ULB UNIVERSITÉ LIBRE DE BRUXELLES

Gembloux Agro-Bio Tech
Université de Liège

FACULTÉ DES SCIENCES

École Interfacultaire de Bioingénieurs

Service d'Écologie du paysage et des Systèmes de Production Végétale

GEMBLOUX AGRO-BIO TECH

Département BIOSE

Unité Biodiversité et Paysage

ESTIMATING THE ABOVEGROUND BIOMASS OF CENTRAL AFRICAN TROPICAL FORESTS AT THE TREE, CANOPY AND REGION LEVEL

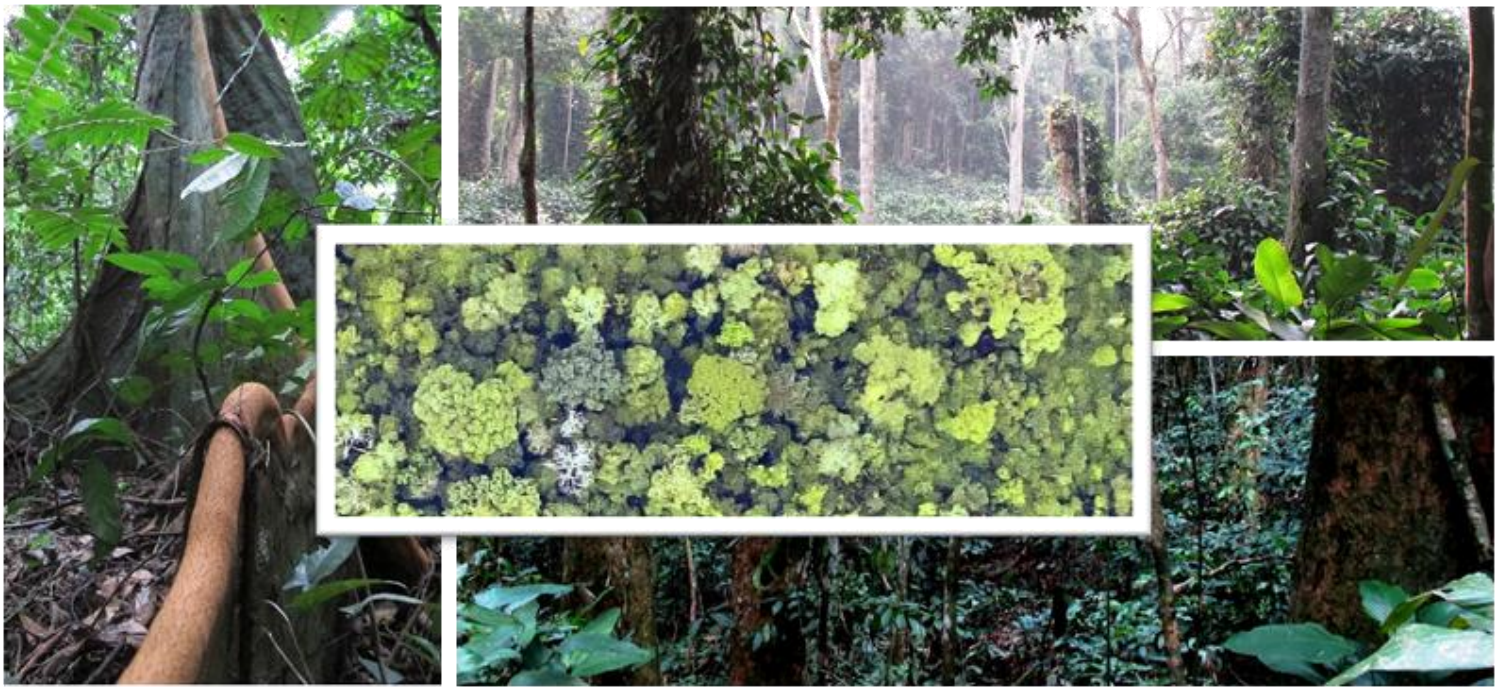

Thesis submitted in fulfillment of the requirements for the degree of Doctor (Ph.D.) in Agronomy and Bioengineering

By

Jean-François Bastin

Collaborations

- Ecole Régionale post-universitaire d'Aménagement et de gestion Intégrés des Forêts et Territoires tropicaux (ERAIFT), Kinshasa, the Democratic Republic of the Congo.
- Botanique et bioinformatique de l'architecture des plantes (AMAP), Montpellier, France.

Bastin J.-F.	Estimating the aboveground biomass of Central African tropical forests

Human pressure on forest resources increased significantly during the past decades through land use and land use change, especially in the tropics where forest clearing is a major source of CO_2 release in the atmosphere. Consequently, forests are the focus of international environmental policies and discussions aiming to reduce emissions from deforestation and forest degradation (i.e., REDD+). The capacity of participating countries to regularly provide accurate forests C stocks measurements at a national scale thus represents an important challenge to address. In dense forests, generally only the above ground biomass (AGB) is measured as it accounts for more than 50% of total C stocks. However, important gaps remain at each scale of measurement, i.e. from felled tree to regional mapping, with the resulting errors propagation through these different scales being probably the most concerning issue.

In the present work, we propose to address these issues by using a multi-scale approach in order to improve our global understanding of AGB variations in dense tropical forests of Central Africa. In particular, we studied (i) forest AGB prediction from remote-sensing textural analysis, (ii) the potential role of largest trees as predictor of the entire forest-stand AGB and (iii) intra- and inter-individual radial variation of wood specific gravity (WSG, i.e. oven-dry mass divided by its green volume) and its potential consequences on the estimation of the AGB of the tree.
First, we analyzed the potential use of textural analysis to predict AGB distribution based on very high spatial resolution satellite scenes. In particular, we used the Fast Fourier Transform Ordination (FOTO) method to predict AGB from heterogeneous forest stands of the Democratic Republic of the Congo (DRC). Here, based on 26 ground plots of 1-ha gathered from the field, plus a successful combination of Geoeye and Quickbird contrasted scenes, we were able to predict and to map AGB with a robust model (R^2 = 0.85; RMSE = 15%) based on textural gradients.
Secondly, the research of AGB indicators was focused on the dissection of the role played by largest trees. Here we found largest trees not only hold large share of forest carbon stock but they contain the print of most of forest-stand structure and diversity. Using a large dataset from western Cameroon to eastern DRC, we developed a non-linear model to predict forest carbon stock from the measurement of only a few large trees. We found the AGB of the 5 % largest stems allow to predict the AGB of the entire forest-stand yielding an R^2 of 0.87 at a regional scale. Focusing on largest trees species composition, we also showed only 5 % of species account for 50 % of total AGB.
In the end, we investigated inter- and intra-individual WSG variations. Despite recognized inter- and intra-specific variations along the radial axis, their ecological determinants and their consequences on trees aboveground biomass assessments remain understudied in tropical regions. To our knowledge, it has never been investigated in Africa. Using a 3-D X-Ray scanner, we studied the radial WSG variation of 14 canopy species of DRC tropical forests. Wood specific gravity variance along the radial profile was dominated by differences between species intercepts (~76%), followed by the differences between their slope (~11%) and between individual cores intercept (~10%). Residual variance was minimal (~3%). Interestingly, no differences were found in the comparison of mean WSG observed on the entire core and the mean WSG at 1-cm under the bark (intercept ~0; coefficient = 1.03). In addition, local values of WSG are strongly correlated with mean value in the global data base at species level.

I deeply believe these results favor the development of promising tools to map and to estimate accurately the AGB of tropical forest-stands. The information provided by largest trees on the entire forest-stand is particularly interesting both for developing new sampling strategies for carbon stocks monitoring and to characterize tropical forest-stand structure. In particular, our results should provide the opportunity to decrease current sampling cost while decreasing its main related uncertainties, and might also favor an increase of the current sampling coverage.

Jury composition

Gregory Mahy	President
Gembloux Agro Bio-Tech, Université de Liège	
Olivier Hardy	Secretary
Université libre de Bruxelles	
Nicolas Barbier	Reporter
Unité Mixte de Recherche, laboratoire de botAnique et bioinforMatique de l'Architecture des Plantes (AMAP), Montpellier, France	
Marius Gilbert	Reporter
Université libre de Bruxelles	
Adeline Fayolle	Reporter
Gembloux Agro Bio-Tech, Université de Liège	
Jan Bogaert	Co-supervisor
Gembloux Agro Bio-Tech, Université de Liège	
Charles De Cannière	Co-supervisor
Université libre de Bruxelles	

Ever failed. Ever tried. No matter.
Try again. Fail again. Fail better.
S.Beckett

ACKNOWLEDGEMENTS

REMERCIEMENTS

Cette thèse de doctorat est le fruit d'un travail collectif initié par le Professeur Jan Bogaert et le Professeur Charles De Cannière. Sans vous, ce travail n'aurait pas pu voir le jour.

Jan, dès le début de notre collaboration lors, de mon mémoire de fin d'études au Bénin, tu as eu confiance en moi et en mes capacités, peut-être même avant que je n'aie moi-même confiance en moi. En venant me chercher en 2010 et en me donnant carte blanche pour la construction d'un projet de thèse ambitieux, tu m'as permis de construire un projet dans lequel je pouvais totalement m'identifier et m'épanouir. En prenant pour exemple ton dynamisme et ta pro-activité, nous avons pu tisser de nombreuses collaborations et développer plusieurs papiers de qualité. Je t'en serai toujours extrêmement reconnaissant. Je voudrais aussi te remercier pour les nombreuses discussions que nous avons tenues au sujet de notre équipe, pour les *update* sur les transferts et les blessures quand j'étais perdu au fin fond du Congo… Cela nous a permis, je crois, de faire régulièrement quelques *break* ponctuant des journées bien souvent trop chargées. Trois fois champions sur quatre ans de thèse, on peut raisonnablement parler de bonne cuvée !

Charles, je ne sais vraiment pas par quel bout commencer. Tu as été présent à mes côtés du premier au dernier jour. La porte de ton bureau a toujours été ouverte et, quel que soit ton planning, tu as toujours su prendre le temps de répondre à mes questions, me donner des conseils, commenter mes papiers, me rassurer et me réorienter subtilement si nécessaire. Tu as toujours su pointer les aspects positifs de mon travail et faire en sorte que je m'appuie sur ces acquis pour aller de l'avant. Tu m'as permis de voir le verre à moitié rempli, ce qui fait qu'il n'y a finalement jamais eu de « bas » lors de ces 4 années de thèse. Au-delà de ce que tu as apporté directement dans ce travail, tu m'as apporté et appris énormément en tant qu'être humain. Suivre ton exemple m'a appris à relativiser et à gérer sereinement certaines situations vraiment délicates. J'ai encore un long chemin à parcourir mais si j'arrive à devenir la moitié de l'homme que tu es, je pourrai être fier de ce que je suis. Merci pour tout.
Par contre, il faudra penser à améliorer ton *shoot* au mini-basket … ;-)

Chaque chapitre constituant cette thèse est le résultat d'une collaboration ou plutôt d'un bout de chemin que j'ai eu la chance de mener avec des scientifiques aussi passionnés que compétents, et parfois aussi pointilleux que perfectionnistes…. Je tiens ici à remercier chaleureusement le Docteur Nicolas Barbier, le Docteur Maxime Réjou-Méchain et le Professeur Adeline Fayolle.

Nicolas, on s'est croisé assez rapidement au début de ma thèse de doctorat. Quand j'y repense, je me rappelle que tu m'avais brièvement montré tes recherches sur le coin d'un banc dans le grenier du bâtiment de botanique. J'avais à l'époque pris cette discussion pour un « cap ou pas cap de travailler sur l'analyse texturale de la canopée par transformée de Fourier … ? ». Un challenge pas évident à relever quand on sait que tu m'avoueras par la suite que même les *reviewers* ont eu du mal à cerner toutes les subtilités de ton dernier article. A travers cette collaboration, tu m'as offert l'un des plus beaux défis intellectuels que j'ai dû relever dans cette thèse. Et au-delà de cela, pour chaque partie de mon travail, tel un troisième promoteur, tu m'as soutenu, tu m'as poussé à être perfectionniste, à me remettre en question et à dépasser mes limites. Enfin, tu m'as mis en contact avec un nombre incalculable de personnes ressources, sans qui je n'aurais pu aujourd'hui produire ce travail. Pour tout cela, et pour tout ce qu'il nous reste encore à faire ensemble, notamment à Montpellier, merci !

Maxime, notre collaboration a également été initiée sur le coin d'un banc, dans le hall d'entrée de l'AMAP où j'ai le souvenir d'avoir passé plus de temps à rallumer la lumière automatique qu'à noter tes commentaires. Ce qui m'a le plus frappé c'est sans doute ta curiosité débordante. Tu t'es intéressé à chaque partie de mon travail et tu y as apporté autant de regards critiques que de conseils avisés. Tu m'as appris à valoriser l'entièreté du potentiel d'un résultat, et tu m'as appris à vendre ce résultat tel un bon marchand de tapis ;-),ce qui est peut-être la partie la plus difficile en sciences. J'espère que le travail que l'on a réalisé, qui dépasse les limites de cette thèse, se

concrétisera prochainement et qu'il n'est que le premier d'une longue série. J'ai en effet bien peur que tes travaux d'intérêts généraux n'en soient qu'à leurs débuts. Pour tout ce que tu as déjà fait, pour le post-doc et pour le travail qui nous attend, encore merci !

Adeline F (pour éviter toute confusion ;-)), bien que notre collaboration ait commencé sur le tard, tu m'as également permis de donner une autre dimension à ce travail. Plus particulièrement une dimension plus « écologiste ». De fait, je ne sais plus très bien si je m'intéresse au REDD+ pour comprendre le fonctionnement des forêts ou l'inverse ;-). Travailler avec quelqu'un d'aussi franc, direct et perfectionniste que toi a été particulièrement agréable. Merci pour tout, j'espère que les différents projets que nous souhaitons développer ensemble se concrétiseront !

Je voudrais ensuite remercier les membres de mon comité d'accompagnement, les professeurs Jean-Louis Doucet, Marius Gilbert et Olivier Hardy. Bien qu'étant chacun très fort chargés et parfois fort éloignés de mes problématiques de thèse, vous avez tous pris le temps nécessaire pour m'écouter et répondre à mes questions quand j'en avais besoin. Marius, Olivier et Jean-Louis, un grand merci pour ces quatre années.

Je voudrais remercier le Professeur Gregory Mahy, pour m'avoir chaleureusement accueilli dans son unité de recherche à Gembloux.

Je voudrais également remercier les différents professeurs pré-cités ayant accepté de faire partie de mon Jury de thèse de doctorat, et pour le temps qu'ils ont consacré à la lecture et à l'évaluation du document.

I also would like to thank the Dr. Danae Maniatis.
First, for having produced a very inspiring PhD thesis on carbon stocks assessment methodologies. I can still remember my first thoughts after reading your PhD, it was something like "How the hell will I ever manage to do something like this?" (after 3 days of continuous crying and despair ☺).
Later, I had the chance to be regularly in contact with you. Your continued support and your constant positive attitude were a great source of energy to keep it up and never give up. Thank you for everything, I hope we'll have the opportunity to finally work or build something together.

Un tout grand merci également aux différentes institutions qui m'ont accueilli, ainsi que les professeurs, scientifiques et techniciens qui m'y ont ouvert leurs portes : ULB (Thomas Drouet, Tariq Stevart, Gilles Dauby, Adrien Parmentier), Gembloux (Jacques Hébert, Phillipe Lejeune, Grégory Mahy, Marc Dufrêne, Jean-François Gillet, Nils Bourland, Pascal Thibaut), ERAIFT (Baudouin Michel, Jean-Pierre Mate, Jean Lejoly), le MRAC (Hans Beeckman, Maaike De Ridder), UGent (Joris Van Acker, Jan Van Der Bulcke), MEISE (Luc Pauwels), WWF Belgique (Geert Lejeune, Gregory Claessens, Françoise Ansay), WWF Germany(Aurelie Shapiro), WWF Congo(Raymond Lumbuenamo, Bruno Perodeau), ONG Mbou-mon-tour (Papa Bokika).

Un tout grand merci à mes collègues bruxellois et gembloutois : Isabelle, Thalès, Adi, Diouf, François, Hady, Sylvain K, Sylvain A, Léon, Chantale, Djibu, Yegor, Line, Alvi, Noémie, Sylvain B, William O, William C, Marie, Mélanie, Aurélie, Carline, Jessica, Justine, Emilie, Julien, Maxime, Valentin, Sebastien, Stéphanie, Julie, Robin, Roel, Olivia, Pitchou, Yannick, Robin, Stéphanie, Sebastien B, Julie M-R, Julien L, Barbara H, Chab et à tout ceux que j'aurais oublié. Pour ceux qui ont encore un bout de chemin à parcourir, je vous souhaite bien du courage… ;-)
Je souhaite aussi particulièrement remercier Cynthia Thomas, qui, malgré mon manque de connaissance du *vade mecum* de l'unité Biodiversité et Paysage, a toujours su faire preuve de patience avec moi. Ta présence et ton soutien à l'unité sont vraiment essentiels. Merci pour ton aide tout au long de ce doctorat !

J'ai également eut la chance d'encadrer trois chouettes petites têtes pour la réalisation de leur mémoire de fin d'étude à l'ULB.
Benoit, encore désolé pour tout ce que tu t'es choppé sur le terrain et merci pour ton investissement physique (qui s'est traduit si je ne m'abuse par une perte nette de 10 kg ;-)).
Judith, cela n'a pas été évident de te trouver un sujet mais finalement je me dis que quelque soit le sujet qu'on t'aurait trouvé tu aurais cartonné. Je ne garde que de bons souvenirs de ton encadrement.
Yegor, merci d'avoir passé des heures à scanner des petits bouts bois dans les caves de l'université de Gand. J'espère qu'on aura l'occasion de continuer à travailler ensemble et j'espère surtout que tu trouveras ta voie et que tu t'épanouiras dans la recherche !

Liboso nakoki kosilisa kotonda bato basuka ia musala oyo, essengli kotonda bato ia mboka.
Pala aka le botaniste, Ngamba aka le maximum, Americain na Leboncoeur, nazali kotonda bino mingi po na basanza totambolaki na zamba, na poto poto, pe na esobe. Biso mitano, tosalaki musala makasi. Nayekolaki mingi na bino. Bozali mayele, bowuti ya mboka kasi tango essengeli koyekola biloko ya zamba bokoki koleka bamundele ya bascientifique bawuti Kinshasa ou Europe. Nazokanisa na bino mingi, mikolo na mikolo, nazobosana bino te. Nakosepela mingi soki nzambe alingi tokokutana.
Bakolo mabele ya GuantaMalebo, yaya Menard, yaya Daniel pe noko Jean. Ngai, mundele mokie, nayekolaki mingi na bino. Liboso, nayekolaki kofandaka kimia liboso makambo : likambo ya zamba, likambo ya nzala, likambo ya musala, pe likambo ya momi ;-). Nayekolaki korespecter coutume ya bino, ya coutume ya Bateke. Sima nayekolaki koloba mwa lingala. Kasi, lingala ya ngai etikali mwa pasi. Nakobosana bino to, nakosepela kokutana bino mikolo ekoya.

Nalingi pe kotonda bakolo ya mabele, Obama ya Nkala ya Kolo ya Mpelu. Natondi bino mingi po na bafête tosalaki ya esika moko. Lelo, nazosepela mingi tango nazokanisa ya mikolo tobinaki ya tomelaki ya esika moko. Awa, nazotonda pe yaya Cicé, papa Paulain ya mama Wivine. Natondi bino mingi po na suka ya biloko ya mboka.

Céline et Fredo, votre présence à Malebo était un véritable bonheur. Pouvoir lâcher de bonnes petites blagues bien crasses avec un bon accent bien de chez nous tout en mangeant une bonne pizza… on a parfois tendance à oublier ce que ça vaut ;-)

Francky four fingers, merci pour les milliers délires qu'on a eu sur le terrain. Je me souviendrai particulièrement de la journée perdue sous une tente, à attendre désespérément que la pluie cesse à proximité des éléphants et à regarder Americain se déchaîner sur du Hard Rock… surréaliste ☺

Je souhaite remercier mes amis. Bien que je n'aie pas pu vous consacrer beaucoup de temps ces 4 dernières années, j'ai souvent pensé à vous. Merci aux vieux dlà vieille (Olivier, John, Manu, Alex, Davy, Edwin, …), toujours là quand on a besoin de vous. Merci aux Zagros et conjoints, merci à mes petits bras cassés du Cercle et merde à H ;-) !!!
Un tout grand merci à My Hanh, pour m'avoir appelé de nombreuses fois quand j'étais perdu au fin fond de la brousse et pour prendre soin de moi dans les moments difficiles.

Je souhaite également remercier mes chats pour être venu me réveiller tous les matins au lever du soleil, afin de s'assurer que je n'arrive pas trop tard à l'université… ou pas

Je souhaite également remercier mes parents, mes frères, mes cousins et cousines, oncles et tantes, ainsi que Chantal, Nathalie et Josée.
Papa et Maman, je ne vous remercierai jamais assez pour tout ce que vous avez fait pour moi depuis le début. Quand je pense à cette thèse, je pense particulièrement à une chose : dès que j'avais tendance à baisser les bras quand j'étais petit, vous étiez toujours les premiers à me faire

comprendre qu'on a tous le potentiel de réussir ce qu'on entreprend, qu'on est tous capable et que, finalement,on se fixe nous-mêmes nos propres limites. Du coup, je ne me suis jamais découragé et j'ai toujours su que j'allais y arriver. Merci pour cela, cela m'a donné de l'énergie tout au long de cette thèse de doctorat !
Chris et Steph, vous êtes particulièrement un exemple d'acharnement, je ne compte pas le nombre de fois où j'ai pensé à vous en forêt en me répétant « lâche rien put***, lâche rien, lâche rien de rien ! Pense à l'autre clette qui était perdu en Chine, lâche rien put*** » ! Merci pour cette source de motivation.

Enfin, et peut-être surtout, je souhaite remercier Adeline.
Ma puce, je n'ai certainement pas assez de pages ici pour te remercier mais je vais tout de même essayer de t'écrire quelques mots. Aussi loin que je me souvienne, tu as commencé en relisant et commentant mon projet FRIA et tu as terminé en relisant et commentant ma thèse de doctorat. La boucle est donc bouclée. Grâce à ta présence et à ton soutien, je n'ai jamais eu le sentiment d'être seul. Tu étais toujours prête à écouter patiemment et attentivement les mêmes histoires barbantes sur mes arbres … (après tout c'est bien normal qu'un gros arbre soit plus lourd qu'un petit arbre non ?) … Sans toi, je n'aurais pas réussi à tenir ce rythme pendant ces 4 années.
En m'apprenant qu'il faut « avoir des rêves assez grands pour ne pas les perdre de vue pendant qu'on les poursuit » (Oscar Wilde), tu m'as permis d'oser devenir ambitieux et de ne jamais reculer devant les obstacles. Ces obstacles, on les a affrontés les uns après les autres, main dans la main. Merci pour tout cela et merci pour tous les rêves qu'il nous reste encore à poursuivre à deux.

Je remercie le FRIA pour avoir financer ces 4 années de thèse de doctorat. Et je remercie l'ERAIFT pour avoir apporté un coup de pouce significatif pour les frais de matériel et les frais logistiques de terrain.

A Fabian, Andrée, Rolande, André, Michel et Jacques…

SUMMARY

Human pressure on forest resources increased significantly during the past decades through land use and land use change, especially in the tropics where forest clearing is a major source of CO_2 release in the atmosphere. Consequently, forests are the focus of international environmental policies and discussions aiming to reduce emissions from deforestation and forest degradation (i.e., REDD+). The capacity of participating countries to regularly provide accurate forests C stocks measurements at a national scale thus represents an important challenge to address. In dense forests, generally only the above ground biomass (AGB) is measured as it accounts for more than 50% of total C stocks. However, important gaps remain at each scale of measurement, i.e. from felled tree to regional mapping, with the resulting errors propagation through these different scales being probably the most concerning issue.

In the present work, we propose to address these issues by using a multi-scale approach in order to improve our global understanding of AGB variations in dense tropical forests of Central Africa. In particular, we studied (i) forest AGB prediction from remote-sensing textural analysis, (ii) the potential role of largest trees as predictor of the entire forest-stand AGB and (iii) intra- and inter-individual radial variation of wood specific gravity (WSG, i.e. oven-dry mass divided by its green volume) and its potential consequences on the estimation of the AGB of the tree.

First, we analyzed the potential use of textural analysis to predict AGB distribution based on very high spatial resolution satellite scenes. In particular, we used the Fast Fourier Transform Ordination (FOTO) method to predict AGB from heterogeneous forest stands of the Democratic Republic of the Congo (DRC). Here, based on 26 ground plots of 1-ha gathered from the field, plus a successful combination of Geoeye and Quickbird contrasted scenes, we were able to predict and to map AGB with a robust model (R^2 = 0.85; RMSE = 15%) based on textural gradients.

Secondly, the research of AGB indicators was focused on the dissection of the role played by largest trees. Here we found largest trees not only hold large share of forest carbon stock but they contain the print of most of forest-stand structure and diversity. Using a large dataset from western Cameroon to eastern DRC, we developed a non-linear model to predict forest carbon stock from the

measurement of only a few large trees. We found the AGB of the 5 % largest stems allow to predict the AGB of the entire forest-stand yielding an R^2 of 0.87 at a regional scale. Focusing on largest trees species composition, we also showed only 5 % of species account for 50 % of total AGB.

In the end, we investigated inter- and intra-individual WSG variations. Despite recognized inter- and intra-specific variations along the radial axis, their ecological determinants and their consequences on trees aboveground biomass assessments remain understudied in tropical regions. To our knowledge, it has never been investigated in Africa.

Using a 3-D X-Ray scanner, we studied the radial WSG variation of 14 canopy species of DRC tropical forests. Wood specific gravity variance along the radial profile was dominated by differences between species intercepts (~76%), followed by the differences between their slope (~11%) and between individual cores intercept (~10%). Residual variance was minimal (~3%).

Interestingly, no differences were found in the comparison of mean WSG observed on the entire core and the mean WSG at 1-cm under the bark (intercept ~0; coefficient = 1.03). In addition, local values of WSG are strongly correlated with mean value in the global data base at species level.

I deeply believe these results favor the development of promising tools to map and to estimate accurately the AGB of tropical forest-stands. The information provided by largest trees on the entire forest-stand is particularly interesting both for developing new sampling strategies for carbon stocks monitoring and to characterize tropical forest-stand structure. In particular, our results should provide the opportunity to decrease current sampling cost while decreasing its main related uncertainties, and might also favor an increase of the current sampling coverage.

RÉSUMÉ

La pression anthropique sur les ressources forestières a augmenté considérablement au cours des dernières décennies, en particulier dans les tropiques où la déforestation est une importante source de rejet de CO_2 dans l'atmosphère. Par conséquent, les forêts sont au cœur des politiques et des discussions internationales visant à réduire les émissions de gaz à effet de serre dues à la déforestation et la dégradation des forêts (i.e., REDD +). La capacité des pays participants à fournir régulièrement le niveau de stocks de carbone des forêts à échelle nationale représente donc un défi important à relever. Dans les forêts denses, la biomasse aérienne ligneuse est plus couramment mesurée car elle représente plus de 50% des stocks totaux de C. Cependant, d'importantes lacunes demeurent à chaque échelle de mesure de la biomasse aérienne ligneuse, partant de l'arbre abattu jusqu'à la cartographie régionale. De plus, la propagation des erreurs à travers ces différentes échelles de travail constituent probablement le problème plus inquiétant.

Dans le présent travail, nous proposons de répondre à ces questions en utilisant une approche multi-échelle afin d'améliorer notre compréhension globale des variations de la biomasse aérienne ligneuse dans les forêts denses de l'Afrique centrale. En particulier, nous avons étudié (i) la prédiction de la biomasse des forêts par l'analyse de la texture de la canopée par télédétection, (ii) le rôle potentiel des arbres les plus grands comme prédicteur de l'ensemble de la biomasse de la forêt et (iii) la variation radiale intra et inter-individuelle de densité de bois et ses conséquences potentielles sur l'estimation de la biomasse de l'arbre.

Tout d'abord, nous avons étudié le potentiel de l'analyse texturale de la canopée pour prédire la distribution de la biomasse aérienne ligneuse sur base d'image satellite très haute résolution spatiale. En particulier, différents gradients de textures ont été quantifiés sur base d'une transformée de Fourier appliquée sur l'image satellite, suivie d'une ordination des spectres de Fourier obtenus. De cette ordination nous avons identifié une série de prédicteur de la biomasse aérienne ligneuse de peuplements forestiers hétérogènes de la République démocratique du Congo (RDC). Ici, sur la base de 26 parcelles de terrain de 1 ha, et de l'association de deux images satellites (Geoeye et Quickbird) prises dans des conditions d'acquisition différentes, nous avons été en mesure de prédire et de

cartographier la biomasse aérienne ligneuse avec un modèle robuste, où 85 % de la variance totale de la biomasse sont expliqués et ne présente que 15 % d'erreur par rapport à la moyenne observée.

Deuxièmement, la recherche d'indicateurs de la biomasse aérienne ligneuse a été axée sur la caractérisation du rôle joué par les arbres plus grands. Ici, nous avons trouvé que les arbres les plus grands, non seulement détiennent une part importante des stocks de carbone forestier, mais ils contiennent une grande part de l'information sur la structure complète du peuplement et sur sa richesse spécifique. Cette étude se base sur un grand set de données (175 parcelles de 1 ha), allant de l'ouest du Cameroun est de la RDC. En particulier, nous avons développé un modèle de prédiction de la biomasse aérienne ligneuse totale sur base de la mesure de quelques grands arbres. Les résultats de ce modèle nous montrent qu'avec seulement 5 % des individus les plus grands, nous pouvons prédire 87 % de la variation de la biomasse aérienne ligneuse totale avec seulement 14 % d'erreur. A échelle régionale, nous avons également montré que la richesse spécifique des 5 % les plus grands constitue un bon indicateur de la richesse spécifique globale vu qu'ils en explique 50 % de la variance.

Enfin, nous avons étudié les variations inter- et intra-individuelles de densité du bois. En dépit des variations de densité reconnues le long de l'axe radial, leurs déterminants, leurs conséquences écologiques et leurs conséquences sur les estimations de la biomasse aérienne ligneuse des arbres ont très peu été étudiées en Afrique. Dans ce chapitre, nous avons étudié la variation radiale de la densité de bois de 14 espèces de la canopée des forêts tropicales de la RDC via l'utilisation d'un scanner à rayon X sur des échantillons de carotte de bois. Nous avons pu y observer que la variation de la densité du bois le long de l'axe radial s’explique principalement par des différences constantes (intercept) propres aux espèces (76 % de la variance), suivie par les différences entre leurs pentes (~ 11 %) et les différences constantes entre les individus (~ 10 %). En outre, nous avons pu observer que les valeurs moyennes de densité de bois obtenues par espèce sont fortement corrélées aux valeurs disponibles dans des bases de données globales. Fait intéressant, aucune différence n'a pu être décelée dans la comparaison de la moyenne de la densité de bois observée sur l'entièreté du profil

des carottes prélevées et de leur densité moyenne à 1 cm sous l'écorce (interception ~ 0; coefficient = 1,03).

Nous pensons que ces résultats favorisent le développement d'outils prometteurs pour cartographier et évaluer avec précision la biomasse aérienne ligneuse des forêts tropicales. En particulier, les informations sur l'entièreté du peuplement forestier contenues dans les plus gros arbres sont intéressantes tant pour le développement de nouvelles stratégies d'échantillonnage que pour comprendre l'écologie des forêts tropicale. En pratique, ces résultats devraient donner l'opportunité de diminuer les coûts d'échantillonnage tout en réduisant ses principales incertitudes connexes. Ces résultats devraient contribuer au renforcement des capacités des pays participant au programme REDD+, et donc leur permettre de diminuer les incertitudes sur leurs estimations de stock de carbone à échelle nationale.

TABLE OF CONTENTS

Table of contents

ACRONYMS

AGB: Aboveground biomass

BRLU: the herbarium and botanical library of the ULB

COP: Conference of the Parties

FAO: Food and Agriculture Organization

FOTO: Fourier textural ordination

GHG: Greenhouse gases

GLAS : Geoscience Laser Altimeter System

GMST: Global mean surface temperature

IPCC: Intergovernmental panel for climate change

LiDAR : Light Detection And Ranging

MRV: Measuring, reporting and verifying

NGO: Nongovernmental organization

REDD: Reduced Emissions from Deforestation and forest Degradation

REDD+: Reduced Emissions from Deforestation and forest Degradation and the role of conservation, sustainable management of forests and enhancement of forest carbon stocks

SAR : Synthetic Aperture Radar

UMR-AMAP: the joint research unit for plant architecture, botany and bioinformatics of Montpellier

UNEP: United Nations Environment Program

UNFCCC: United Nation Framework Convention on Climate Change

VHR: Very high spatial resolution (pixel resolution < 1 m)

WMO: World Meteorological Organization

WSG: Wood specific gravity, i.e. the wood oven-dry mass divided by its green volume

WWF: World wide fund for nature

FIGURES

TABLES

FOREWORD

Foreword

Anthropogenic greenhouse gases (GHG) emissions are the main reported driver of climate change (IPCC 2013). After fossil fuels combustion, tropical deforestation is the second most important source of GHG (van der Werf et al. 2009), contributing from 7 to 16 % of total emissions (Pan et al. 2011). As a consequence, international policies have emerged with the aim to reduce emissions due to deforestation and forest degradation, i.e. the REDD program (Agrawal et al. 2011). The application of such program requires from each participating country to implement a national forest monitoring system, and to support the Measurement, the Reporting and the Verification (MRV) of forest carbon stocks. As a priority, the REDD program aims to create a new financial incentive for developing countries by valorizing forest resources conservation through the carbon market (Agrawal et al. 2011). Here, Central African countries constitute the main challenge because their forests are reported to be the less studied (Gibbs et al. 2007, Lewis et al. 2013) while they are arguably the less prepared to meet international programs requirements (Agrawal et al. 2011).

In the tropics, the largest shares of forest carbon stocks are contained within the aboveground living biomass (Pan et al. 2011), and as forest above-ground carbon stocks correspond to the half of their dry aboveground biomass (AGB) (Gibbs et al. 2007) the main challenge for scientists is then to develop accurate, precise and effective methods to assess forest AGB.

Tropical forest AGB estimation is one the 'hottest' topic in the current research on climate change, forestry, remote-sensing and tropical ecology. Despite considerable efforts in the past few years to improve our knowledge in each domain (e.g. Lewis et al. 2013, Chave et al. 2014, Mitchard et al. 2014), important gaps remain at each scale of measurement, i.e. from felled tree to regional mapping (Chave et al. 2004, Clark and Kellner 2012, Réjou-Méchain et al. 2014, Mitchard et al. 2014). The propagation of errors (Figure 0-1) through these different scales of work is probably the most concerning issue (e.g. Chave et al. 2004, Clark and Kellner 2012). Regional mapping relies on remote-sensing methods but also on ground sampling quality, which themselves depend on the quality of AGB measurement based on felled trees. Identification of these problems led Clark and Kellner (2012) publishing a paper on the 'tropical forest biomass estimation and the fallacy of misplaced

concreteness'. The motivation of this publication was the ascertainment that most of published works on AGB measurement and estimations don't do it properly. In order to improve the quality of AGB estimations, Clark and Kellner propose to consider a new framework in which forests are seen as a set of 'forest units', i.e. an assemblage of individual trees constituting the 'forest-stand', accounted at each scale of measurement. This 'unit' or 'forest-stand' conception mirrors the 'layered forest' of Hallé et al. (1978), in which tropical forests were compared considering an assemblage of trees composing each layer of the forest, constituting a 'forest unit' or 'forest-stand' comparable between the different locations.

These observations form the foundation of our work, where our main objective is to provide new elements to improve our understanding of AGB distribution and variation throughout Central Africa based on a multi-scale approach : the tree, the forest-stand ('forest unit') and the region (assemblage of 'forest units'). The work performed at each scale considered aims to decrease uncertainties in AGB estimation and to favour the implementation of the REDD program.

The introduction of this manuscript aims to provide a useful background on several levels:

- The role played by forests as carbon stocks and the resulting international policies that have been developed. In particular we provide recent figures on the distribution and on the dynamics of carbon stocks in the different forests of the world, with more detailed information for the different tropical forests.
- The up-to-date methodologies and recent results obtained at each scale of AGB measurement.
- A general history and description of the Congo Basin Forests and of the study site in which I collected the data used in Papers 1 and 3.

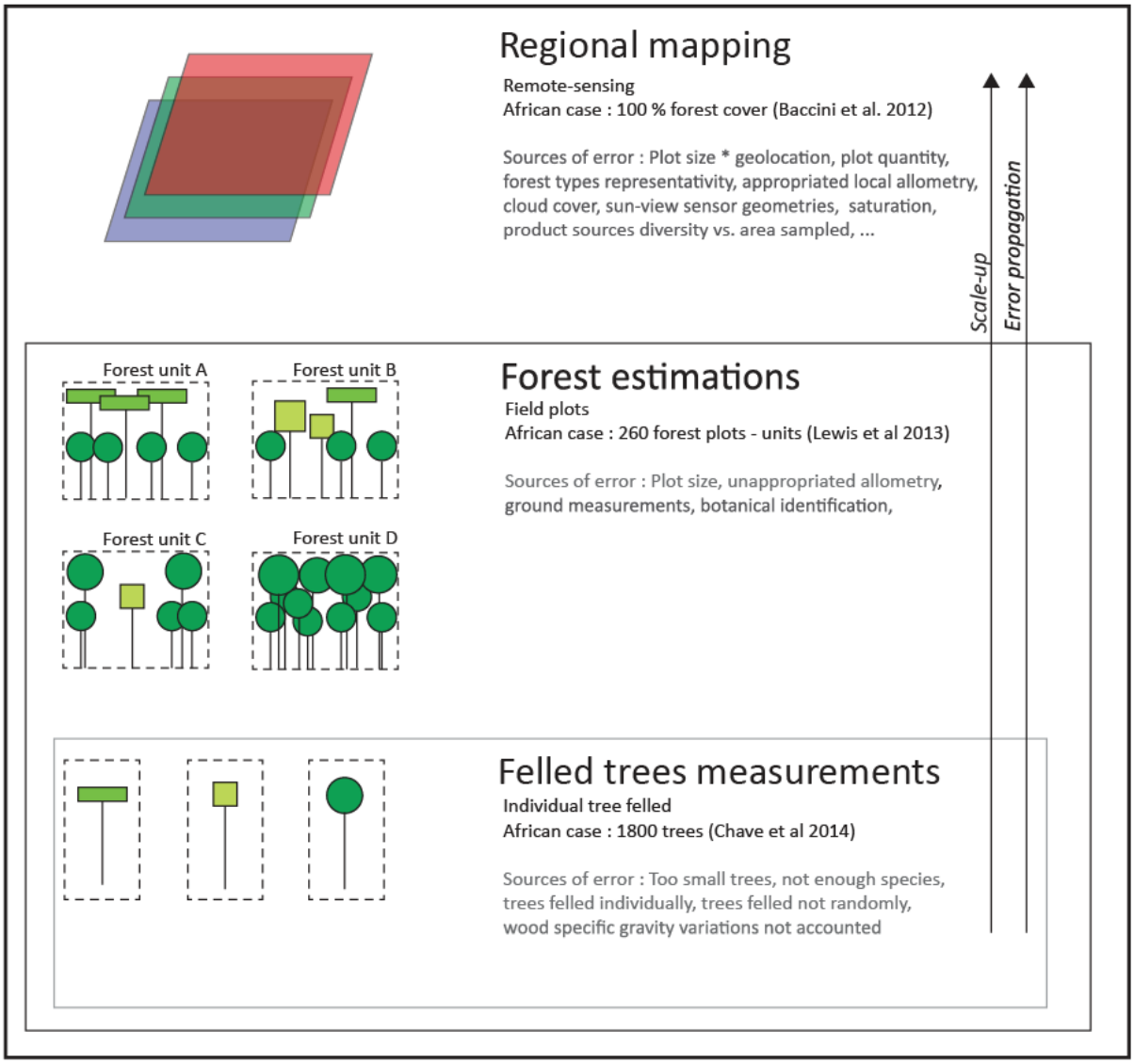

Figure 0- 1. Error propagation in forest AGB estimations. Illustration through the main scale of work generally considered. Numbers and references are given as an example for the case of Africa. Some examples of common sources of errors are cited for each level (in grey). The figure is inspired from Chave et al. (2004) and Clark and Kellner (2012).

INTRODUCTION

PART 1: FORESTS AND CLIMATE CHANGE

Partially Includes the following publication :

Bastin et al 2011. Multiscalar analysis of the spatial pattern of forest ecosystems in Central Africa justified by the pattern/process paradigm: two case studies.

1. Climate change and carbon emissions

According to the fifth's assessment report of the Intergovernmental Panel on Climate Change (IPCC) published in 2013, the Earth's radiative budget is imbalanced since at least the 1970s, with more energy from the Sun entering than exiting the atmosphere (IPCC 2013). This uptake of energy has impacted the climate system equilibrium and led to several changes, the main being a global warming of the Earth's surface.

The global mean surface temperature (GMST) has continuously increased on Earth since the 19th century (IPCC 2013). The measured temperature, accounting land and ocean temperature data, show a warming of 0.85 °C from 1880 to 2012 and about 0.72 °C from 1951 to 2012 (Figure 0-2). These observations are consistent between different datasets recorded independently, accounting the Global Historical Climatology Network Version 3 (GHCNv3; Lawrimore et al. 2011), Goddard Institute of Space Studies (GISS; Hansen et al. 2010), the Center Research Unit gridded surface Temperature 4 (CRUTEM4; Jones et al. 2012) and a new data product from a group based predominantly at Berkeley (Rohde et al. 2013). Furthermore, the global increase in temperature is confirmed by many complementary observations realized in the last decades, such as the melting of Arctic sea-ice which is about 10^6 km² per decades since 1979 (Figure 0-3; Cavalieri et al. 1984, Markus and Cavalieri 2000, Walsh and Chapman 2001, Rayner 2003, Comiso and Nishio 2008, Cavalieri and Parkinson 2008, Parkinson and Cavalieri 2012), and the increase of the sea level of about 2 millimeters per year since 1870s (Figure 0-3; Jevrejeva et al. 2008, Ablain et al. 2009, Leuliette and Scharroo 2010, Nerem et al. 2010, Church and White 2011, Ray and Douglas 2011). Other climate parameters are investigated to describe and understand the current climate change and the consequences of a global warming (e.g. the shrinking of glaciers, the increase of oceans' salinity, the increase of oceans' acidity, the increase of occurrence of extreme climate events, the stability of the precipitations ...) but these are not developed in the present section. For more information, we recommend to consult the fifth assessment report of the IPCC which is available online on their website.

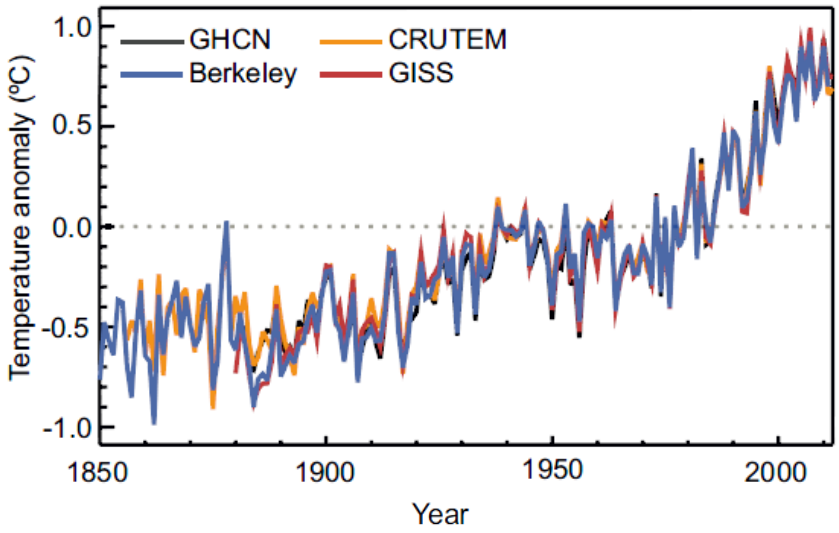

Figure 0- 2: Observed global mean land and ocean surface temperature anomalies relative to the 1961 – 1990 period. Annual and decadal averages are displayed (IPCC 2013). Black : Lawrimore et al. (2011); orange: Jones et al. (2012); red: Hansen et al. (2010) and blue (Rohdes et al. 2013).

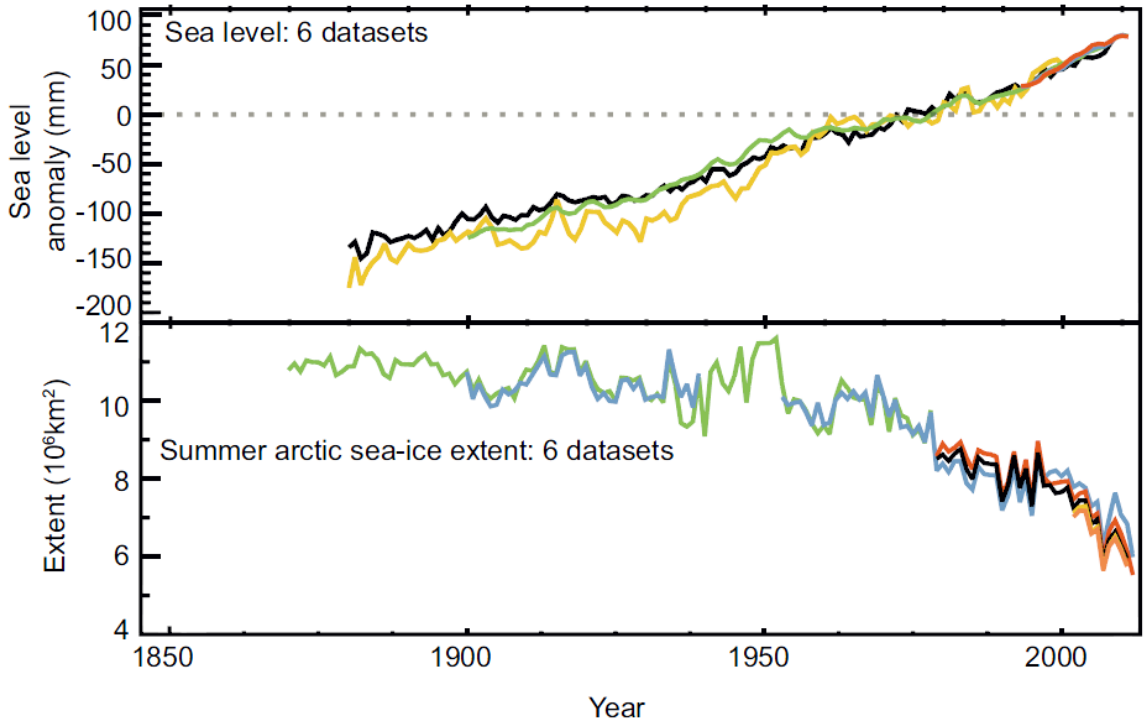

Figure 0- 3: Observed global mean Sea level and Artic sea-ice extent anomalies relative to the 1961 – 1990 period (IPCC 2013). Arctic sea-ice extent sources: Green: Walsh and Chapman (2001), Blue: Rayner et al., (2003), Red: Comiso and Nishio (2008), Black: Cavalieri and Parkinson (2008) and Parkinson and Cavalieri (2012), Yellow: Comiso and Nishio (2008), Orange: Markus and Cavalieri (2000). Sea-level sources : Black: Church and White (2011), Yellow: Jevrejeva et al. (2008), Green: Ray and Douglas (2011), Red: Nerem et al. (2010), Orange: Ablain et al. (2009), Blue: Leuliette and Scharroo (2010)).

Drivers of climate change are assessed through the measurement of 'Radiative Forcing' (RF) which quantifies the changes in energy fluxes caused by alteration processes since the 'Industrial era', i.e. from 1750 to 2011 (IPCC, 2013). Natural and anthropogenic processes can alter Earth's energy budget which reacts through a modification of the climate system equilibrium. Basically, positive RF leads to an increase in earth surface temperature, while a negative RF leads to surface cooling. The strength of climate change drivers can be therefore quantified through specific RF, expressed in Watt per square meter (Wm^{-2}). The main potential anthropogenic drivers of climate change are: the well mixed greenhouse gases (WMGHG; CO_2, CH_4 and NO_2), the Ozone, Aerosols and the Albedo resulting from land surface changes. Main natural sources are the solar irradiance and the volcanic RF. RF of each driver is generally assessed from the differences of concentrations between 1750 and the present and translated in Wm^{-2} from Myhre et al. (1998) formula. These are measured directly (*in situ*) or indirectly (remote sensing) in the troposphere or at the top of the atmosphere (IPCC 2013).

Among aforementioned drivers, the largest contribution to total RF is caused by the increase of CO_2 (IPCC 2013), which account for about 80 % of the total RF due to well-mixed greenhouse gases (WMGHG; CO_2, CH_4 and NO_2). To assess anthropogenic impact on WMGHG emissions, past concentrations of WMGHG have been estimated with high confidence through the analysis of the air enclosed in polar ice cores (Joos and Spahni 2008, Köhler et al. 2011). It appears that today concentration of WMGHG are the highest found since the last 800 000 years. From this period, the pre-industrial ice core WMGHG concentrations stayed within well-defined natural limits with maximum interglacial concentrations of approximately 300 ppm for CO_2 and minimum glacial concentrations of approximately 180 ppm. Such variations have been successfully modeled from natural orbital forcing. This term is used to denote the incoming solar radiation changes originating from variations in the Earth's orbital parameters as well as changes in its axial tilt. Orbital forcing is well known from precise astronomical calculations for the past and future (Laskar et al. 2004).

It is now a fact that present-day (2014) concentrations of CO_2 (398.83 ppm, Dlugokencky and Tans 2014) exceed by far the range of concentrations recorded in the ice core records during the past 800

000 years, and such increase cannot be explained by natural forcings only. Consequently, CO_2 deserves a particular attention, especially considering anthropogenic sources of emissions.

The current carbon cycle on Earth can be described as a network of different reservoirs (Atmosphere, Oceans, Vegetation, Soils and Permafrost) storing or emitting fluxes of CO_2. On Figure 0-4, we represented this carbon cycle, which is a simplified and updated version of the figure 6.1 of the IPCC report of 2013. Basically, we can see the stock of all compartments (in PgC) and fluxes (in PgC per year) between them. Natural fluxes (Pre-industrial era) are displayed in black and anthropogenic fluxes (according to 2000 – 2009 emissions) are displayed in red.

The atmosphere store about 830 PgC (Prather et al. 2012, Joos et al. 2013), an amount that increases each year of 4PgC due to human activities. The vegetation live biomass store about 360 PgC and 500 PgC in soils, deadwood and litter (Pan et al. 2011). CO_2 is removed from the atmosphere by plant photosynthesis (Gross Primary Production (GPP), 123 PgC yr^{-1}, (Beer et al. 2010) and can be released back into the atmosphere by autotrophic (plant) and heterotrophic (soil microbial and animal) respiration and additional disturbance processes (119 PgC yr–1, (Beer et al. 2010). A fraction of soil carbon is transported by freshwaters and is outgazed as CO_2 (~1 PgC yr^{-1}) is delivered by rivers to the coastal ocean as dissolved inorganic carbon, dissolved organic carbon and particulate organic carbon (Tranvik et al., 2009). Atmospheric CO_2 is exchanged with the surface ocean through gas exchange. This exchange flux is driven by the partial CO_2 pressure difference between the air and the sea. The total amount of carbon in the oceans account about 40 000 PgC (Hansell et al. 2009). Note there is an additional amount of in permafrost soils of about 1700 PgC (Tarnocai et al. 2009).

Fossil fuels and deforestation are the main sources of anthropogenic CO_2 emissions accounting respectively for 7.8 PgC yr-1 (GEA 2006) and 1.1 PgC yr-1 (Pan et al. 2011). Interestingly, these exceedings are partly stored back (55 %) in the Ocean and the Vegetation reservoirs, where they are almost equally distributed (IPCC 2013). However, 45 % of each year emissions remain in the atmosphere and mainly contribute to the current climate change. These numbers emphasize the key

role played by forests in climate change. In the next section we consequently focus on the relationship between forest and their carbon stocks.

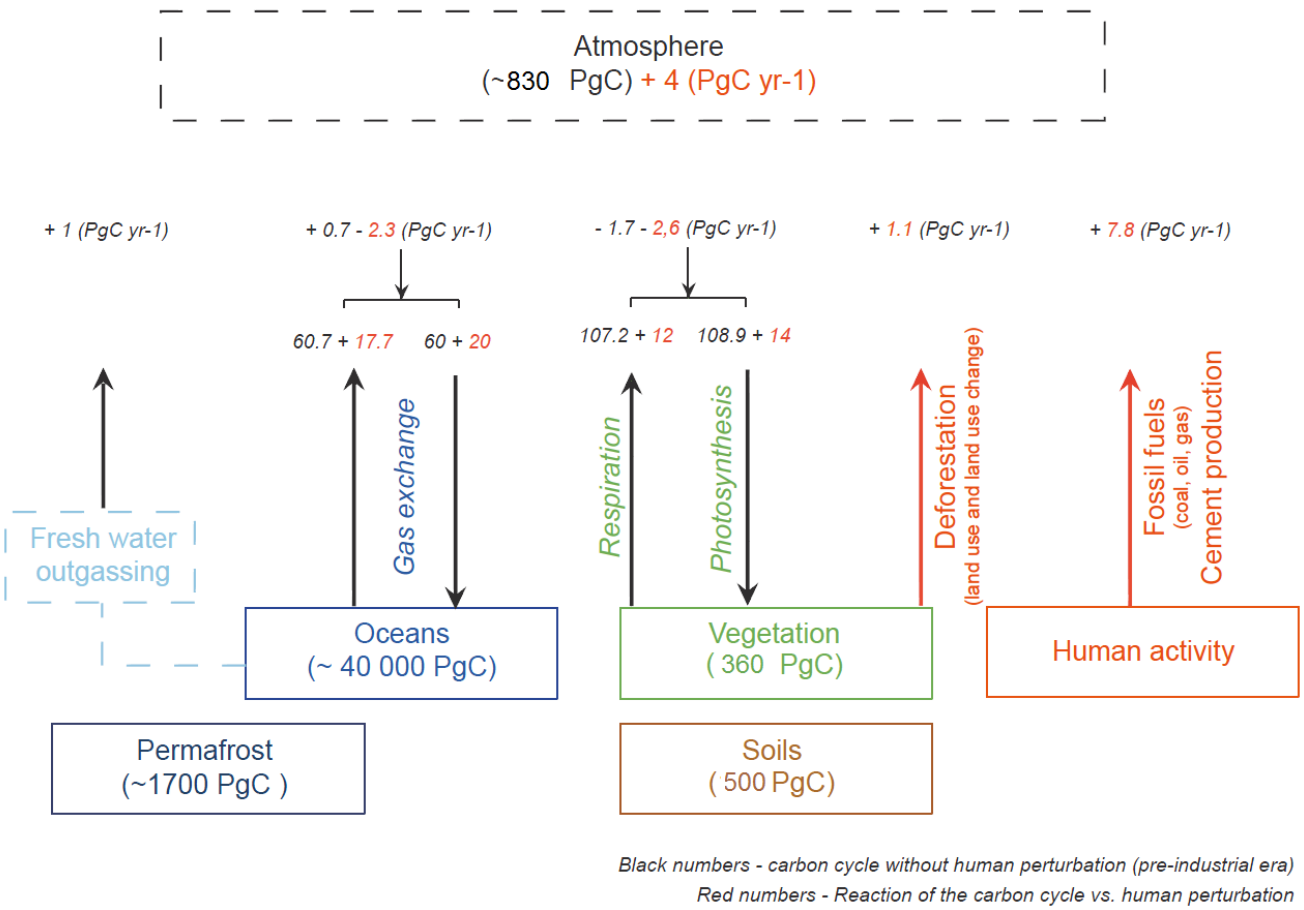

Figure 0-4 : The carbon cycle – reservoirs and fluxes (adapted from IPCC 2013). The atmosphere store about 830 PgC (Prather et al. 2012, Joos et al. 2013), an amount that increases each year of 4PgC due to human activities. The vegetation live biomass store about 360 PgC and 500 PgC in soils, deadwood and litter (Pan et al. 2011). CO_2 is removed from the atmosphere by plant photosynthesis and can be released back into the atmosphere by autotrophic (plant) and heterotrophic (soil microbial and animal) respiration and additional disturbance processes (119 PgC yr–1, (Beer et al. 2010). A fraction of soil carbon is transported by freshwaters and is outgazed as CO_2 (~1 PgC yr^{-1}) is delivered by rivers to the coastal ocean as dissolved inorganic carbon, dissolved organic carbon and particulate organic carbon (Tranvik et al., 2009). Atmospheric CO_2 is exchanged with the surface ocean through gas exchange. This exchange flux is driven by the partial CO_2 pressure difference between the air and the sea. The total amount of carbon in the oceans account about 40 000 PgC (Hansell et al. 2009). Note there is an additional amount of in permafrost soils of about 1700 PgC (Tarnocai et al. 2009). Fossil fuels and deforestation are the main sources of anthropogenic CO_2 emissions accounting respectively for 7.8 PgC yr-1 (GEA 2006) and 1.1 PgC yr-1 (Pan et al. 2011).

2. Carbon stocks and forests

Worldwide forests cover about 42 millions of km² across tropical, temperate and boreal regions, corresponding to about 30 % of the total land surface (Bonan 2008). Besides numerous and various services provided to the society, forests play an important role in the global carbon cycle (Bonan 2008, van der Werf et al. 2009, Pan et al. 2011). Pan and colleagues (2011) have estimated that forests store in average about 861± 66 Pg C, with 383 ± 30 Pg C (44 %) in soil, 363 ± 28 Pg C (42 %) in live biomass, 73 ± 6 Pg (8 %) in deadwood and 43 ± 6 Pg C (5 %) in litter.

Most of the carbon stocks are found in the tropics, i.e. 55 % of the total (Figure 0-5A), while boreal and temperate forests contain respectively 32 % and 14 % of the total. On the other hand, carbon density (MgC ha^{-1}) are present in same amounts in tropical and boreal forests, i.e. 240 MgC ha^{-1}; while temperate forests only contain 155 MgC ha^{-1}. An important difference between boreal and tropical forests concerns the distribution of the stocks through the different carbon pools; tropical forests have most of their carbon stored in the living biomass (56 %), i.e. the aboveground part of the trees and their roots, while boreal forest have the most in the soil (60 %).

Although the differences in forest carbon sinks appear consistent since the 1990's, contrasted dynamics are observed in the different biomes. While the sinks in temperate forests increased by 17 %, tropical sinks decreased by 23 % between 1990 and 2007 (Figure-0 5B). The dynamics are also slightly different between the tropical regions: for example, the gross deforestation of tropical intact forests is clearly more important in South Asia than in the other tropical biomes (Figure-0 5D). In Africa, forests exhibit lower rates of deforestation than other continents (CBFP 2012). Indeed, the current clearing is still generally very localized and is often associated with shifting agricultural activities (CBFP 2012).

These numbers shed light on the particular case of tropical forests: while storing most of the world forest carbon, they are the only one undergoing a net deforestation.

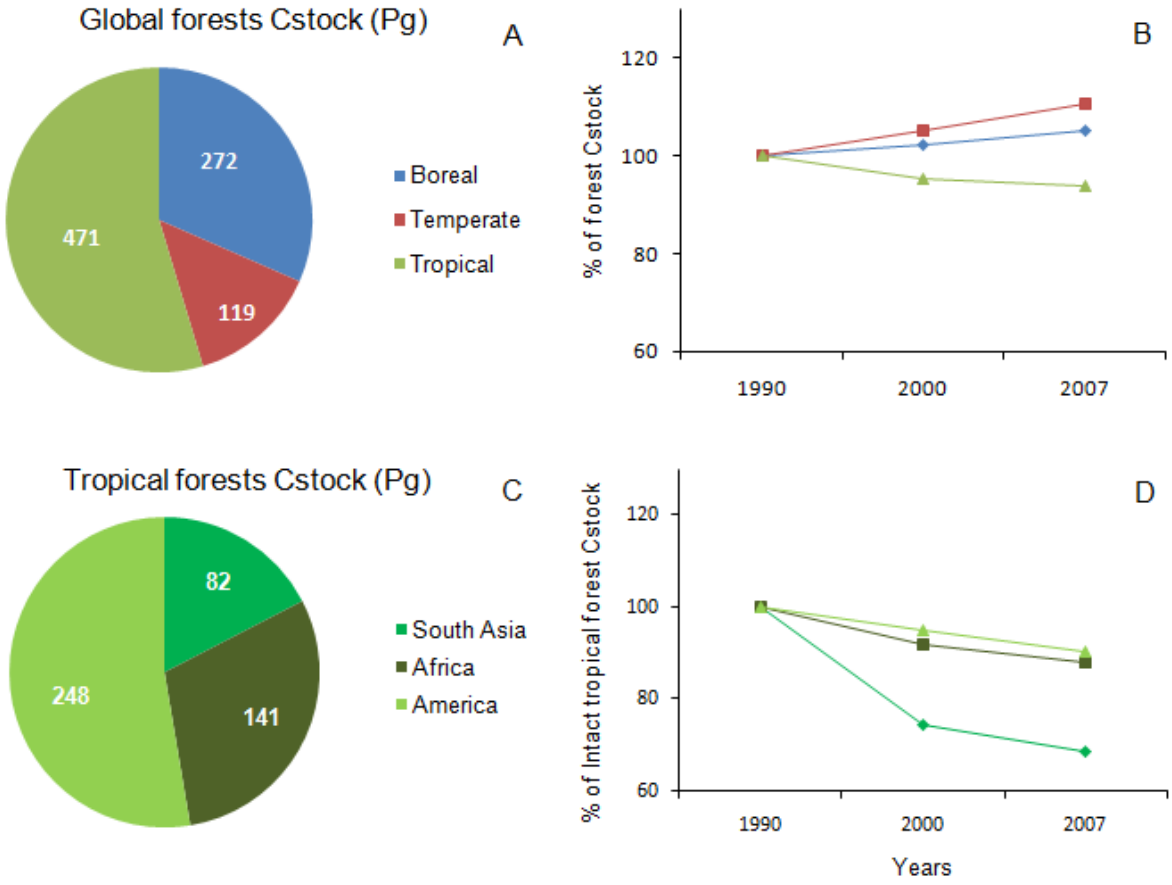

Figure 0-5.Carbon stocks of world and tropical forests. Distribution of Carbon stocks in world's forests in 2007 (A, C). Evolution of the percentage of forest carbon stocks in world forest (B) and in tropical forest (D) using 1990's at the reference level. The figure is inspired from Pan et al. (2011).

According to the last technical report of the Intergovernmental Panel on Climate Change (IPCC 2013), tropical gross deforestation is between 0.9 PgC year^{-1}(Harris et al. 2012) and 2.9 PgC year^{-1}(Pan et al. 2011). The difference between the two estimations lies in the use of different methodologies. Pan et al. (2011) based their estimations on field permanent plots (mainly from Food and Agriculture Organization - FAO) and on a bookkeeping model (based field recording on permanent plots) for the characterization of land-use change. They further extrapolated a mean value at the regional scale. Harris et al. (2012) built a world map from field plots and the use of satellite imagery to identify land-use change dynamics. If the second has the advantage of being spatially explicit (characterizing from the deforestation, the degradation and the regrowth dynamics from satellite) and more transparent, it does not mean the result is more accurate when considering carbon stocks dynamics; since carbon

stocks are not homogeneously distributed within and between the different forest types. Therefore, depending on the forest types accounted, conclusions on forests cover and on forest loss may greatly vary. This is illustrated on Figure 0-6 which represents different scenarios of forest type aggregation in the Katanga province of the Democratic Republic of the Congo (Bastin et al. 2011). The variation of forest cover between the different scenarios emphasize conclusion of deforestation and carbon loss as to be handled with caution and with a particular care on the forest types accounted.

In the following section, I remind briefly the main steps that led the countries from the world to face the climate change issue, from the creation of the Intergovernmental Panel on Climate Change (IPCC) to the potential valorization of forest lands in developing countries.

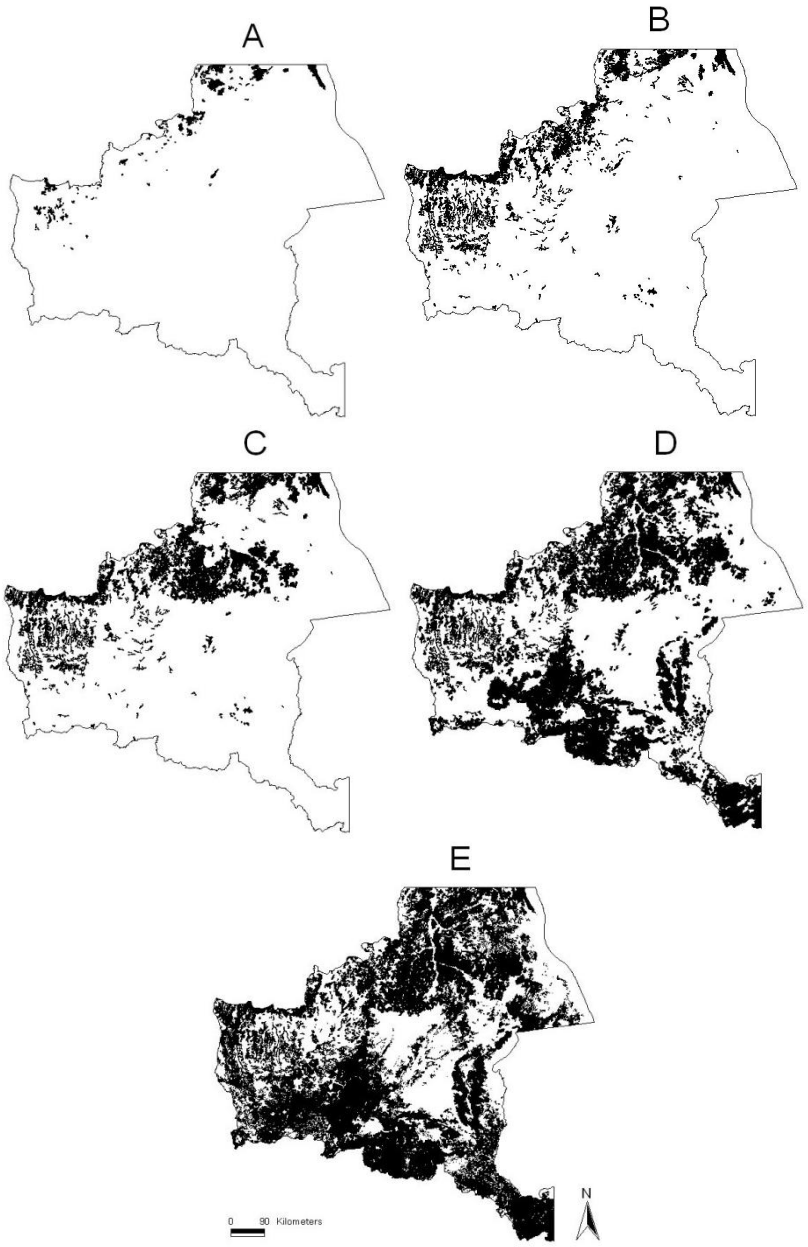

Figure 0-6. Illustration of five scenarios of forest cover in Katanga province (Democratic Republic of the Congo), considering the combination of five different forest types. A: Dense rainforest; B: A + Edaphic forests; C: B + secondary forests; D: C + woodlands; E: D+ savannah woodlands. Map based on Lagmouch and Hardy (2008).

3. The intergovernmental Panel on Climate Change

The Intergovernmental Panel on Climate Change (IPCC) was created in 1988 by the World Meteorological Organization (WMO) and the United Nations Environment Program (UNEP) in order to assess the evolution of climate. In 1992, during the 'Earth Summit' organized in Rio, participating countries started to realize the importance of climate change and its potential consequences. One hundred ninety two world's nations adopted the international treaty that led to the formation of the United Nation Framework Convention on Climate Change (UNFCCC). This formal treaty led to the creation of a legally binding instrument in 1997, known as the 'Kyoto Protocol' (KP), which was ratified by 184 countries. With the KP, 37 industrialized countries and the European Community committed in a first commitment to reduce their emissions of GHG by an average of 5 % by 2012 against 1990 levels. The KP's first commitment period started in 2008 and ended in 2012. Several countries decided to withdraw from the protocol to avoid any financial penalties (e.g. United States of America, Canada, Japan ...), but others performed better than expected: the 15 EU countries that ratified originally the KP present together emissions below 14.9 % against 1990 levels. The second commitment period started in Doha in 2012. Parties are now committed to reduce emissions by at least 18 percent below 1990 levels in the eight-year period from 2013 to 2020, and to investigate new options to reduce emissions from anthropogenic sources.

4. The REDD+ program

The negotiations and the investigations on the options to mitigate climate change began in 2005 in the context of UNFCCC. They started to consider the forest lands in developing countries as a possible key mechanism to reduce the climate change. The most significant decision has been taken in 2009 during the 15th meeting of the Conference of the Parties (COP) in Copenhagen: an agreement was found on 'Reduced Emissions from Deforestation and Forest Degradation and the role of conservation, sustainable management of forests and enhancement of forest carbon stocks', or in short REDD+ (Decision 4/CP.15). This is the first international agreement of this kind, including forests and tropical forests in particular, which aim to favor developing countries economy while

conserving most of their forest resources. In particular, the REDD+ program aims to create a new financial incentive for developing countries by valorizing forest resources conservation through the carbon market. Participating countries will have to establish two points (1) a Reference Level and/or Reference Emission Level (RL/REL) and (2) a national forest monitoring system to support the Measurement, Reporting and Verification (MRV) function of the Convention. The present work is entirely dedicated to this second point.

INTRODUCTION

PART 2: ABOVEGROUND BIOMASS ESTIMATES

1. The aboveground biomass of the tree

In this section, we first remind the origins of tree biomass measurements in the tropics and focus on the main recent improvements, particularly considering the case of Africa. We will further provide more details on the Wood Specific Gravity (WSG), which is the focus of the third paper.

1.1. The need of standard approach in the tropics

Originally, one of the main issue in tropical forest AGB assessment was the lack of standard models, hereafter referenced as 'allometric model', enabling to convert tree measurements into AGB estimates (Chave et al. 2005). In temperate regions, mono-species allometric models are generally used to estimate forest AGB (e.g. Brown and Schroeder 1999). However, the transposition of such model to the tropics is difficult to apply considering the diversity of tree species in such forests, they account as many as 300 different species on 1-ha in South America and as many as 100 on 1-ha in Africa (Phillips et al. 1994, Turner 2001). Therefore, mixed-species models are generally preferred (e.g. Brown 1997, see Table 1).

However, the first mixed-species models developed present large uncertainties and low consistency between sites because they are generally site-dependent and based on a small number of harvested trees (Chave et al. 2005). This has led to an important source of bias in AGB assessment of the forests until now (Brown 1997, Clark and Clark 2000, Houghton et al. 2001, Chave et al. 2004). Moreover, the selection of the most appropriated model is a problematic step, due to the multiplicity of their mathematical formulations. While the three main variables to consider (the diameter at 130 cm - DBH, the total height - H, the wood specific gravity - WSG) constitute a consensus since a long time (e.g. Schumacher and Hall 1933), their implementation in allometric models presents various options (e.g. linear, power, exponential). Generally the best formulation is selected according to model selection criteria (goodness of fit, AIC, ...) but rarely according to the principle of parsimony (Burnham and Anderson 2002), which stipulates that the quality of a fit should depend on the model complexity – as measured by the number of parameter in a model, and consequently leads to the selection of complex models. Moreover, considering the difficulties related to H and WSG field

measurements, simple allometric model have been built (e.g. Brown 1997) by assuming a power-law relationship between the logarithm of tree diameter and the logarithm of its height (Niklas 1995), and a mean WSG value for tropical trees of 0.64 g/cm³ (Chave et al. 2004). By doing this, the number of variables involved can be reduced to one data easy to collect : the DBH. However, such models will generally lead to important errors when applied outside the training area (with over- or under-estimation superior to 25 % according to Mitchard and colleagues 2014).

1.2. The main advance: Chave 2005

In 1997, Sandra Brown from the FAO developed the first main contribution to the standardization of the AGB estimations (Table 1). Based on 371 harvested trees (DBH ≥ 5 cm), she was the first to propose three simple models, only requiring the measurement of diameter at breast height (DBH), and this for three forest types defined according to their precipitations regimes (i.e. Wet forest: > 4000 mm $year^{-1}$, no dry season; moist forest: between 1500 and 4000 mm $year^{-1}$, short dry season; dry forest: < 1500mm $year^{-1}$, several months of dry season). The following and main advance in the field was delivered by Chave and colleagues in 2005. Based on an unprecedented database, i.e. counting 2410 harvested trees (DBH ≥ 5 cm) from tropical America and tropical Asia, they significantly improve pan-tropical mixed-species model accuracy. Two sets of models were developed, one including the measurement of tree height (model I) and one without it (model II). The models always performed better when the three parameters were considered (Chave et al. 2005). For each set, they developed both one global model and one model per forest type (Table 1). Forest types were also defined according to the precipitation regimes, with slight differences when comparing to Sandra Brown's definitions (i.e. Wet forest : > 3500 mm $year^{-1}$, no dry season; Moist forest: between 1500 and 3500 mm $year^{-1}$, between 1 and 4 months of dry season; Dry forest: < 1500mm $year^{-1}$, + 5 months of dry season).

Chave's best model presented a maximum of 20 % of error in AGB estimates, with variables ranked by decreasing importance being: the DBH, the WSG and H.

Interestingly, Chave and collaborators (2005) showed that the inclusion of a continental-effect didn't help to improve models accuracy. This conservation of tree allometry across sites and, since no species are shared between the sites, proved that this character is conserved across the phylogeny of self-supporting trees. As a consequence, this result suggested Chave's models should perform well even in non-sampled areas such as tropical Africa. Yet, since no trees were harvested in Africa for his study, it remained the main issue discussed in the literature in the recent years (Gibbs et al. 2007).

1.3. From Chave 2005 to Chave 2014

The paper of Chave and colleagues (2005) combined to the emergence of the REDD+ program led to a profusion of researches on local allometries in different regions of the African continent (e.g. Henry et al. 2010, Djomo et al. 2010, Vieilledent et al. 2012, Fayolle et al. 2013, Ngomanda et al. 2014). Each paper published a set of local allometric models and compared them to the most cited pan-tropical models, i.e. Brown (1997) and Chave et al. (2005). In each investigated case, local models performed better than pan-tropical models, which is not surprising considering the specificity of each dataset (few sampled trees, few species). However, all the studies performed in Africa, except the one performed by Ngomanda et al (2014), confirmed the validity of Chave's model. Indeed, when including all the variables (i.e. model I), Henry et al. (2010) obtained no significant bias using the model for the proper forest type, Djomo et al. (2010) obtained an average error of 20 % (similar to the error mentioned in Chave et al. 2005); Vieilledent et al. (2012) noted a bias inferior to 6 %. Using the two most important variables (DBH, WSG), Fayolle et. al (2013) obtained no significant bias either. Only Ngomanda et al. (2014) obtained an important overestimation when using Chave's model (~40 %). Despite being the only case questioning the accuracy of Chave's model for Africa, this overestimation underlined the need of further investigations on African tree allometries.

Binding these new datasets on Africa to the previous database and adding new ones from other tropical regions), Chave and colleagues (2014) built a single pan-tropical mixed-species model based on a total of 4004 harvested trees (Chave et al. 2014). When all the variables are available (DBH, H, WSG), the single model held across all the tropical regions without any effect from the region or from

the environment. This model was also very close to the model for moist forests (model I) which was developed in 2005. This (1) underlined the quality of the former study and (2) confirmed the conservation of the allometry across the whole tropical phylogeny of self-supporting trees.

Furthermore, Chave and colleagues addressed, in their paper of 2014, a particular attention to recent considerations about DBH:H relationship. This relationship have been shown to vary between the tropical regions (Feldpausch et al. 2011, Banin et al. 2012). Here, Chave and colleagues (2014) showed that the DBH:H relationship linearly depends on a bioclimatic stress factor combining temperature variability, precipitations variability and drought intensity. As a consequence, accounting for bioclimatic parameters when total height is not measured outperforms significantly all the previous models developed without height (e.g. Chave 2005 model ll). Chave and colleagues (2014) however recommended to use local DBH:H allometries prior than the estimation of height from bioclimatic parameters.

1.4. The case of wood density

WSG is the second most important predictor of the AGB of a tree, after DBH (Chave et al. 2005, 2014). WSG ranges from 0.08 to 1.39 $g.cm^{-3}$ among tropical tree species (Zanne et al. 2009) and is strongly conserved across the phylogeny (Slik 2006, Chave et al. 2006): a nested analysis performed on 2456 Amazonian species showed that 74 % of WSG variance is explained by the genus, 34 % by the family and 19 % by the order (Chave et al. 2006). This finding offered the possibility to use the genus average instead of species-specific values when there are no data available on the species(Baker et al. 2004, Slik 2006).

Due to difficulties related to field measurements, WSG has often been extracted from global database (Zanne et al. 2009) and then merged with species inventory records. As a consequence, the potential variation of WSG within a given species or even within a tree has been completely neglected. Hence, potential large intra-individual and intra-species radial and vertical variation of WSG are reported in the literature (e.g. Wiemann and Williamson 1988, Fearnside 1997, Woodcock and Shier 2002, Nock et al. 2009, Hietz et al. 2013, Osazuwa-Peters et al. 2014). The most striking

results were found for gap-pioneer species, exhibiting a radial WSG variation that could reach 200 to 300 % from pith-to-bark (Wiemann and Williamson 1988). In addition, the potential local or global environmental impact on WSG has never been controlled, such as climate and soil fertility (Baker et al. 2004, Muller-Landau 2004, Gourlet-Fleury et al. 2011).

Consequently, the use of WSG from global database is one of the main problem often mentioned in potential error of AGB estimations (Maniatis et al. 2011a, Clark and Kellner 2012). However, some interesting results have recently emerged, emphasizing the stability of the mean WSG among species, between measured WSG and tabulated WSG. Fayolle and colleagues(2013) showed the mean WSG measured from harvested trees are strongly correlated to WSG measured from global databases (e.g. Zanne et al. 2009).

Contradictory information also resulted from the literature. Whether or not we must account for the different sources of WSG variations is still then not clear. It thus requires further investigations to better understand the stability of WSG variations and its potential consequences on the estimation of the AGB of a tree. This is the main focus of paper 3.

Table 0- 1. Pan-tropical allometric models developed recently to predict the AGB of the tree. Forest types are defined considering the precipitation regime. D is the diameter at breast height (130cm), BA is the basal area (m^2/ha), H is the total height and WSG is the wood specific gravity (oven-dry mass divided by the green volume). E is the bioclimatic index resulting from: TS is the temperature seasonality, PS is the precipitation seasonality and CWD is the maximum climatological water deficit.

Ref	Forest type	Equation formulation	Parameters
Brown 1997	dry	<AGB> =10^[-0.535+log10 (BA)]	[D]
	moist	<AGB> = 42.69-12.800(D)+1.242(D^2)	[D]
	wet	<AGB> = 21.297-6.953(D)+0.740(D^2)	[D]
Chave 2005	dry	<AGB> = 0.112 (WSG D^2 H)^(0.916)	[D, H, WSG]
	moist	<AGB> = 0.0509 * (WSG D^2 H)	[D, H, WSG]
	wet	<AGB> = 0.0776 (WSG D^2 H)^(0.940)	[D, H, WSG]
	dry	<AGB> = WSG * exp[(−0.667 + 1.784(D)+ 0.207$(\ln(D))^2$- 0.0281$(\ln(D))^3$]	[D, WSG]
	moist	<AGB> = WSG * exp[(−1,499 + 2,148(D)+ 0.207$(\ln(D))^2$ - 0.0281$(\ln(D))^3$]	[D, WSG]
	wet	<AGB> = WSG * exp[(−1,239 + 1.980(D)+ 0.207$(\ln(D))^2$ - 0.0281$(\ln(D))^3$]	[D, WSG]
Chave 2014	all	<AGB> = 0.0559 (WSG D^2H)	[D, H, WSG]
	all	<AGB> = 0.0673 (WSG D^2H)^(0.976)	[D, H, WSG]
	all	<AGB> = exp[(−1.803− 0.976E + 0.976ln(WSG)+ 2.673ln(D)− 0.0299$(\ln(D))^2$]	[D, WSG]
		ln(H) = 0.893− E + 0.760ln(D)− 0.0340$(\ln(D))^2$	*Bioclim*
		E = ((0.178) (TS-0.938) (CWD-6.61) (PS))×10−3	*Bioclim*

2. The aboveground biomass of the forest

In this section, we first present the main points to consider when selecting an allometric model to estimate the AGB of a given forest. We further explain the main sources of errors in forest AGB assessment resulting from field plot design.

2.1. The choice of allometry

As detailed before, the selection of the appropriate allometric model is the major potential source of errors when estimating the AGB of a given forest on the ground (Chave et al. 2005, 2014, Clark and Kellner 2012). According to the IPPC guidelines (IPCC 2006) and to the recommendations from the literature, we should select the allometric model, depending on data available, in the following order of preference, using :

i. A local model (with local harvested trees)
ii. A pan-tropical model (with DBH, H and WSG measurements)
iii. A pan-tropical model (with DBH, WSG and a local DBH:H allometry developed on subsamples)
iv. A pan-tropical model (with DBH, WSG and bioclimatic factors sensu Chave et al. (2014))
v. A pan-tropical model only based on DBH and WSG
vi. A pan-tropical model only based on DBH

Today, thanks to the development of the global WSG database (Zanne et al. 2009) and the better understanding of WSG variations the option (vi) can be easily outperformed.

The transition from level (v) to level (ii) mainly relies on our capacities to measure and to estimate the tree height on the field. Chave and colleagues (2014) suggested that the best method to measure tree height without felling the tree would be to climb to the bole and to use a laser rangefinder with decimetric accuracy. However, such method is difficult to apply systematically on the field. The parsimonious use of hypsometers, with multiple measurements and combined with calibration cross-check operations is thus advised (Chave et al. 2014). Also, many uncertainties remain between level (ii) and level (iii). In order to illustrate them, we fitted DBH:H relationships, using an exponential 3-

parameters regression model (Banin et al. 2012), and plotted the results for two contrasted species we investigated during our field work : *Staudtia kamerunensis* and *Klainedoxa gabonensis* (Figure 0-7). The figure enables to compare the estimation of H by using a multi-species study-site DBH:H allometry (black dotted line; i.e., level iii), a species-specific DBH:H allometry (colored lines; a situation between level iii and level ii) or by directly measuring the height with an hypsometer (colored points; i.e., level ii). The differences between the asymptotes of the regression and the spread of the points illustrate well the differences of precision between level (iii) and level (ii). For example, *Klainedoxa gabonensis* can reach 50 m but the asymptote is fixed at 40 m.

If the transition from level (vi) to level (ii) is workable, the transition from level (ii) to level (i) is clearly more difficult. The corresponding cost and the required logistical supports are generally too important (Gibbs et al. 2007).

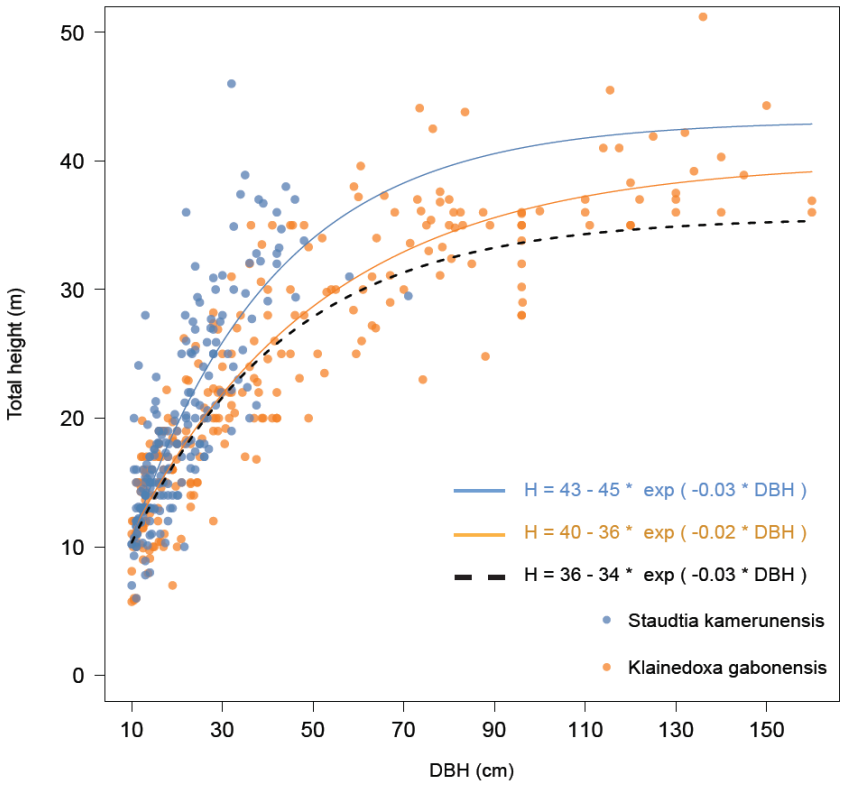

Figure 0- 7. DBH:H allometry of contrasted species measured in the Malebo study site of the Democratic Republic of the Congo. *Staudtia kamerunensis* (blue) and *Klainedoxa gabonensis* (orange). The continuous curves represent the fitted exponential 3-parameters regressions for both species. The dotted curves represent the fitted 3-parameters exponential regression for all the trees measured in the Malebo study site.

2.2. The sampling design

Sampling a forest to estimate its AGB requires the establishment of a sampling design, for which two major concerns are addressed in the literature : (i) the position of the plot and (ii) the size of the plot (Clark and Clark 2000, Chave et al. 2004, Patenaude et al. 2005, Gibbs et al. 2007, Picard and Gourlet-Fleury 2008, Clark and Kellner 2012, Réjou-Méchain et al. 2014).

Due to the heterogeneity of AGB distribution within a tropical forest, the average AGB of the sampled plots is not used to estimate the mean AGB of a whole region: plots are generally used to calibrate and validate AGB prediction from remote-sensing products. Therefore, in order to establish the plots at appropriated locations, it is required to stratify the area according to the forest types (Gibbs et al. 2007) but especially considering their integration in remote-sensing based approaches (Clark and Kellner 2012). Within each forest types (defined during the stratification) of a given landscape, at least 5-ha are recommended to be sampled to properly assess AGB (Picard and Gourlet-Fleury 2008). Similarly, Baraloto and collaborators (2013) showed, based on the investigation of 6 tropical forests of South-America, that the sampling of at least 5-ha enables to keep the coefficient of variation of the AGB estimate (CV_{AGB}) consistently below 10 %. The CV_{AGB} is defined as a normalized measured of the AGB dispersion between plots, and a low CV_{AGB} allows to detect the significant differences between forest-stands (Hall et al. 1998), i.e. without any bias due too small sample size.

Subsequently, the decision about the number and the size of the plots will depend on several aspects: the AGB variance (Chave et al. 2004), the cost (Baraloto et al. 2013) and the interaction with remote-sensing signals (Mascaro et al. 2011, Réjou-Méchain et al. 2014).

2.2.1. AGB variance

Forest AGB variance within a given landscape is strongly correlated to the size of the plot (Chave et al. 2004). Chave and colleagues (2004) showed that the decrease of CV_{AGB} is correlated with the increase of the plot size. In order to define an adequate minimal size of plots which minimizes CV_{AGB}, they performed a normality test of AGB distribution, the same way Clark and Clark realized in Costa

Rica (2000). The smallest plot size satisfying the normality criterion was the same in both studies and exhibited an area of 0.25-ha (Clark and Clark 2000, Chave et al. 2004). Similarly, Wagner and colleagues (2010) underlined for French Guyana forests the CV_{AGB} was always below 20 % as long as 1-ha plot is sampled. These different findings argue in favor of a minimal plot size between 0.25 and 1 ha, with a total area sampled of each forest stratum of 5-ha. Nonetheless, we should bear in mind that these results are strongly correlated to forest locations (Chave et al. 2004), which suggests further analyses should be conducted in other tropical regions to fully understand the correlation between CV_{AGB} and plot size.

2.2.2. Sampling cost

When drawing the field sampling design, we have to gauge between sampling cost effort and the representativeness of forest types or forest strata (Picard and Gourlet-Fleury 2008). Such sampling cost is difficult to assess and has been poorly investigated until now. A first interesting attempt has recently been realized by Baraloto and collaborators (2013). They did not consider the logistical costs in relation to the number of investigated locations but they calculated a sampling effort in terms of 'persons per day' for various designs. They also compared the effort of each design for equivalent level of CV_{AGB}. Their results showed (i) that the effort relies on the specificity of the forest, since different 'persons per day' were attributed for equivalent sampled areas in different locations and (ii) that plots of 0.5-ha and 1-ha always presented smaller cost than plots of 0.1 ha. These are interesting information, but from my personal experience (32 plots of 1-ha), I would suggest that we should also consider the spread of the plot locations in costs evaluations. These considerations will undoubtedly require further investigations, and this especially in the framework of the REDD+ program, for which numerous field datasets are needed to implement the MRV.

2.2.3. Field sampling and remote-sensing

The remote-sensing methods developed for predicting and mapping forest AGB are based on a field calibration. Therefore, the quality AGB maps relies on the capacity of the field plots to intercept the AGB of entire pixels (Réjou-Méchain et al. 2014). Hence, in most studies the footprint of space-borne

remote-sensing products largely exceeds the size of the field plots used for the calibration (Baccini et al. 2007). Consequently, the level of uncertainties depends on the heterogeneity of the forest, which is often important in the tropics (Hallé et al. 1978, Turner 2001). For example, Mascaro and collaborators (2011) showed, in tropical forests in Panama, that we need to establish 1-ha plots in order to present error in AGB estimations below 10 % when using LiDAR airborne remote-sensing products presenting a footprint of 0.36 ha.

Furthermore, several errors resulting from remote-sensing specificities have to be considered. These main issues have recently been identified and quantified by Réjou-Méchain and colleagues (2014). They particularly investigated the geo-localization errors, the post-geoprocessing conversion of the ellipsoidal footprint into a square pixel and the difference between the object measured from space and on the ground (canopy vs. trunk). Their results show plots of 0.1-ha and plots of 1-ha lead respectively to 46.3 % and 16.6 % of spatial sampling error in AGB due to geo-localization problems. Moreover, they found that when field calibration plots are smaller than the pixel resolution, the local heterogeneity in AGB leads to a substantial bias that cannot be removed with current statistical methods.

In the end, they draw attention of the impact of topography on geo-localization issues, urging the need to explicitly take it into account for future sampling strategies.

3. Mapping aboveground biomass

Given the extent of tropical forests, access limitations and structural complexity (Hallé et al. 1978, Turner 2001, Gibbs et al. 2007), remote sensing methods are long seen as crucial tools for assessing tropical forest AGB (Patenaude et al. 2005, DeFries et al. 2007). No remote-sensing instrument may directly measure the AGB of the forests. Space- and air-borne products measure various properties of forest canopy (radiance, texture, canopy height profile), which are subsequently used as potential predictors of forest AGB. As a consequence, all techniques still require ground estimations of AGB for calibration and validation of the metrics resulting from remote-sensing products.

Remote-sensing is powerful in predicting forest AGB of boreal, temperate and even-aged forests (e.g. Lefsky et al. 2001, Drake et al. 2003, Zheng et al. 2004). However, inferring AGB in tropical forests is much more challenging due to the complexity and the density of the forest stands (Hallé et al. 1978, Turner 2001, Lu 2006, Gibbs et al. 2007). The first tests performed on AGB estimations in the tropics were rapidly confronted to a saturation issue at about 250 $Mgha^{-1}$(Imhoff 1995, Mougin et al. 1999) whereas African tropical forests have been shown to reach up to 700 $Mgha^{-1}$(Lewis et al. 2013). This problem has encouraged the development of various and new methods, both regarding passive (optical – spectral properties; only receiving a signal) and active (RADAR, LiDAR – three dimensional structure; receiving and emitting a signal) remote-sensing signals. Each product presents advantages and disadvantages (spatial extent, pixel resolution, spectral resolution, time resolution, and sensitivity to clouds); both techniques are thus often used jointly in order to fill each other weaknesses, and this especially to produce regional maps. This is actually the 'state of the art' maps that have recently been developed by Saatchi and collaborators (2011) and Baccini and collaborators (2012).

In this section, I will briefly remind the functioning of the main signal types in remote-sensing. I will further focus on the ‘state of the art’ AGB maps and discuss their main weaknesses. I will finally introduce one of the main promising techniques on the processing of VHR optical imagery, i.e. the Fourier Textural Ordination (FOTO), which is the focus of paper 1.

3.1. The main products in remote-sensing

3.1.1. Optical

Optical remote-sensing is defined as a passive technique where space- and air-borne sensors intercept the solar energy reflected from Earth's surface (Lu 2006). The intercepted spectral range is generally comprised between 0.4 and 2.5 µm and often dissects the reflectance of the visible, the near, the middle and the far infrared. Optical remote-sensing provides the opportunity to work with a variety of products presenting varying pixel spatial resolutions (coarse > 250 m; medium ~ 30-100 m; fine < 1 m). The most known optical satellites are MODIS (coarse), Landsat (medium), Spot (medium), Quickbird (fine) and Ikonos (fine).

Optical datasets present the advantage to cover large extents, and to easily gather repeated measurements since the launch-date of the satellites. But, contrariwise to actives sensors (RADAR, LiDAR, detailed hereafter), all satellite images are very sensitive to the acquisition conditions, i.e. the cloud cover, the atmospheric and the radiometric effects (e.g., sun-scene-sensor angles and corresponding illumination conditions). Except from the cloud cover, the other problems can usually be overcome. For instance, interactions with atmosphere can be corrected through the use of a modified dark object subtraction technique (Chavez 1996); radiometric effect such as BRDF (Bidirectional Reflectance Distribution Function) can be partly filtered through the use of specific algorithm (e.g. Vermote et al. 2002).

One of the main attempt initially performed to assess forest AGB from optical datasets is the use of vegetation indices in 'neural network' processing (Foody et al. 2001). This network corresponds to a complex optimization of multiple linear regressions which yields the best estimate of AGB but which is based on calibration from ground measurements. Consequently, the resulting coefficients are generally site-specific and cannot be transposed or interpreted biologically.

Today, the improvement of VHR images processing from optical remote-sensing have enable to develop promising techniques to predict forest AGB. This is detailed in a specific section on the Fourier Textural Ordination method.

3.1.2. RADAR

Originally, Synthetic Aperture Radars (SARs) were developed for military purpose (in the 1960's) but, it is now often used to characterize the forest cover. They constitute active sensors (i.e. they transmit and receive their own signal) in the microwave part of the electromagnetic spectrum. The wavelengths of SARs are commonly represented as 'bands', with L and P-bands for long wavelengths (20 – 80 cm) and with C- and X-bands for short wavelengths (3-5 cm).

Basically, SAR maps a 'portion of energy' which is re-emitted from the targeted object (the forest) to the sensor receiver. The measure of this 'portion of energy' is called the backscatter. When the forest is aimed, the backscatter can be decomposed as follows: a double bounce for trunk-ground interaction, a rough surface scattering from the ground and a volume scattering from the canopy (Balzter et al. 2007). As forests with different structures will induce differences in each component of the backscatter, SARs present the potential to directly quantify variations in vegetation volumes. We can thus use it to predict variations of AGB between the different forests.

The particular advantage of SARs in the tropics is that they are much less affected by the cloud cover than optical or LiDAR sensors (Lu 2006). On the other hand, the main limit concerns the above-mentioned saturation issue, which often occurs with the L- and the P-bands for SARs systems (Zolkos et al. 2013). Typically, in the tropics, the signal of these bands saturates for AGB of about 150-200 $Mgha^{-1}$ (Mitchard et al. 2012). This has encouraged the development of alternative products to predict AGB (i.e. the LiDAR), but SARs datasets remained very useful in the evaluation of forested area variations.

Nonetheless, promising development were recently shown with the combination of polarimetric and interferometric synthetic aperture radar (Pol-InSAR) which has the potential to estimate biomass at higher densities (Goetz and Dubayah 2011). These may offer new opportunities in the upcoming years.

3.1.3. LiDAR

Like SARs systems, Light Detection And Ranging (LiDAR) is based on the active sensing of Earth's surface, with the emission and reception of near-infrared wavelengths. Like SARs systems, the energy emitted is capable of penetrating through forest canopies down to the ground surface. The defining characteristics of LiDAR systems are related to the width of the laser beam (small footprint or large footprint) and the way in which the reflected laser energy is digitized (Dubayah and Drake 2000).

Large footprint LiDAR presents a ground resolution of 5 m of diameter when processed from aircraft but presents much larger footprint when processed from satellite. For instance, the Geoscience Laser Altimetry System (GLAS) presents a footprint of about 65 m. This presents the advantage to correspond well to the data used to develop regional 'state of the art' AGB maps (e.g. Saatchi et al. 2011, Baccini et al. 2012) which are discussed in the further section.

Small footprints LiDAR illuminates a surface area of about 50 cm (or less) of diameter and are always processed from aircraft. When forests are scanned with small footprint systems, the received signal can be translated into various forest structure metrics such as maximum canopy height and multi-strata heights above ground. This provides the opportunity to reconstruct precisely the vertical structure of the forest. However, despite promising results in tropical forests with low AGB levels (~ 100 Mg/ha), biomass prediction models from single LiDAR metrics generally exceed the 20 % of relative residual standard error (RSE(%)) recommended by the MRV guidelines (Houghton et al. 2009, Zolkos et al. 2013). Also, they only cover small extents (tens of km²) and depend on the consistency of DBH-H allometries. In addition, LiDAR-based forest canopy metrics used to predict AGB, such as the mean forest height profiles (Mascaro et al. 2011), do not consider an important share of the horizontal structure of the forest stands, i.e. regarding the variations of crown size and shape in the canopy layer (Hallé et al. 1978, Barbier et al. 2010).

3.2. 'State of the art' global AGB maps

As two maps are mainly cited in the literature (i.e. Saatchi et al. (2011) and Baccini et al. (2012)), here we present the two methods by comparing them to each other and to field dataset. Maps comparison is based on the excellent review of Mitchard and colleagues (2013) and the comparison to field dataset is based on the work of Mitchard and colleagues (2014).

The maps of Saatchi (map1) and Baccini (map2) both follow a similar workflow (Figure 0-7). They both (i) used space-borne datasets from GLAS satellite, (ii) used ground AGB estimates to predict forest AGB on all the GLAS footprints and (iii) fused these predictions with other remote-sensing products (MODIS, elevations models, ...) to extrapolate their prediction at a global scale.

However, some important differences exist between the two workflows:

- For map1, they first calculated a forest canopy metric and predicted AGB variation in a second stage while in map2 they used raw GLAS signals to predict directly AGB variations;
- In map1, they estimated field AGB based on 3 parameters (DBH,H,WSG) while in map2 they only used two parameters (DBH, WSG);
- They extracted different vegetation indices from MODIS and implemented different extrapolation models for the two maps.

Despite presenting several similarities in their development, the two maps present huge differences in AGB prediction : especially for central Amazonia, the Congo basin, the south of Papua New Guinea, the Miombo woodlands of Africa, and the dry forests and savannas of South America (Mitchard et al. 2013). The differences in AGB predictions were not systematic which makes it difficult to compare the methodological differences (Mitchard et al. 2013). Furthermore, in a new publication, Mitchard and collaborators (2014) compared each of these maps with an independent and large ground sampling design in South America. They stressed here that both maps failed to intercept the main gradient of AGB when confronted to 413 grounds plots estimations. The observed differences far exceeded the results mentioned in each of the former study (Saatchi et al. 2011, Baccini et al. 2012). Some regions were indeed over- or under-estimated by more than 25 %.

As a conclusion, mapping AGB on large scale only based on large-footprint LiDAR (~65 m) and canopy profiles estimates seem to yields inevitable large and spatially correlated errors (Mitchard et al. 2014). Therefore, new products, based on criteria able to better intercept forest community assembly specificities and complexity have to be developed.

In that framework, interesting results have recently been produced in the realm of very high spatial resolution datasets.

3.3. The Fourier Textural Ordination

The Fourier Transform Textural Ordination, hereafter called FOTO, aims at characterizing the existing gradients of canopy crown size distribution throughout the forest and is based on the spatial variation in pixel radiance observed on VHR images.

Originally developed to study geomorphology (Mugglestone and Renshaw 1998), it has been adapted to study landscape patterns in arid vegetation and canopy structure with the use of aerial photography and satellite imagery (Couteron et al. 2005, Barbier et al. 2006, Deblauwe et al. 2008). Technically, the method decomposes the spatial variation of pixel values within a given optical image extract (window) of the canopy into spatially periodic functions (sine and cosine) of varying amplitudes and frequencies to yield Fourier spectra (Figure 0-8). The algorithm used, i.e. the 2-Dimensional Fast Fourier Transform, performs a spatial decomposition of the radiometric signal of a given image window (Figure 0-8 - step1) in order to yield a set of periodic functions (Figure 0-8 - step2). The Fourier transform yields complex numbers, the squared amplitudes of which form a 2D-periodogram or r-spectrum (Figure 0-8 - step3). This r-spectrum expresses the variance partition intercepted by the periodic function at each considered frequency. R-spectrum of all windows are at the end summarized in a single table called the r-spectra table (Figure 0-8 - step4).

To summarize, the r-spectrum constitutes a simple descriptor (i.e., a set of features using image analysis wording) describing the spatial structure within the window in terms of the variance contributions of a limited number of spatial frequencies.

The FOTO method then compares the windows through the r-spectra (Figure 0-9 - step 4) using standard multivariate methods to identify the main gradients of canopy texture in the region (Proisy et al. 2007, Barbier et al. 2010, Ploton et al. 2012). Ordination scores are used as textural indices and constitute the characteristic dimensions of the FOTO analysis (Figure 0-9 - step 5).

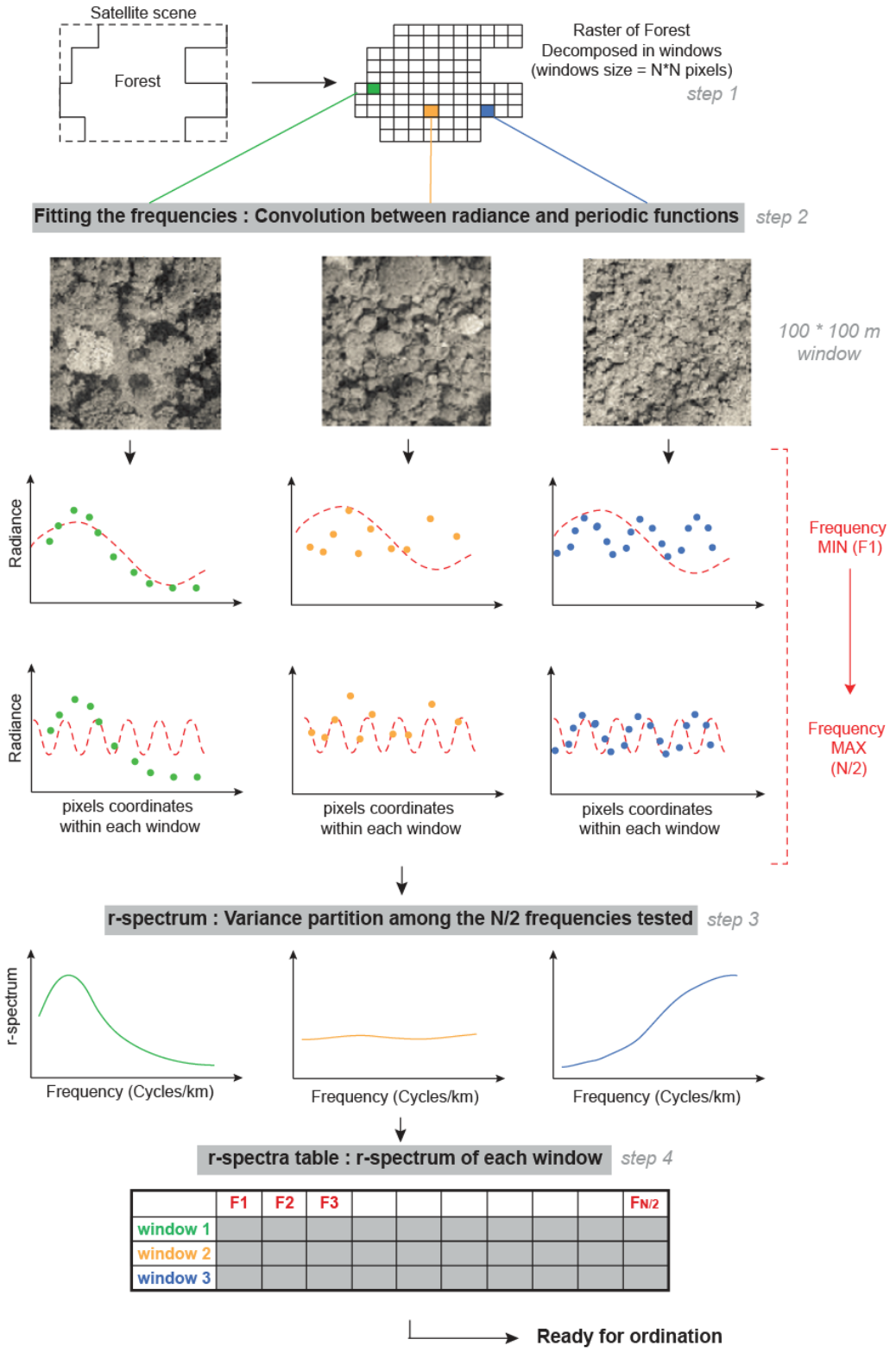

Figure 0- 8. Flowchart of the method. Step1: Fourier Textural Ordination (FOTO) of the raw satellite images (Quickbird-2 and Geoeye-1). Step2: Correction of Geoeye-1 texture r-spectra through a correspondence between the two satellite scenes calculated from the shared areas. Step3a: Ordination of the r-spectra through a PCA analysis and extraction of texture indices. Step3b: Classification of the textural class with the k-means method. Step4: Aboveground biomass (AGB) prediction model developed for each texture class, using texture indices as predictors. Step5: Cross validation of the model with a Leave-One-Out method.

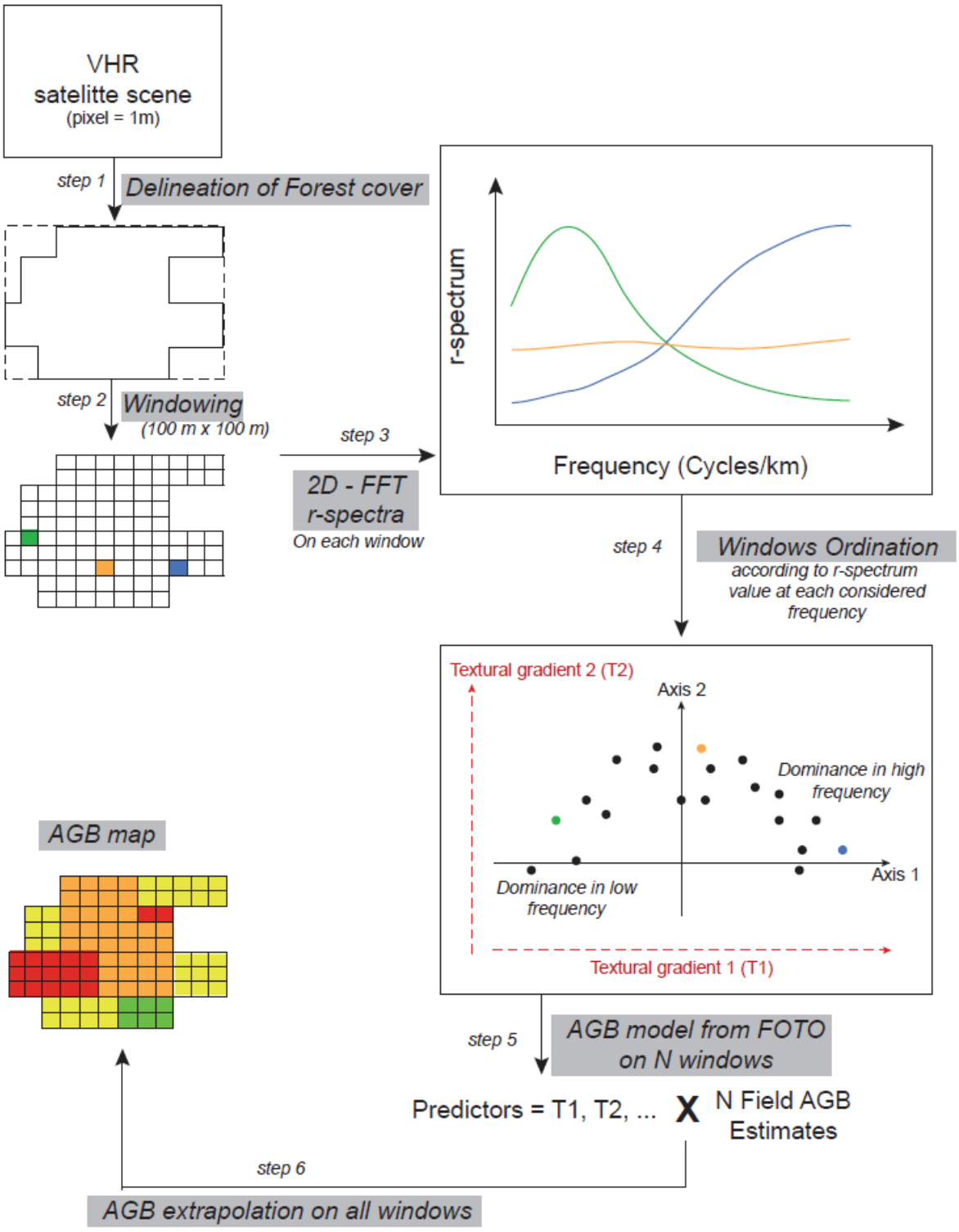

Figure 0- 9. Fourier Textural Ordination workflow. From image delineation to the production of an AGB map.

The FOTO method presents the advantage of being unsupervised and providing quantitative results that are interpretable in terms of canopy grain, canopy heterogeneity and crown size distribution. Consequently, due to the allometric relations between crown and trunk dimensions (West et al. 2009, Barbier et al. 2012, Antin et al. 2013), FOTO indices correlate well with stand structural parameters measured in the field (e.g. Couteron et al. 2005, Proisy et al. 2007, Barbier et al. 2010, Ploton et al. 2012). For instance, images of closed canopies exhibiting a stronger contribution of high spatial frequencies often correspond to the small-sized trees (early successional stages or unfavorable soils) with low forest-stand AGB, whereas low frequencies are prevalent when large trees emerge, resulting in higher AGB (Proisy et al. 2007). Interestingly, in all investigated cases, FOTO indices did not appear to saturate in stands of high AGB, even up to 500 Mg/ha (Proisy et al. 2007, Ploton et al. 2012).

In the present thesis, this method has been tested to predict the distribution of AGB in complex forest stands of Central Africa. This is the focus of paper 1.

INTRODUCTION

PART 3: CENTRAL AFRICAN FORESTS

1. Central African forests cover

Tropical forests of Central Africa present the second largest area of contiguous rainforests (from the Gulf of Guinea to the Albertine Rift) after the Amazonian Basin. They cover about 2 millions of km² (Gibbs et al. 2007, Duveiller et al. 2008). Given the high density of the river network, they present the world's largest tropical edaphic forest in the central part of the Congo Basin (CBFP 2012). Montane forests also exist in the Albertine Rift and in the west of Cameroon (i.e. foothills of Mount Cameroon, Bamenda and Bamileke highlands). The largest blocks of intact natural forests remains in the Democratic Republic of the Congo, Gabon and the Congo, with DRC holding 63 % of the total remaining forest (Laporte et al. 2007). Central African forests are estimated to hold about 8000 species of tree species (White 1983) and to store an average of 200 $MgC.ha^{-1}$ (Lewis et al. 2009, 2013).

Interestingly, while containing most of Central African intact forests, the DRC appears to be the less investigated by scientific inventories. Indeed, regarding the existing biomass inventory plots distribution recorded in the African Tropical Observation Network (AfriTRON, see Lewis et al. 2013), DRC appears to be characterized by huge “gap of knowledge” (Figure 0-10). However, considering the potential valorization of commercial forest inventory data as suggested by Maniatis et al. (2011), this gap could be rapidly filled.

2. Central African forest history and composition

Africa’s tropical forest appears as the driest of the world tropical regions, with precipitations ranging from 1600 to 2000 mm $year^{-1}$(Malhi and Wright 2004), and their extent appears more vulnerable to small shifts in ocean-atmosphere circulation than Amazonian forests (Malhi and Wright 2004). During the peak of the last Ice Age which occurred in the Pleistocene, 15000 – 18000 years ago, precipitations were very low and deserts covered almost the entire continent (White 2001b). Forests were probably highly fragmented and were only present under the form of refugia (White 2001b, Maley 2002), which are today recognized to be located in the Cameroon and Gabon mountains and the eastern DRC mountains (White 1983, Fayolle et al. 2014b). Based on recent results on the

patterns of tree species composition in Central African forests (Fayolle et al. 2014b), most species endemism is suggested to pre-date the Pleistocene and are consequently not related to the successive cold and arid periods of the Ice Age. Indeed, Fayolle and colleagues identified a major floristic discontinuity located at the Albertine rift which separates the dry, moist and wet forests of West and Central Africa (the entire Guineo-Congolian region) from the upland and coastal forests of East Africa. Therefore, refugia probably acted as sinks for already existing species that may have progressively spread under a stable climate (Plana 2004). Nonetheless, today cover of Central African forests is the result of an expansion of forest refugia that started at the end of the last glacial period, more than 8000 years before present (Justice et al. 2001).

These centers of endemism are mainly covered of wet forests, while the area between the two is mainly covered of lowland semi-deciduous moist forests (White 1983, Fayolle et al. 2014b). Their composition has recently been characterized based on the inventories of 22 logging concession, which account 49 711 plots of 0.5-ha, with records of trees starting at a DBH of 30 cm (Fayolle et al. 2014a). Mostly in agreement with independent description of the vegetation (Réjou-Méchain et al. 2008, Gourlet-Fleury et al. 2011) and vegetation maps developed recently from various remote-sensing products (Gond et al. 2013, Viennois et al. 2013, Betbeder et al. 2014), Fayolle and colleagues (2014a) highlighted that most of the lowland semi-deciduous moist forests are covered by a range of *Celtis* forests (from young to old-growth successions), forests near villages and roads are dominated by *Musanga* secondary forests, rivers are sparsely covered by old-growth monodominant forest of *Gilbertiodendron dewevrei*, and the southern part of the Central African Republic and the northern part of the Republic of Congo are covered by mixed *Manilkara* forests.

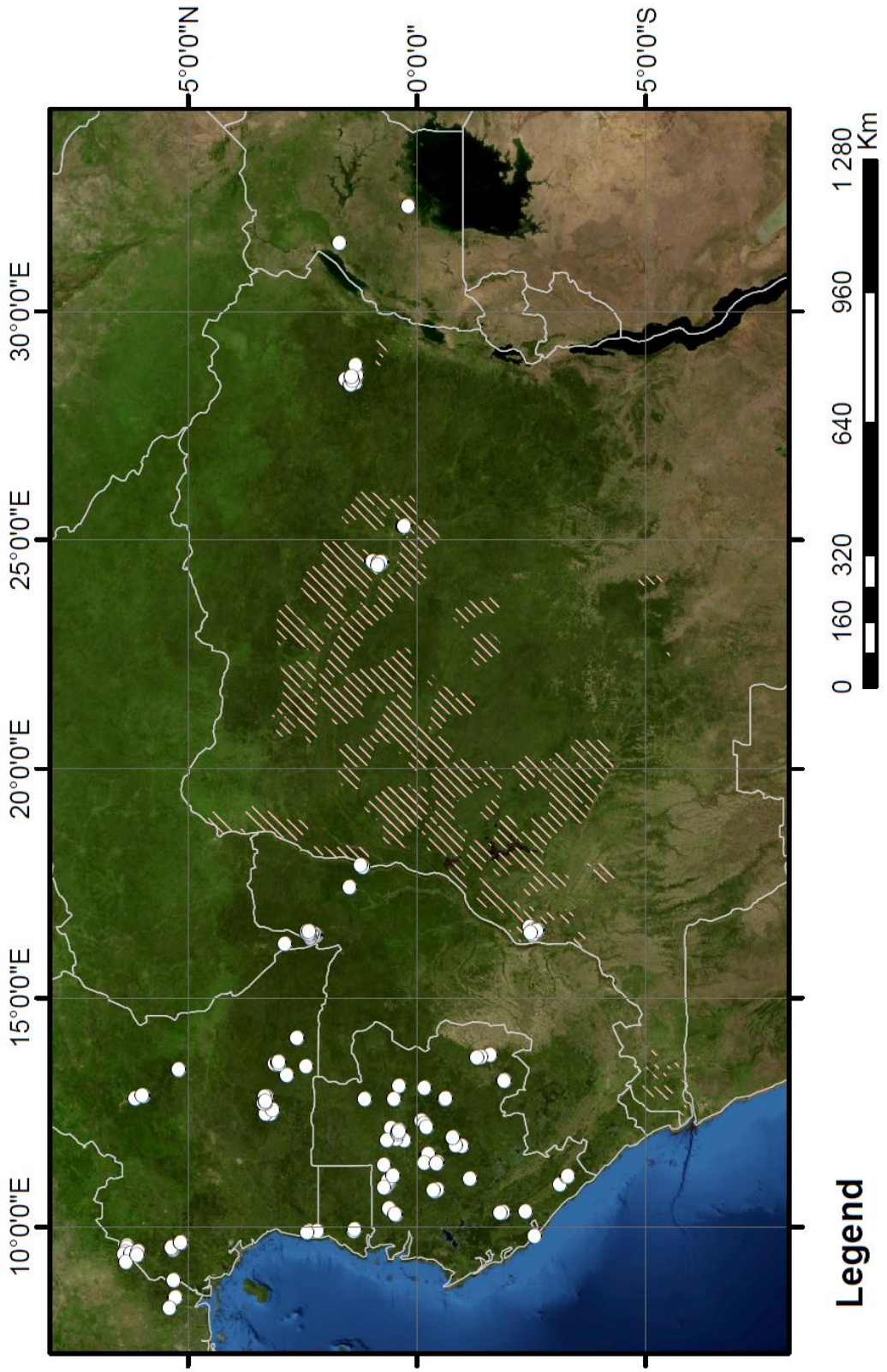

Figure 0- 10. The Congo Basin Forests, biomass inventory plots and DRC forest logging concession areas. Whitedots represent the distribution of the plots of the African Tropical Observation Network(AfriTRON, consulted the 27.05.2014). Red hatched lines represent areas occupied forest logging concession in activity in DRC registered to the 'Direction des Inventaires et Aménagementsforestiers' (DIAF).

3. The Malebo study site

3.1. Focus on the area

Our fieldwork was located at the edge of the Congo Basin Forest, in the Bandundu province of the Democratic Republic of the Congo (DRC). It covers an area of nearly 400 km², centered on the WWF Malebo research station (WGS1984; N -2°29'4.35" E 16°30'5.528"). The area was first known because of the presence of bonobos (*Pan paniscus*) for which forest surveys conducted by the World Wide Fund for Nature (WWF) highlighted large population densities (Inogwabini et al. 2008). This led to the initial presence of the WWF which rapidly started to encourage REDD+ initiatives. The area has even been recognized as a "REDD+ pilot site" for DRC since the conference of the parties held in Cancun in November 2010. Consequently, WWF plays a leading part in its development through two main projects: the REDD+ for People and Nature -RPAN project- and the Carbon mapping project. The first project aims to prepare local population to the REDD+ program and the second project, conducted in collaboration with the Jet Propulsing Laboratory led by Sassan Saatchi, aims to map forest carbon stocks on the whole area with an airborne lidar-based approach.

3.2. Forest and environment

The forests that we investigated are located on the northern part of the Bateke Plateau, between Lake Maï-Ndombe, the Congo River and the Kasaï-KwaRiver, with an altitude ranging from 300 to 500 m above sea level (Shuttel Radar Topography Mission data, SRTM). According to soil data from FAO, the dominant soil types are Ferralic Arenosols (FAO 2007), which comprise sandy soils with low fertility. In this equatorial zone, rain occurs for most of the year with two dry seasons around February and June to August. Precipitation varies between 1500 and 1600 mm/year, and the average monthly temperature is stable around 25°C (Vancutsem et al. 2006). The presence of a cattle ranching society and their consequent savanna's management, i.e. with multiple fires per year, maintained today's state of 'forest-savanna mosaics'(Figure 0-11). However, fires regimes started to decrease in the past few years, which led to an interesting re-colonization dynamics of *terra firme*

savannas led by *Uapaca guineensis* (Figure 0-12A). The landscape includes a wide diversity of *terra firme* forests stands along with riverine gallery forests, old secondary forests, *Marantaceae* forests (Figure 0-12B) with understories dominated by *Haumania liebrechtsiana* and *Megaphrynium macrostachyum* (Inogwabini, 2008), mature forests dominated by a mix of *Annonaceae*, *Caesalpinoideae and Olacaceae* trees and old growth monodominant *Gilbertiodendron dewevrei* forests (Figure 0-13A). The most frequent species present in the canopy in terms of the total basal area are *Klainedoxa gabonensis* (9.87 %; Figure 0-13B), *Plagiostyles africana* (6.67%), *Pentaclethra eetveldeana* (5.53 %), *Strombosia grandifolia* (4.41 %), *Millettia laurentii* (3.66%; Figure 0-13C), *Polyalthia suaveolens* (3.5 %), *Gilbertiodendron dewevrei* (3.28 %), *Pycnanthus angolensis* (3.12 %), *Dialium* spp.(2.56 %) and *Uapaca* spp. (2.5%). During my PhD thesis, 178 tree species belonging to 44 families were recorded in the herbarium and botanical library of the ULB (BRLU), with reference IDs Bastin-Serckx#1-474. In particular, a correspondence table was built between vernacular (Kiteke) and scientific names (See Appendix A). Interestingly, the species composition that we described is very similar to the forest sketches realized by Professor Bouillenne in 1955 (Figure 0-14) in their description of *terra firme* forests along the Lake Tumba, i.e. 200 km North from the Malebo region.

3.3. A word on the local communities

The majority of the local people belongs to the Teke ethnic group. They live from shifting agriculture and hunting in the forests. Their fields are generally located in forest edges and do not surpass 1-ha per household. All animals are hunted, except buffalos, elephants and bonobos. While the first two are not hunted only due to legal prohibition, bonobos are also protected due to a local taboo: bonobos are locally believed to be related to human ancestors (Serckx et al. 2014). Teke people seem to manage their environment with quite a sustainable way, but pressure on forest resources often come from outside the region, such as illegal forest logging companies. Consequently, since 2013, the WWF and a local NGO (Mbou-Mon-Tour) are working together on the elaboration of a “community natural reserve” status to better protect forest resources (for fauna and flora).

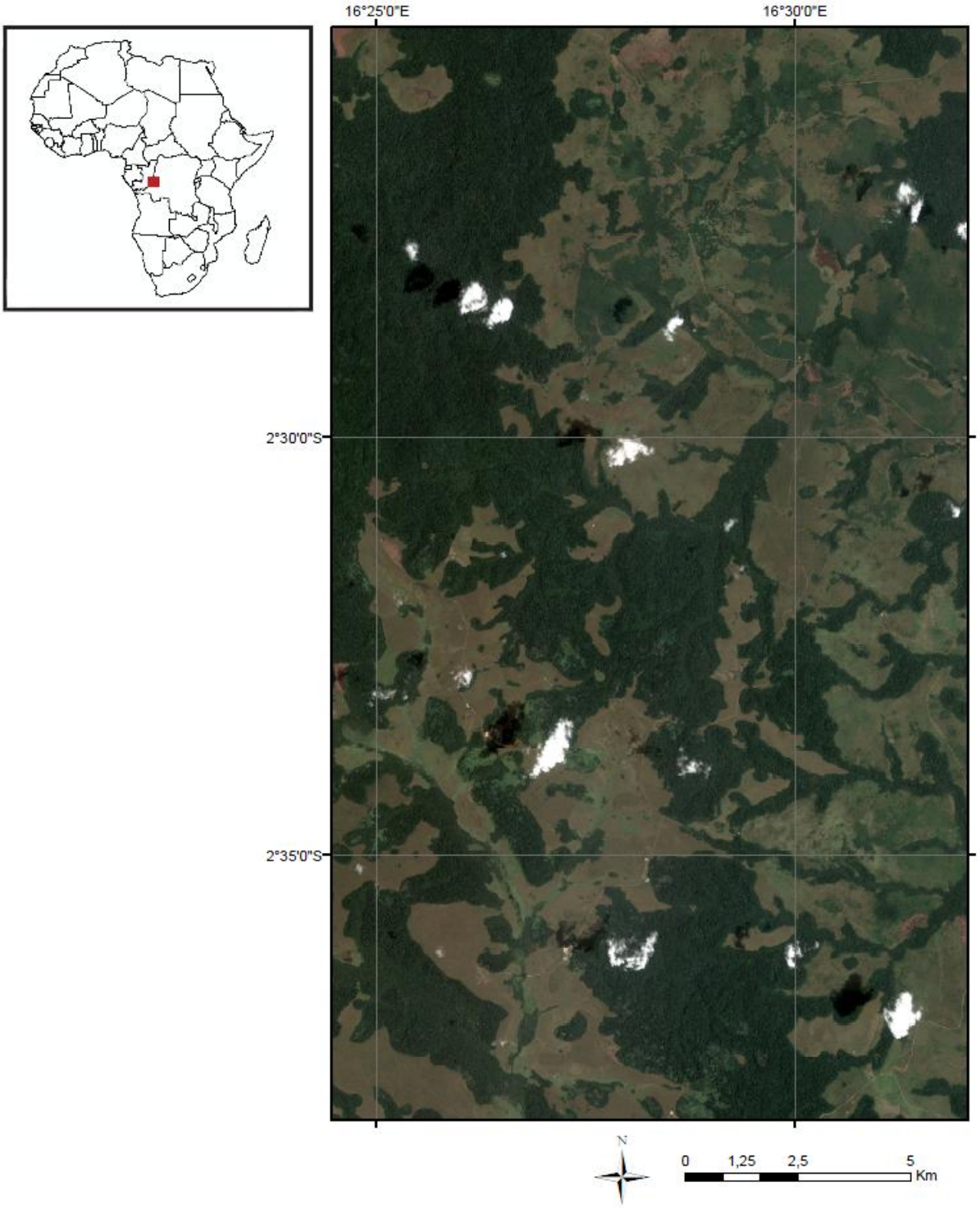

Figure 0- 11. The Malebo area, Bandundu Province, The Democratic Republic of the Congo. Snapshot from a True Color raster image taken with the Pleiades satellite in July 2013. Dark green corresponds to dense forests, light green to colonizing forests, edaphic forests and woody savannah and light brown correspond to herbaceous savannah and bare soils.

Figure 0- 12. Forest stands representative of the Malebo area. *Uapaca guineensis* colonizing forests (A), composed of many small trees (< 15 m of height), and *Marantaceae forests* (B) with a few large trees (> 30 m of height) in the middle of an empty understory fulfilled with *Marantaceae*.

Forest stands representative of the Malebo area. *Gilbertiodendron dewevrei* forests (A), *Klainedoxa gabonensis* and its fruit (B), *Millettia laurentii* and its pods (C).

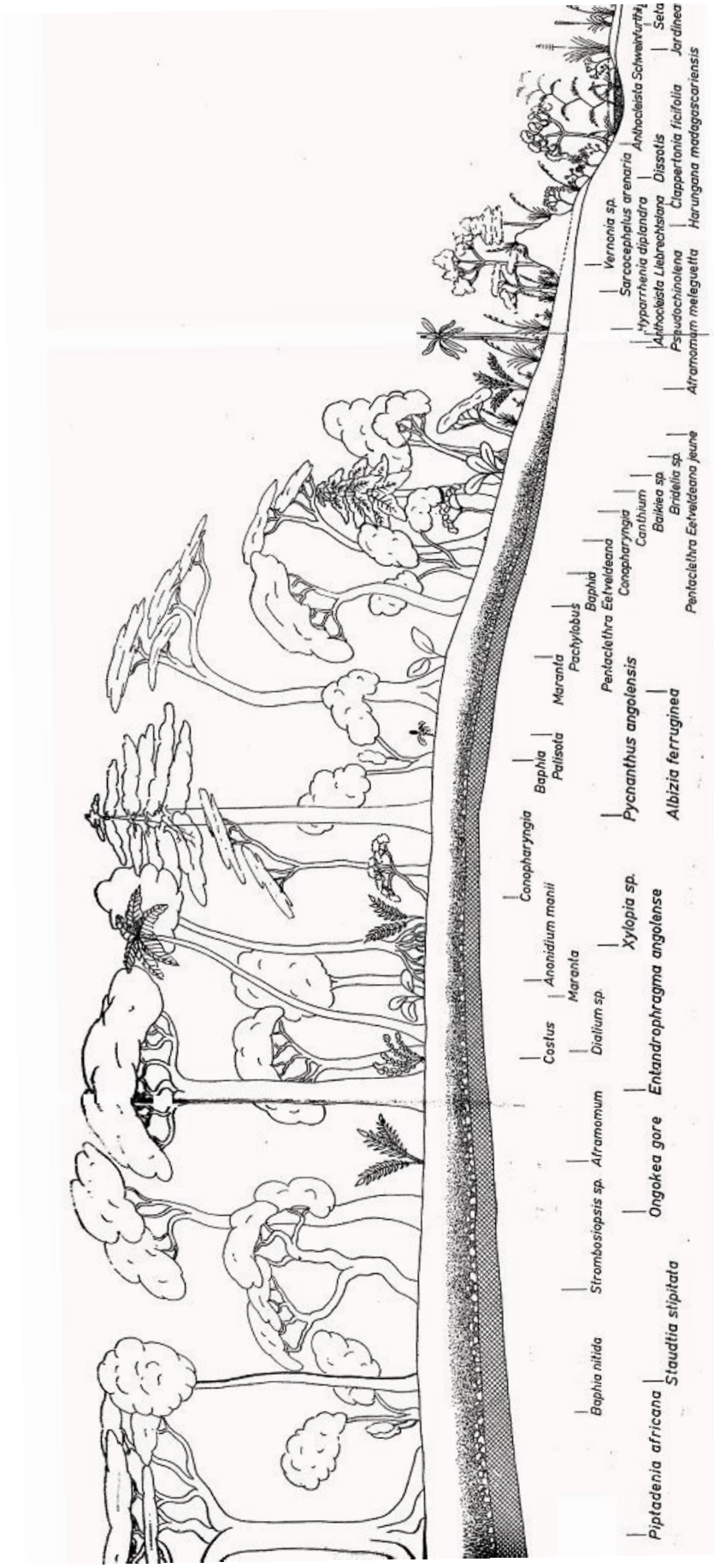

Figure 0- 13. **Sketch of *Terra firme* forest situated near the Lake Tumba.** This forest description was realized in 1955 by Pr.Bouillenne and illustrates well the kind of forest encountered in the Malebo area. Note *Piptadenia Africana* corresponds to *Piptadeniastrum africanum*.

MAIN DOCUMENT

STRUCTURE

Willing to contribute concretely to some of the existing issues, the present work was thought and built to address relevant questions at each scale of AGB measurement and estimation in Central Africa. Each one of these will constitute an entire chapter of the present work:

- Regional mapping: Can we develop accurate and precise methods to assess 'forest units' AGB from very high spatial resolution (VHR, pixel ≤ 1 m) optical imagery?
- Forest estimations: Can we find any predictor of 'forest units' to develop a cost-effective field methodology and to increase the amount of sampling point for remote-sensing calibration and validation?
- Individual tree variations: Can we afford to neglect intra-individual, intra-species and inter-site variations of wood density when we estimate the AGB at the tree or the forest level?

Paper 1 - Regional mapping

Through our collaborations with WWF Germany and the joint research unit for plant architecture, botany and bioinformatics of Montpellier (UMR-AMAP) we had the opportunity to work on very high resolution (VHR, pixel ≤ 1 m) optical imagery. Despite offering interesting perspectives, such tools have remained so far underused in the framework of AGB estimations. Therefore, in this paper we tested and improved an existing method, i.e. the Fourier Textural Ordination (FOTO), to depict forest canopy structure and to map forest AGB in Africa. The FOTO method has been developed at AMAP and tested with success in a variety of tropical forests outside Africa (Couteron et al. 2005, Proisy et al. 2007, Ploton et al. 2012). However, such method had yet to be tested at a regional scale and in different types of 'forest units'. This has required to overcome two difficulties: (i) the instrumental effects due to variations in sun-scene-sensor geometry or sensor-specific responses and (ii) the forest structural heterogeneity including monodominant or open canopy forests, which are of particular importance in Central Africa. Here we addressed the two issues successfully, using images combination and textural classification.

Paper 2 – Forest estimations

Today, the remaining uncertainties related to the combination of ground and remote-sensing techniques to predict the AGB of tropical forests is a call for developing alternative strategies but also requires a better understanding of dynamics in tropical forest ecosystems (Mitchard et al. 2013, 2014, Réjou-Méchain et al. 2014). In tropical forest ecosystems, large trees are known to monopolize a large share of the forest carbon stocks within their AGB (Chave et al. 2001, Slik et al. 2013) and to accumulate it faster than smaller trees (Stephenson et al. 2014). In this context, largest trees appear progressively as the key common denominator to consider (Harms et al. 2000, Bagchi et al. 2010, Remm and Lõhmus 2011, Lindenmayer et al. 2012, Slik et al. 2013, Stephenson et al. 2014).

In this chapter, based on a large dataset gathered in Central Africa (203 1-ha plots), we tested the full potential of largest trees as predictor of the entire 'forest unit' structure and species richness. Our objective was to answer to the following questions: Do the largest trees reflect the entire forest biomass and diversity? Is there a species hyperdominance in carbon accumulation? Despite their simplicity, answering these questions have provided a better understanding of African forests structure and species richness distribution. This has also allowed us to suggest the development of a cost-efficient forest monitoring programs which is particularly important in a REDD+ context.

Paper 3 – Individual tree

The wood specific gravity (WSG), i.e. the oven-dry mass divided by its green volume, is the second most important predictor of the AGB of the tree (Chave et al. 2005, 2014) (the first being the tree diameter). However, most studies reporting AGB estimations have extracted their WSG values from global databases (e.g. Zanne et al. 2009) and, consequently, have neglected WSG radial intra-individual, intra-species and inter-species variations (Maniatis et al. 2011b, Clark and Kellner 2012). Selecting representative species in terms of AGB ha^{-1} and forests successional stages, we addressed these questions depicting the wood density profile of 120 wood cores through 3D X-ray tomography scans. We characterized the importance of such variations, their relationship with tree life-history strategies and the consequences of the absence of their inclusion in tree AGB estimates.

DATASETS AND SAMPLING DESIGN

Paper 1 - Regional mapping

The mapping of forest AGB through the FOTO method was based on a set of 26 1-ha plots covering an area of about 400 km^2. Texture signals were calibrated using two field datasets obtained during two different field campaigns realized in the study site of Malebo (DRC). A first set of 11 1-ha plots were inventoried in 2011 according to a systematic (grid 1 km²) and randomized field sampling design (Gibbs et al. 2007). A second set of 15 1-ha plots were collected in 2012, based on the limits of available satellite images and stratified in order to cover the entire range of the texture gradient obtained after FOTO pre-processing. To avoid geolocation issues, plot centroid coordinates were calculated from location records collected with a GPS GARMIN ™ 62S every 25 m along the plot contour, resulting in 25 points per plot.

All the trees presenting a diameter at 130 cm ≥ 10 cm (DBH) were measured and identified. Note stem diameter were measured at 130 cm or 50 cm above buttresses or trunk deformations if present. Total heights were estimated with Laser rangefinder (LazerACE™ 2D Hypsometer) using the 3-shot method, i.e. measuring the horizontal distance calibrated for the last object encountered and measuring the angles formed between the observer and the bottom and the top of the trees (Rondeux 1999). Four hundred seventy-four samples of 178 tree species belonging to 44 families were recorded in the herbarium and botanical library of the ULB (BRLU), with reference IDs Bastin-Serckx#1-474. Wood specific gravity values were extracted from the Dryad global wood density database (Zanne et al. 2009). All these parameters were used as input data to Chave's allometric model to predict AGB for moist forest stands (Chave et al. 2005). The latter equation was considered, at the time of writing, the best pan-tropical allometric model available to estimate AGB, including Central Africa (Henry et al. 2010, Djomo et al. 2010, Vieilledent et al. 2012, Fayolle et al. 2013).

The imagery used in paper 1 consists of two satellite optical images of very high spatial resolution (< 1 m) that overlap over more than 60 km². The first image, covering 100 km², was acquired and shared by the UMR-AMAP (Nicolas Barbier, Pierre Couteron) from the Geoeye-1 sensor in January

2012. The second image, covering 360 km², was acquired and shared by the WWF-Germany (Aurelie Shapiro) from the QuickBird-2 sensor in July 2012.

Paper 2 - Forest estimations

For our second study, we tested, based on datasets inventoried in 9 different sites across Central Africa, the potential of largest trees as predictor of the entire forest-stand AGB and species richness. We gathered permanent and non-permanent large plots from non-logged forests, comprising Ituri-Lenda (20 ha; CTFS; DRC), Korup (50 ha; CTFS; Cameroon), Korup2 (2 ha; IRD; Cameroon), Lomie Kongo (3 ha; IRD; Cameroon), Mabounie (12 ha; IRD; Gabon), Malebo[1] (31 ha; Bastin. J-.F.; DRC), Mbaïki (12 ha; ICRA/CIRAD; Central African Republic), Mindourou (10 ha; IRD; Cameroon), Ngovayang massif (15 ha; Ngonmadje C.; Cameroon) and Yangambi (20 ha; de Haulleville T.; DRC). The floristic composition of Korup, Mabounie and Ngovayang are representative of Wet Central African forests and the rest is composed of species characteristic of Moist Central African forest (Fayolle et al. 2014b). To ensure a sufficient sampling size for each site, Korup-IRD plots were merged with Korup-CTFS plots and Mindourou and Lomie Kongo plots were merged to form the South-East Cameroon site. Prior to analyses, each site was divided into 1-ha plots or subplots, totalizing 176 plots.

Diameter at breast height (DBH; measured at 130 cm or 50 cm above buttresses if any or at 450 cm in Mbaïki) has been measured for all trees presenting a DBH superior-or-equal to 10 cm. Measured trees were identified up to the species-level and samples were recorded into the collection of the herbarium and botanical library of the ULB (BRLU) for DRC-Malebo (Bastin-Serckx #1-474), Gabon and Cameroon (IRD) datasets and of the National Botanic Garden of Belgium in MEISE for DRC-Yangambi (COBIMFO) datasets. Tree height was measured in Malebo on each single stem and in Yangambi on sub-samples using laser rangefinder hypsometers (Nikon, LaserACE 2D) with multiple

[1] Note Malebo site is here composed of 31 1-ha plots instead of the 26 used in paper 1 because 5 plots of the first field campaign were located outside satellite images extents.

[2] More than 1000 woodcores were actually extracted from the field but the cost of wood density radial profiles

and multi-angle measurements. When available, measured and estimated heights were implemented into three parameters exponential models (Banin et al. 2012), to develop local height-diameter allometries.

For the entire dataset, wood density was extrapolated from standardized species records using the Dryad database (Zanne et al. 2009) (using genus or family averages if the species-level was not available).

Paper 3 - Individual tree

Radial variations of wood density were studied on woodcores samples extracted from the Malebo study site (cf. paper 1).

Based on our two field campaigns, we selected 14 common tree species to sample belonging to 14 genera and 8 families, in order to cover a wide range of wood density, AGB and regeneration guilds *sensu* Hawthorne (1995): with non-pioneer light demanding (NPLD; n = 7 species) which can establish in the shade but need gap to reach the canopy, shade-bearer species (SB; n = 5 species) which can establish and grow in the shade and swamp species (Swamp; n = 2 species). For each species, woodcores were sampled in order to maximize the representativeness of DBH classes. A total of 120 woodcores[2] were studied in paper 3.

Non-used datasets

Several extra-measurements were realized during our field campaigns in the region of Malebo but they weren't used in the present PhD thesis : (i) we realized 25 hemispheric photography of the canopy openness per plot, at each coordinates recorded with the GPS, (ii) we extracted 16 soils samples on the first 30 cm per plot during our second field campaign, and (iii) we established 40 0.25-ha plots in the edge of the forest (< 400 m from the forest-savannah limits (Laurance 2008) during our first field campaign. These 'edge plots' were established originally to evaluate the

[2] More than 1000 woodcores were actually extracted from the field but the cost of wood density radial profiles analyses limited our investigation to 120 trees. Woodcores are currently stored in Gent university.

potential influence of the edge on forest AGB but preliminary results were unsatisfying and the idea was sidelined.

PAPER 1

AGB MAPPING FROM CANOPY TEXTURE ANALYSIS

Title

Aboveground biomass mapping of African forest mosaics using canopy texture analysis: towards a regional approach.

Authors

Bastin J.-F., Barbier N., Couteron P., Adams B., Shapiro A., Bogaert J. and De Cannière C.

Paper accepted in Ecological Applications from the Ecological Society of America, the **19 April 2014**.

Authors contribution :

- Paper conception : Bastin, Barbier
- Field collection : Bastin, Adams
- Field design : Bastin, Barbier, Bogaert, De Cannière
- Satellite datasets acquisition : Barbier, Couteron, Shapiro
- Methodology and Statistics : Bastin, Barbier, Couteron
- Text : Bastin, Barbier, Bogaert, De Cannière, Couteron

Abstract

In the context of the reduction of greenhouse gas emissions caused by deforestation and forest degradation (the REDD+ program), optical very high resolution (VHR) satellite images provide an opportunity to characterize forest canopy structure and to quantify aboveground biomass (AGB) at less expense than methods based on airborne remote sensing data. Among the methods for processing these VHR images, Fourier textural ordination (FOTO) presents a good potential to detect forest canopy structural heterogeneity and therefore to predict AGB variations. Notably, the method does not saturate at intermediate AGB values as do pixelwise processing of available space borne optical and radar signals. However, a regional scale application requires to overcome two difficulties: (i) instrumental effects due to variations in sun-scene-sensor geometry or sensor-specific responses that preclude the use of wide arrays of images acquired under heterogeneous conditions and (ii) forest structural diversity including monodominant or open canopy forests, which are of particular importance in Central Africa. In this study, we demonstrate the feasibility of a rigorous regional study of canopy texture by harmonizing FOTO indices of images acquired from two different sensors (Geoeye-1 and QuickBird-2) and different sun-scene-sensor geometries and by calibrating a piecewise biomass inversion model using 26 inventory plots (1 ha) sampled across very heterogeneous forest types. A good agreement was found between observed and predicted AGB (RSE=15%; R^2=0.85; p-value<0.001) across a wide range of AGB levels from 26 Mg/ha to 460 Mg/ha, and was confirmed by cross validation. A high-resolution biomass map (100 m pixels) was produced for a 400 km² area, and predictions obtained from both imagery sources were consistent with each other (r=0.86; slope=1.03; intercept=12.01 Mg/ha). These results highlight the horizontal structure of forest canopy as a powerful descriptor of the entire forest stand structure and heterogeneity. In particular, we show that quantitative metrics resulting from such textural analysis offer new opportunities to characterize the spatial and temporal variation of the structure of dense forests and may complement the toolbox used by tropical forest ecologists, managers or REDD+ national monitoring, reporting and verification bodies.

Keywords

Canopy structure, Aboveground biomass, Canopy texture analysis, Fourier Transform, Remote-sensing, Very High Resolution imagery, Forest-stand structure, Forest classification, Congo Basin Forest, Central Africa.

Introduction

Monitoring carbon emissions from tropical forests has become a major issue in past decades (van der Werf et al. 2009, Pan et al. 2011, IPCC 2013). Because anthropogenic forest loss is responsible for 6 to 17% of total carbon emissions (Pan et al. 2011, Harris et al. 2012), mostly occurring in the tropics (Houghton 2005), the United Nations Framework Convention on Climate Change (UNFCCC) developed an international program aiming at "Reducing Emissions due to Deforestation and forest Degradation", i.e. the REDD+ program (UNFCCC 2010). The implementation of such program relates on the capacities to assess properly the current state of forest carbon stocks on large scale, particularly the fraction stored in aboveground biomass (AGB) (Houghton et al. 2009), and its evolution through time (DeFries et al. 2007, Maniatis and Mollicone 2010).

Given the extent of tropical forests, access limitations (Gibbs et al. 2007) and structural complexity (Hallé et al. 1978), remote sensing methods are since long seen as crucial tools for assessing tropical forest AGB (Patenaude et al. 2005, DeFries et al. 2007). However, despite notable improvement and diversification of the techniques (e.g. Asner et al. 2010, Saatchi et al. 2011, Baccini et al. 2012), consistent mapping of AGB within the realm of intermediate to high AGB tropical forests has so far remained elusive, at least with existing space-borne instruments (Mitchard et al. 2013). Currently, the best reported results are obtained with the use of space- or air-borne LiDAR proxies of forest and canopy height to estimate AGB at local scale, i.e. over a few tens of km² (Zolkos et al. 2013). These are then consequently used as a way to feed into larger-scale AGB prediction models (Asner et al. 2010, Baccini and Asner 2013). Resulting predictions from LiDAR-techniques show relative residual standard errors (RSE(%)) ranging from 10 to 40% depending on the sensor and the forest types considered (Zolkos et al. 2013). One of the best reported results, i.e. a RSE(%) of about 10%, was obtained within the 50 ha permanent plot of Barro Colorado Island (BCI) in Panama, with an average AGB of 103 Mg/ha (Mascaro et al. 2011). However, despite promising results in tropical forest with low AGB levels (~ 100 Mg/ha), biomass prediction models from single LiDAR metrics generally exceed the 20% of RSE(%) recommended by the MRV (measuring, reporting and verification) guidelines

(Houghton et al. 2009, Zolkos et al. 2013), cover small extents (tens of km²) and depend on the consistency of DBH-H allometries. In addition, LiDAR-based forest canopy metrics used to predict AGB, such as the mean forest height profiles (Mascaro et al. 2011), do not consider an important share of the horizontal structure of the forest-stand, i.e. when regarding the variations of crowns size and abundance in the canopy layer related to variations of forest successions (Hallé et al. 1978, Barbier et al. 2010). Of course, this needs not always to be the case, and - at least with high density small footprint airborne LiDAR data - other descriptors could be obtained (e.g. Mascaro et al. 2012, Kellner and Asner 2014).

Despite offering interesting perspectives for the characterization of the canopy layer, very high resolution (VHR, pixel ≤ 1 m) optical imagery has remained underused since the launch of the first IKONOS and QuickBird sensors in the early 2000s. Although approaches aimed at the delineation of individual crowns have proven to be disappointing in natural forests due to overlap or aggregation between crowns (Keller et al. 2002, Palace et al. 2008, Zhou et al. 2010), textural indices computed at the stand level (~1 ha) exhibit encouraging results for describing forest-stand structure (Frazer et al. 2005) and thereby predicting AGB. One method in particular, the Fourier Transform Textural Ordination, hereafter called FOTO, has been tested in a variety of tropical forest contexts (Couteron et al. 2005, Proisy et al. 2007, Barbier et al. 2010, Ploton et al. 2012). The FOTO method aims at characterizing the existing gradients of canopy crown size distribution throughout the forest based on the spatial variation in pixel radiance observed on VHR images. Technically, the method decomposes the spatial variation of pixel values within a given optical image extract (window) of the canopy into spatially periodic functions (sine and cosine) of varying amplitudes and frequencies to yield Fourier spectra (Couteron 2002). The method then compares the windows through the spectra using standard multivariate methods to identify the main gradients of canopy texture in the region (Proisy et al. 2007, Barbier et al. 2010, Ploton et al. 2012). Ordination scores are used as textural indices and constitute the characteristic dimensions of the FOTO analysis. Compared to classical textural classification (e.g., Sarker et al. 2011) and object-based methods (e.g., Duveiller et al. 2008),

the FOTO method presents the advantage of being unsupervised and providing quantitative results that are interpretable in terms of canopy grain, canopy heterogeneity and crown size distribution. Consequently, due to the allometric relations between crown and trunk dimensions (West et al. 2009, Barbier et al. 2012, Antin et al. 2013), FOTO indices correlate well with stand structural parameters measured in the field (e.g. Couteron et al. 2005, Proisy et al. 2007, Barbier et al. 2010, Ploton et al. 2012). For instance, images of closed canopies exhibiting a stronger contribution of high spatial frequencies often correspond to the small-sized trees (early successional stages or unfavorable soils) with low forest-stand AGB, whereas low frequencies are prevalent when large trees emerge, resulting in higher AGB (Proisy et al. 2007). Interestingly, in all cases investigated, FOTO indices did not appear to saturate in stands of high AGB, even up to 500 Mg/ha (Proisy et al. 2007, Ploton et al. 2012).

In some cases, the relationship between ground stand structure metrics and FOTO metrics (e.g., between stand density and canopy texture, hereafter referred to as structure-texture relationships) appears to change between sites, suggesting the existence of local differences in forest structural dynamics (Ploton et al. 2013). In preliminary tests performed in Central African forests, FOTO metrics appeared to be poorly correlated to all standard structural parameters when applied without distinction across forest types. In particular, some extensive African forest types, such as open canopy Marantaceae forests (White 2001a, Gillet and Doucet 2012, Viennois et al. 2013), young secondary forest made of *Uapaca guineensis* or *Musanga cecropioides* (Lubini and Mandango 1981, Inogwabini et al. 2008), semi-deciduous mixed *terra firme* forests (Evrard 1968) or *Gilbertiodendron dewevrei* monodominant old growth forest types (Lebrun and Gilbert 1954, Evrard 1968, Mosango and Lejoly 1990, Lubini and Kusehuluka 1991), do present unique canopy textures and are likely to differ in terms of texture-structure relationships. The very existence of different texture-structure groups could improve our global understanding of the ecological significance of forest structure and will be investigated in the present study.

At last, processing VHR images to implement the method over regional extents or through time, as required by international programs (Maniatis and Mollicone 2010), involves specific issues that have yet to be addressed. In particular, the fusion of satellite images from different sensors displaying variation in both raw-data preprocessing (Ryan et al. 2003) and acquisition configurations (Asner and Warner 2003) is often problematic. Changes in the sun-scene-sensor geometry have been shown to induce measurable textural changes (Gastellu-Etchegorry 2008, Barbier et al. 2010, 2011, Proisy et al. 2012). This effect is summarized in the bidirectional texture function (BTF), which is a function analogous and similar to the bidirectional reflectance distribution function (BRDF) (Kimes 1983, Gastellu-Etchegorry et al. 1999). In particular, differences in sun elevation and sun-sensor azimuth angle induce discrepancies in the observed distribution of tree shadows, and have a major impact on texture (Asner and Warner 2003, Barbier et al. 2011, Ploton et al. 2012). Here, we will evaluate the potential use of scene overlap to overcome resulting biases in texture-based forest structural parameter predictions.

The aim of this paper is to assess the potential use of FOTO indices, extracted from the analysis of forest canopy analysis from VHR optical imagery, to predict AGB variations, to assess the interdependence between forest structure and forest type and infer regional-scale AGB variations for Central African forests. We will account particularly for (i) a mosaic of distinct forest types presenting low to high AGB gradients and (ii) the use of VHR images acquired in contrasted acquisition conditions.

Material and methods

Study site

Our study region is located at the edge of the Congo Basin Forest, located in the Bandundu province of the Democratic Republic of the Congo. It covers an area of nearly 400 km², centered on the WWF Malebo research station (WGS1984; N -2°29'4.35" E 16°30'5.528") with sampling limits defined by the availability of VHR imagery (Figure I.1). At a regional scale, the investigated forests are located on the northern part of the Bateke Plateau, between Lake MaïNdombe, the Congo river and the Kasaï-Kwa river, with an altitude ranging from 300 to 500 m above sea level (Shuttel Radar Topography Mission data, SRTM). According to soil data from FAO, the dominant soil types are Ferralic Arenosols (FAO 2007), which comprise sandy soils with low fertility. In this equatorial zone, rain occurs for most of the year with two dry seasons around February and July. Precipitation varies between 1500 and 1600 mm/year, and the average monthly temperature is stable around 25°C (Vancutsem et al. 2006).

This landscape (Figure I-1) is properly described as a forest-savanna mosaic (Inogwabini et al. 2008) and includes a wide diversity of *terra firme* forests stands along with riverine gallery forests, re-colonizing *Uapaca guineensis* transition forests, old secondary forests, *Marantaceae* forests with understories dominated by *Haumania liebrechtsiana* and *Megaphrynium macrostachyum* (Inogwabini, 2008), mature forests dominated by a mix of *Annonaceae*, *Caesalpinoideae and Olacaceae* trees and old growth monodominant *Gilbertiodendron dewevrei* forests. The most frequent species present in the canopy in terms of the total basal area are *Klainedoxa gabonensis* (9.87%), *Plagiostyles Africana* (6.67%), *Pentaclethra eetveldeana* (5.53%), *Strombosia grandifolia* (4.41%), *Millettia laurentii* (3.66%), *Polyalthia suaveolens* (3.5%), *Gilbertiodendron dewevrei* (3.28%), *Pycnanthus angolensis* (3.12%), *Dialium* spp.(2.56%) and *Uapaca* spp. (2.5%).

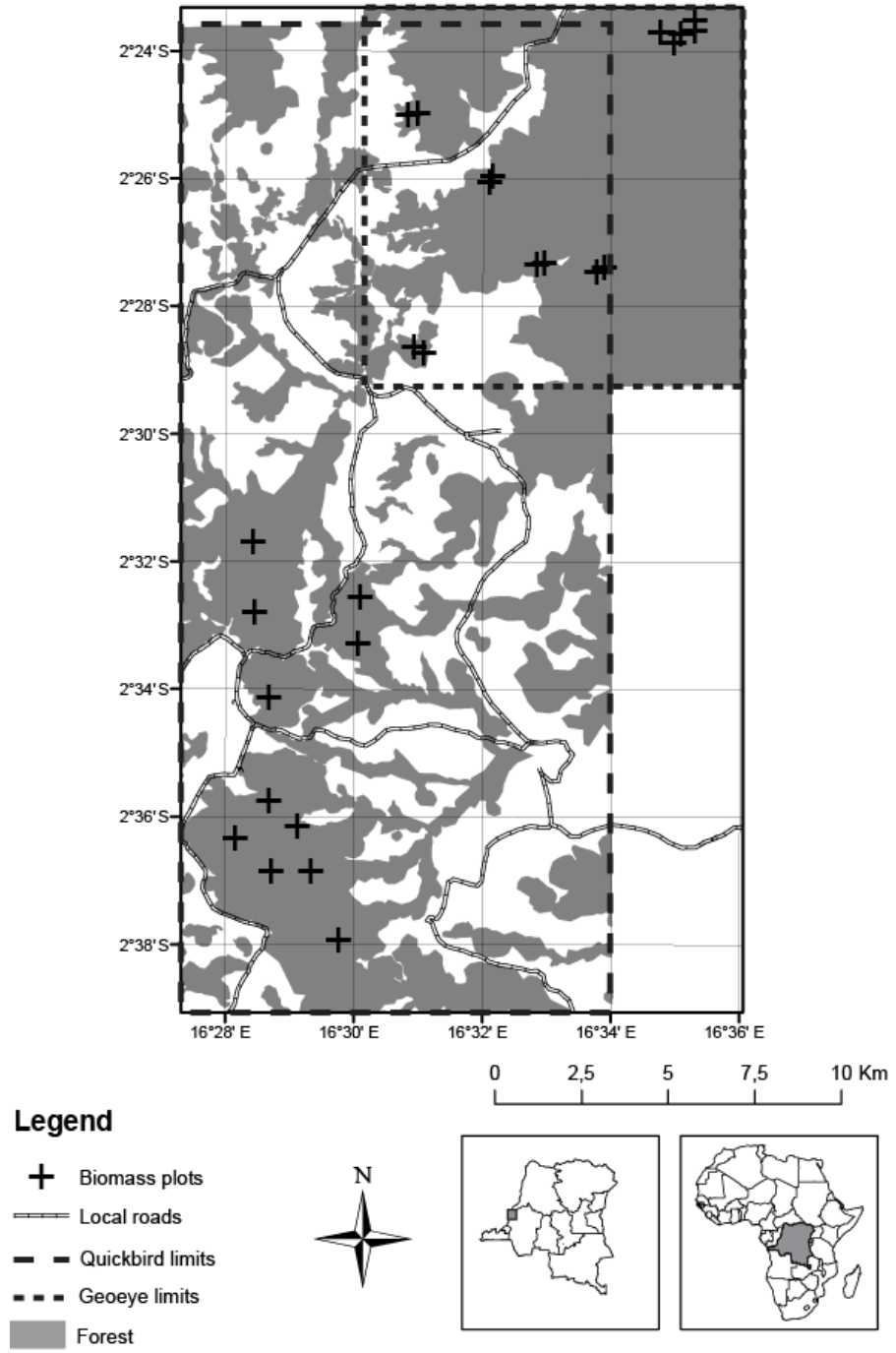

Figure I- 1. Study area with forest cover binary map (forest in grey vs. non-forest in white) over a complex mosaic of heterogeneous forest stands and savannas at the edge of the Congo Basin Forest, Democratic Republic of Congo, Bandundu. The footprints of the Geoeye-1 and Quickbird-2 scenes used in this study are represented by dashed rectangular boxes. Crosses represent the location of the 26 field plots (1 hectare each).

Image database

The imagery used in this study consists of two satellite optical images of very high spatial resolution (< 1 m) that overlap over more than 60 km² (Figure I-1). The first image, covering 100 km², was acquired by the Geoeye-1 sensor in January 2012 (acquisition parameters: view zenith angle = 16.56°; sun azimuth angle = 125.3°; sun elevation = 57.2°, sun-sensor azimuth angle = 31.78°, product catalog ID = 2012011909114141603031601696) and the second, covering 360 km², was acquired by the QuickBird-2 sensor in July 2012 (acquisition parameters: viewer zenith angle = 5.4°; sun azimuth angle = 53.5°; sun-elevation = 49.4°, sun-sensor azimuth angle = 95.1°, product catalog ID =A0100100BC44F600). Because both images were taken in the same year, with a difference of less than a year between the image dates and field measurements, potential biases in the analysis due to changes in the vegetation cover can be ignored. Furthermore, as both dates correspond to dry seasons, major variations in forest cover due to phenology are not expected. In this paper, these images will be referred to, respectively, as GE1 and QB2.

Because canopy texture analysis with the FOTO method provides a better insight on complete forest structural gradients when resolutions are smaller than a 2 m pixel size (Proisy et al. 2007), we only used the panchromatic bands, corresponding to spectral intervals ranging from 0.450 to 0.900 µm for GE1 and 0.450 to 0.800 µm for QB2. The spatial resolution of the two images was standardized to 1 m × 1 m pixels.

The primary focus of this study was the prediction of forest AGB; therefore, a supervised delimitation of non-forested areas (incl. villages, fields, bare soils and savannas) was performed to mask them out prior to texture analysis.

Forest structure field dataset

This study combines two field datasets obtained during different campaigns. The first set of forest inventory plots was collected in 2011 based on the QB2 limits and was established according to a systematic (grid 1 km²) and randomized design (Gibbs et al. 2007). The second set of plots was

collected in 2012 based on the GE1 limits and stratified from a FOTO pre-processing analysis in order to represent the complete texture coarseness gradient. A total of 26 plots, 1 ha each, was used (Table I-1). To avoid geolocation issues, plot centroid coordinates were calculated from location records collected with a GPS GARMIN™ 62S every 25 m along the plot contour, resulting in 25 points per plot. Because of the absence of differential correction, phase information and limitation to the GPS constellation, the use of such a navigation grade device reduces both the accuracy and precision of the positions. However, when comparing to differential methods, we found a bias in per-plot averaged horizontal positions of less than 3 m in four plots and less than 6 m for two other plots. These results are comparable to those obtained by Yoshimura and Hasegawa (2003) and by Valbuena et al. (2010). This suggests that the approach of multiplying position readings at different locations within the plot is a valid workaround for the effect of dense vegetation on positioning precision, whereas maximum levels of bias can be considered as acceptable when considering the hectare scale approach taken here. Stem diameters were collected at 130 cm (DBH) or above buttresses or trunk deformations if present. Total height (LazerACE™ 2D Hypsometer) and tree species were recorded for each tree with a DBH ≥ 10cm. Four hundred seventy-four samples of 178 tree species belonging to 44 families were recorded in the herbarium and botanical library of the ULB (BRLU), with reference IDs Bastin-Serckx#1-474. Wood specific gravity values were taken from the Global Wood Density Database (Zanne et al. 2009). All these parameters were used as input data to Chave's allometric model to predict AGB for moist forest stands (Chave et al. 2005). The latter equation was considered, at the time of writing, the best pan-tropical allometric model available to estimate AGB, including Central Africa (Henry et al. 2010, Djomo et al. 2010, Vieilledent et al. 2012, Fayolle et al. 2013). The computed AGB values of our plots ranged between 25 and 460 Mg/ha (table I-1).

Table I- 1. Characteristics of the forest plots collected during the two field campaigns for this study, and FOTO *PCA* scores of corresponding canopy windows. *AGB*=aboveground biomass estimated from field measurements with Chave'spantropical moist model (Chave et al. 2005), *PCA*1-3=scores along the corresponding axes of the *PCA* on the table of corrected spectra

plot reference	X coordinates	Y coordinates	Canopy dominant genus	*AGB* (Mg/ha)	*PCA1*	*PCA2*	*PCA3*	Texture classes (k=3)
M1P1	16°28´25"	-2°31´41"	*Dialium*	345.36	1.36	1.59	0.12	intermediate
M1P2	16°28´26"	-2°32´46"	*Millettia*	311.98	-5.87	-0.81	-0.78	coarse
M1P3	16°30´6"	-2°32´33"	*Klainedoxa, Santiria*	327.25	-1.6	1.24	0.33	intermediate
M1P4	16°30´3"	-2°33´16"	*Pycnanthus, Klainedoxa*	400.23	1.06	0.31	0.18	intermediate
M1P5	16°28´40"	-2°34´8"	*Piptadeniastrum*	287.1	4.87	-1.16	0.1	fine
M1P6	16°28´40"	-2°35´45"	*Copaifera, Scorodophloeus*	357.12	1.28	-0.43	0.55	intermediate
M1P7	16°28´9"	-2°36´19"	*Klainedoxa, Uapaca*	395.95	3.18	-0.72	0.73	fine
M1P8	16°28´42"	-2°36´52"	*Pentaclethra, Klainedoxa*	412.39	-3.32	-2.15	-0.03	coarse
M1P9	16°29´19"	-2°36´52"	*Klainedoxa*	409.92	0.95	0.02	0.44	intermediate
M1P10	16°29´46"	-2°37´55"	*Klainedoxa*	461.42	-0.29	-1.48	0.41	intermediate
M1P11	16°29´6"	-2°36´8"	*Pycnanthus, Pentaclethra*	337.54	1.6	-1.56	0.01	fine
M2P1	16°32´57"	-2°27´19"	*Millettia*	285.89	1.29	0.94	0.53	intermediate
M2P2	16°34´58"	-2°23´51"	*Pentaclethra*	299.85	5.25	1.08	-0.66	fine
M2P3	16°35´17"	-2°23´31"	*Klainedoxa*	161.84	-1.94	-0.37	-1.92	intermediate
M2P4	16°35´18"	-2°23´41"	*Millettia*	183.12	1.38	1.39	-0.39	intermediate
M2P5	16°35´4"	-2°23´43"	*Gilbertiodendron*	284.48	5.56	-3.84	1.6	fine
M2P6	16°31´4"	-2°28´43"	*Millettia*	189.98	0.47	1.97	0.39	intermediate
M2P7	16°30´56"	-2°28´38"	*Plagiostyles*	112.57	5.12	2.23	-1.88	fine
M2P8	16°32´50"	-2°27´21"	*Brachystegia, Gilbertiodendron*	331.15	-2.59	0.61	1.31	intermediate
M2P9	16°33´46"	-2°27´28"	*Millettia*	198.56	-5.05	0.33	0.9	coarse
M2P10	16°33´53"	-2°27´24"	*Maranthes*	235.14	7.21	-2.42	0.18	fine
M2P11	16°30´49"	-2°24´59"	*Millettia*	188.47	5.39	0.66	-0.99	fine
M2P12	16°30´59"	-2°24´58"	*Entandrophragma*	220.39	-6.25	0.84	1.33	coarse
M2P13	16°32´9"	-2°25´58"	*Pentaclethra, Klainedoxa*	175.53	6.38	0.56	-0.96	fine
M2P14	16°32´6"	-2°26´4"	*Xylopia*	124.96	6.4	0.16	-0.58	fine
M2P15	16°34´45"	-2°23´43"	*Uapaca*	27.45	21.19	-8.36	2.07	fine

The 2D Fast Fourier Transform

The textural analysis applied in this paper is the Fourier Transform Textural Ordination (FOTO) method. Originally developed to study geomorphology (Mugglestone and Renshaw 1998), it has been adapted to study landscape patterns in arid vegetation and canopy structure based on aerial photography and satellite imagery (Couteron et al. 2005, Barbier et al. 2006, Deblauwe et al. 2008). The reader is referred to previous studies (Couteron 2002) for more details; here, we will focus on the key features.

The algorithm, programmed in MATLAB © on the basis of the fft2 function, performs a spatial decomposition of the radiometric signal of a given image extract (hereafter the window). Specification of window size (N x N pixels) depends on the objects of interest. As we focused on canopy features, we worked with 100 m × 100 m windows, an area directly comparable with the size of the field inventory plots (1 ha). To improve the spatial resolution of the output texture and AGB maps, overlap was allowed between consecutive windows, resulting in a 25 m final (pseudo-) resolution.

The 2D Fourier transform characterizes the image via a convolution with sine-cosine functions at integer frequencies, i.e., wavenumbers (1, 2, …, N/2), along the two major Cartesian directions. These frequencies are afterwards expressed in cycles/km to ease interpretation. The Fourier transform yields complex numbers, the squared amplitudes of which form a 2D-periodogram or power spectrum that has the advantage of being an additive partitioning of the image variance into frequency components. Directional information in the periodogram was not considered here and was averaged through the computation of the r-spectrum (Figure I-2, *step1*). To summarize, the r-spectrum constitutes a simple descriptor describing the spatial structure within the window in terms of the variance contribution of a limited number of spatial frequencies. As a high redundancy was found in the higher frequencies, only the first 33 frequencies were analyzed. In other words, we considered frequencies ranging from 10 cycles/km (FMIN), corresponding to large objects having a

period/wavelength of 100 m, up to 330 cycles/km (FMAX), i.e., small objects with wavelengths of ca. 3 m.

Combining r-spectra from different sensors and acquisition conditions

The observed canopy texture is influenced by acquisition geometry, i.e., the sun-scene-sensor angles (Barbier et al. 2011) but also by the sensor's modulation transfer function (Ryan et al. 2003). Barbier et al. (2011) showed that bias induced in FOTO indices by changes in acquisition geometry could be linearly corrected. In this study, we took advantage of the geographical overlap between the two images (Figure I-1) to empirically derive linear correction coefficients directly for each frequency of the r-spectrum (Figure I-2, *step2*). To do so, a linear regression model was computed for each frequency (column) of the r-spectra table between the two images across all windows (lines) within the overlap. As the two tables *a priori* present comparable levels of uncertainty, model II major axis linear regressions were performed (Sokal and Rohlf 1995). The coefficients and intercepts obtained were then used to correct the whole GE1 r-spectra dataset, hereafter referred to as GE1-corr. Note that GE1 was chosen to be corrected because its scene was smaller and covered fewer plots than the QB2 scene.

Texture ordination and classification

An ordination of windows was performed using a standardized principal component analysis (PCA) (Figure I-2, *step3a*) on the basis of the concatenated (GE1-corr and QB2) r-spectra table, considering each frequency (column) of the table as a quantitative variable. In applications dealing with closed canopy forests, the first axis of the *PCA* generally expresses a fineness-coarseness gradient of canopy grain (Couteron et al. 2005) and has been shown from simulated images to be closely correlated with the mean crown size of canopy trees (Barbier et al. 2010). Due to the allometric properties of tree stands (Enquist et al. 2009, Antin et al. 2013) as well as the preponderance of large trees influencing AGB (Chave et al. 2001, Slik et al. 2013), the main *PCA* axes have already shown good correlations with AGB in French Guyana mangrove forests and in homogenous forests stands in India (Proisy et al.

2007, Ploton et al. 2012). Here, Central African forests present contrasting forest types with likely varying structure-texture relationships, notably due to the peculiarities of *Marantaceae* forest stands (open canopy) or mono-dominant *Gilbertiodendron dewevrei* forests (tightly closed, very homogeneous canopy). We therefore investigated the relationships between FOTO metrics and stand parameters separately by delineating forest classes from a first round of analysis of the canopy texture itself. We first classified windows on the basis of the concatenated r-spectra table (Figure12, *step3b*) using an unsupervised non-hierarchical clustering approach (k-means) and testing different numbers of classes, as it was difficult to know a *priori* how many and which forest classes it would be necessary to distinguish.

Biomass models and cross-validation

AGB-texture prediction models were calibrated between FOTO indices and field plot AGB data. Linear multiple regression models were developed using the main textural characteristics (i.e., scores along the three *PCA* main axes) from the windows extracted around plot locations as predictors and the AGB estimated from field data as the response variable.

To test the sensitivity to the number of k-means classes, between one and six classes were used, and for each class an independent AGB-texture model was calibrated (Figure12, *step4*). Use of more than six classes was not considered, as we needed sufficient field plots within each class to calibrate the global AGB model. This approach is analogous to the piecewise linear regression from the data mining statistics family (Hastie et al. 2009), which divides the dataset into segmented consecutive linear regressions with different coefficients. However, in the present case, the classification was performed for the whole r-spectra table (329 808 windows) and not only on the field plot points, thereby enhancing the representativeness of the classes for the area and reducing the risk of overfitting. For each scenario (number of k-means groups), the average R^2 and RSE were computed and a Leave-one-out cross-validation was performed (Figure I-2, *step5*). The best set of models was then used for mapping AGB over the study site.

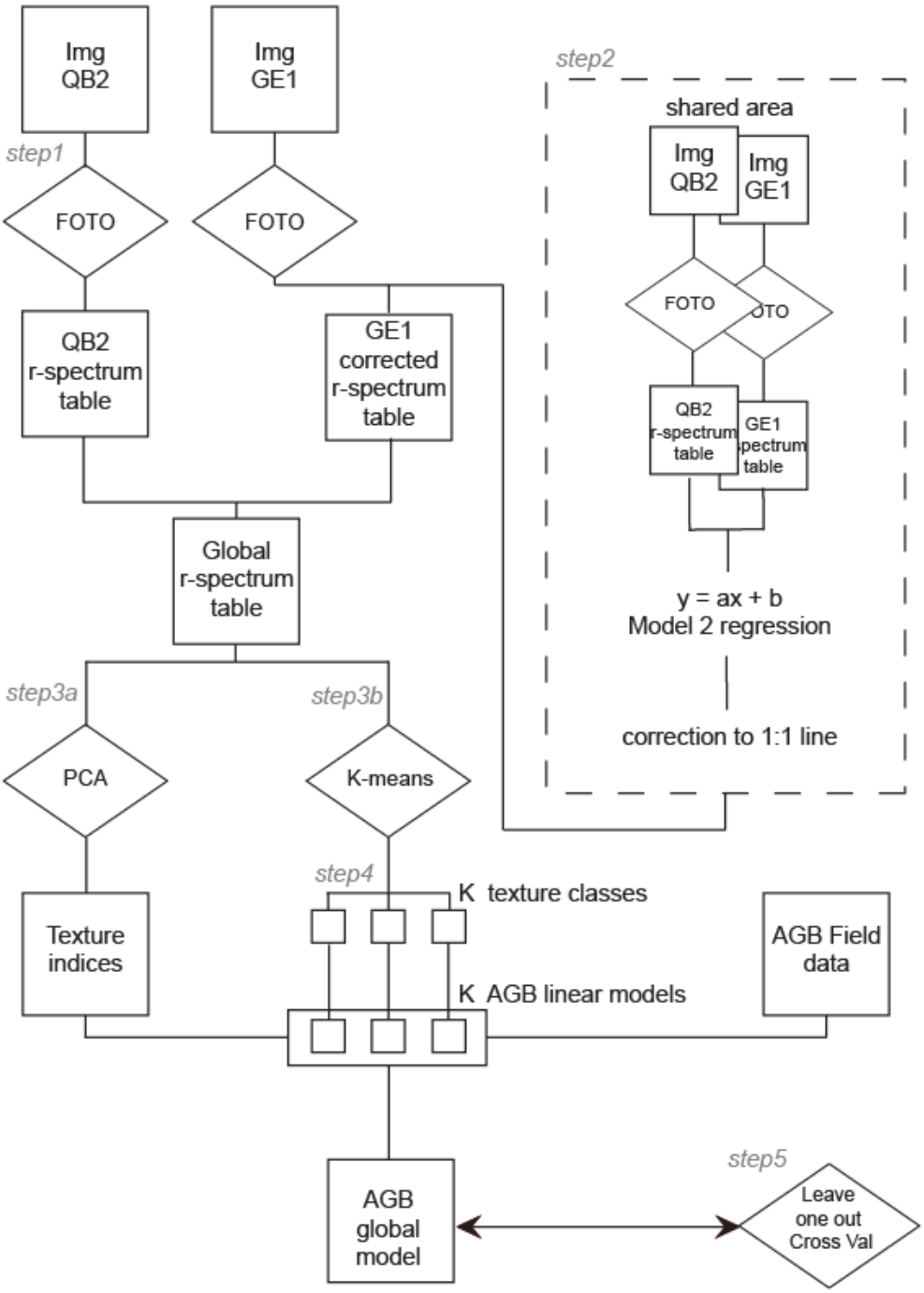

Figure I- 2. Flowchart of the method.

Results

Instrumental effects

We first addressed the issue of textural variations caused by instrumental effects and differences in acquisition geometry (See workflow, Figure I-2). The impact of these effects is illustrated through a close-up of the GE1 and QB2 panchromatic images of the same location (Figure I-3A). The results of the textural ordination and classification realized on the combined (raw) r-spectra tables were mapped (Figures 3B-C). In the ordination maps (Figure I-3B), the scores along the three first *PCA* axes are represented in shades of red, green and blue (RGB composite), respectively (see next section for an interpretation of the meaning of the axes). Due to specific acquisition geometry and sensor specificities, the GE1 image (Figure I-3A, right) exhibited a much finer grain than QB2 (Figure I-3A, left), resulting in completely different texture and classification maps even for the same forest types (Figure I-3B, Figure I-3C). In more statistical terms, these discrepancies translated into an important bias in both the slope and the intercept of the regressions between the textural values (*PCA* axes scores) obtained for the GE1 and QB2 images (Figure I-4, gray dots and regression lines). As the two images have a common area, we were able to derive empirical linear correction coefficients for each frequency bin of the Fourier r-spectra. This simple correction results in a notable reduction of the bias of the *PCA* texture axes (Figure I-4, black dots and regression lines). In fact, after correction, the regressions between the first three axes for the two images presented null intercepts and slope coefficients of 1.1, 0.9 and 1, respectively, compared to non-null intercepts and slope coefficients of 0.7, 1 and 0.5 for the raw data. Bias removal was clearly apparent on the mapped results in terms of both ordination scores and k-means classification (Figures 13D, E) and resulted in similar predicted AGB distributions, as illustrated in Figure I-3F (pixel resolution of 25m, filtering of 3*3). However, the noise, expressed by the R^2, did not appear to be reduced.

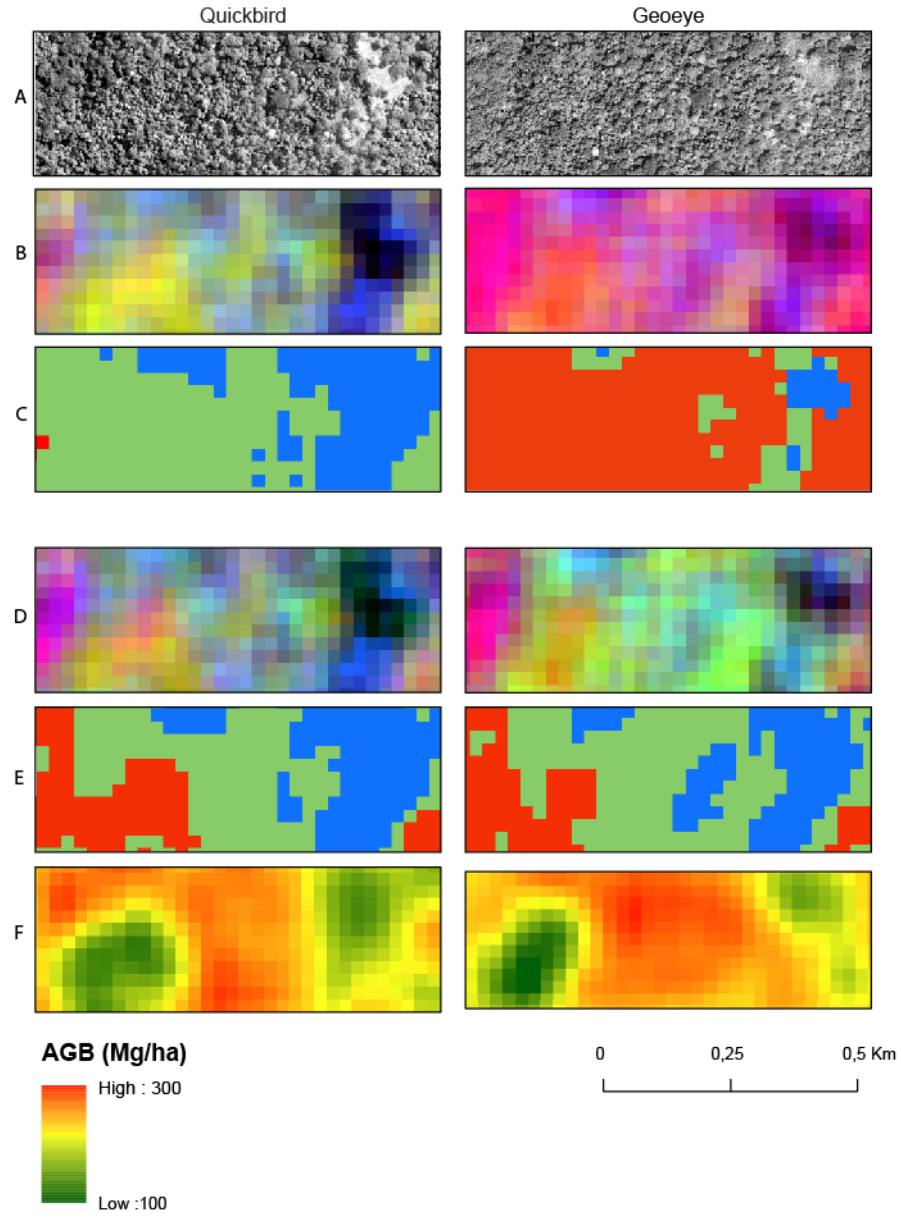

Figure I- 3. Close-up (750 m × 250 m) within the shared area between Geoeye-1 andQuickbird-2 scenes showing the results of the different processing steps. A/ panchromatic images (spatial resolution = 1 m); B-C/ Red-green-blue composites mapping the scores along the three first *PCA* axes on the uncorrected (B) and corrected (D) Fourier r-spectra (pseudo-resolution = 25 m); C-E/Cluster maps of the 3-classes k-means classification on the uncorrected (C) and corrected (E) Fourier r-spectra; F/ Inverted biomass maps with pixel resolution of 25m and mean filtering window of 3*3 pixels.

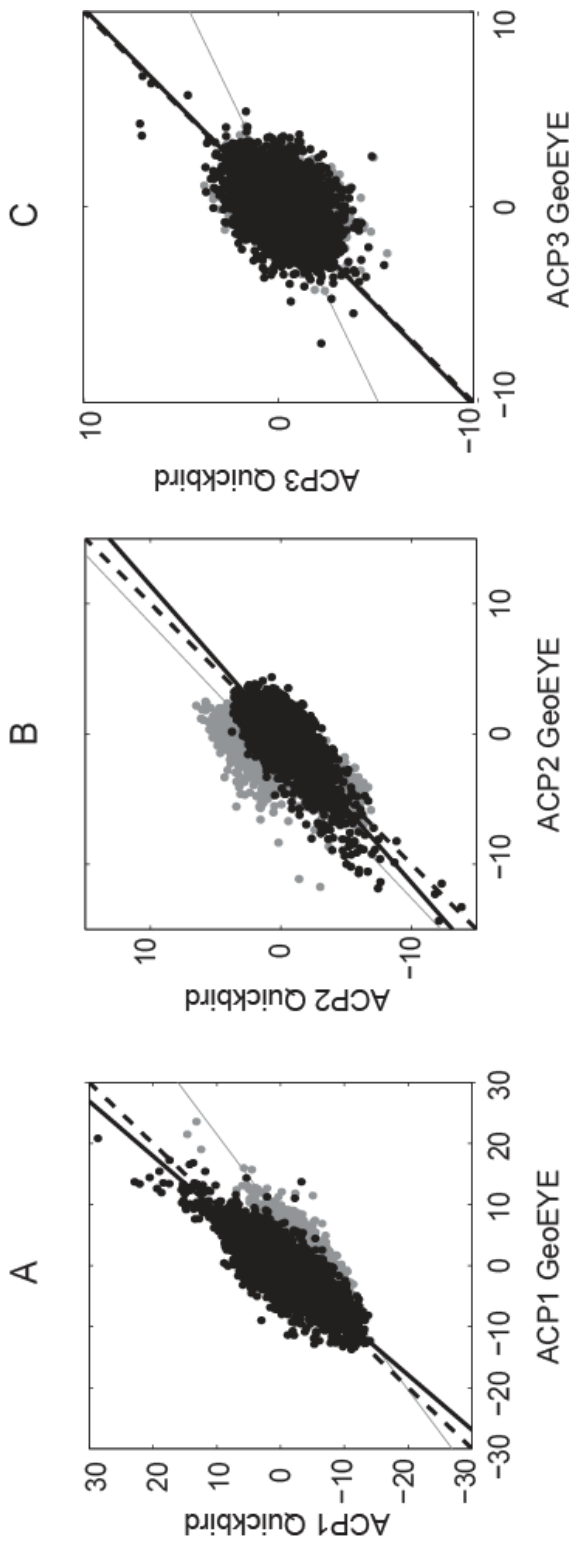

Figure I- 4. Comparison of FOTO PCA axes scores for Geoeye-1and Quickbird-2 scenes obtained within the shared area with (black) and without (gray) r-spectra correction. Fits are obtained by model II major axis linear regressions. A/ scores along PCA axis 1: black: y=1.11x, R^2=0.657; gray: y=0.72x-5.4, R^2=0.665; B/ scores along PCA axis 2: black: y=0.88x, R^2=0.506; gray: y=0.95x+1.93, R^2=0.448; C/ scores along PCA axis 3 black: y=0.98x, R^2=0.190; gray: y=0.48x-0.27, R^2=0.178.

Global texture map

Windowing into 100-pixel windows (with 1 pixel = 1m² and a window taken every 25 m) and subsequent r-spectra computation were performed on the GE1 and QB2 images (Figure I-2), resulting in 122 900 and 206 908 r-spectra, respectively. After applying the above correction on the GE1 r-spectra (Figure12), the ordination was computed on the concatenated matrix of GE1-corr and QB2 r-spectra, with individual windows as observations and Fourier frequencies as variables.

The three main axes accounted for more than 65% of the total variability observed in the *PCA* (Figure I-5C), with the first axis being clearly prominent, as shown in the scatterplots of *PCA* scores (Figures 15A, B) and in the plot of loadings (Figure I-5C). However, the two subsequent axes presented non-negligible contributions and were hence retained. The correlation circle between the main *PCA* plans and the Fourier frequencies (Figures 15D, E) indicated, as was expected, that *PCA*1 expressed a gradient from low frequencies (FMIN) to high frequencies (FMAX). The two other axes presented more complex frequency contributions. *PCA*2 expressed a gradient from a co-existence of low and high frequencies (FMIN and FMAX) progressively converging towards intermediate frequencies (F60). *PCA*3 started in the low frequency domain (FMIN) and ended in intermediate frequencies (F60), passing by a co-contribution of several frequencies.

When mapped as Red-Green-Blue (RGB) composites, the three first axes exhibited contrasting and coherent spatial patterns, providing useful visual information about canopy structure variation as shown in Figure I-3D, with pink-red values corresponding to dense/closed canopy structure and dark-blue values to open canopy structure. However, given the complexity of forest structural variation in the study area, texture-structure relationships proved subtler than in previous studies, as we found both high and low AGB levels at the two extremes of the main texture gradient (*PCA* axis 1), suggesting a relatively low interdependence between forest types and AGB. Coarse grained canopy texture corresponded to low-AGB open-canopy *Marantaceae* forests as well as to high-AGB closed stands with large crowns. At the opposite end of the gradient, fine canopy textures corresponded to

both low-AGB pioneer stands or to high-AGB monospecific *Gilbertiodendron dewevrei* forests (Table I-1). Consequently, establishing texture-AGB relationships required the derivation of piecewise relationships specific to more homogeneous textural groups.

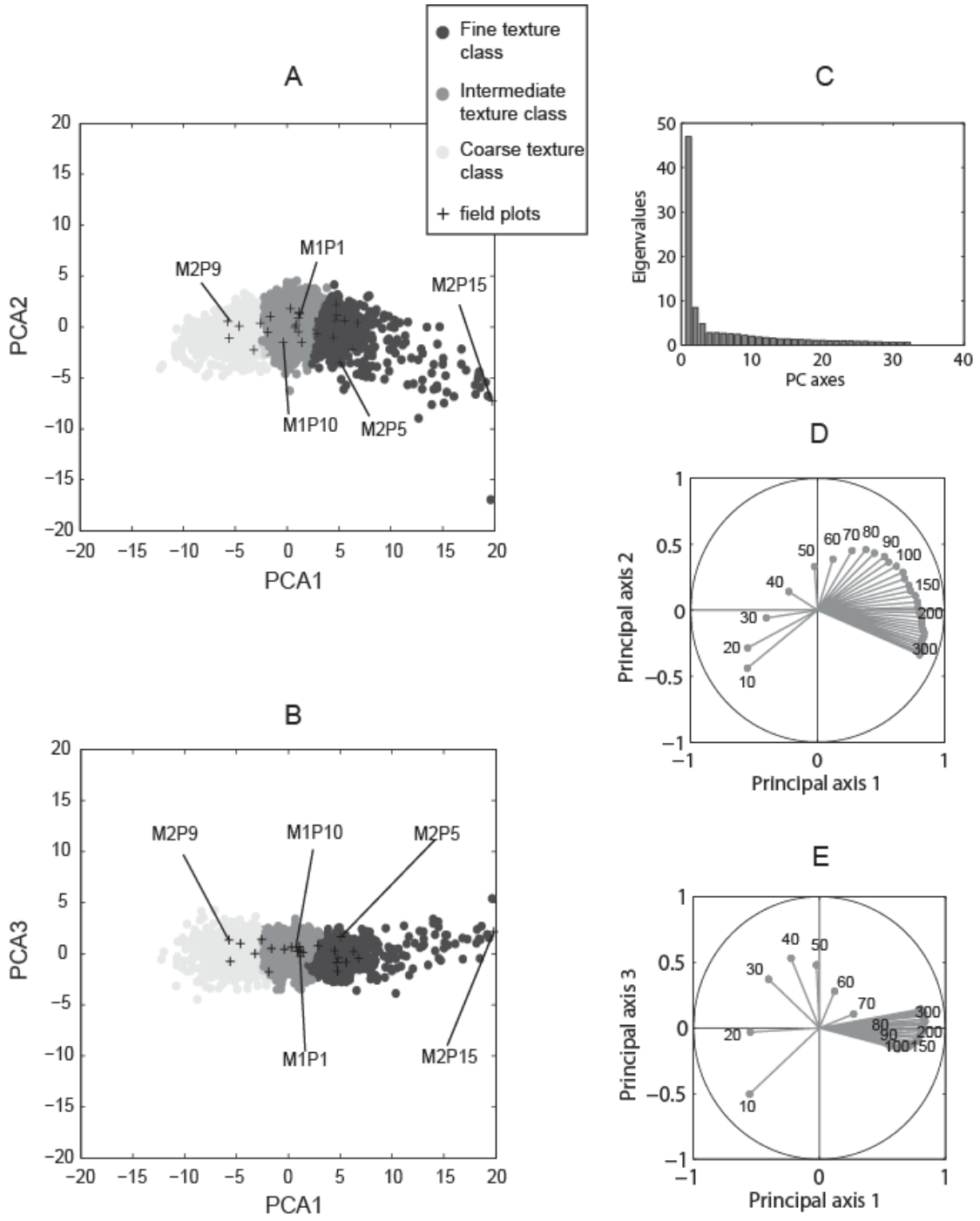

Figure I- 5. Synoptic results of the *PCA* on corrected Fourier r-spectra from 329 808 square Geoeye-1 and Quickbird-2, 100 m sides canopy image windows. A-B/ the two first factorial planes are represented with grey dots with shading indicating the k-means texture class concerned. The black crosses correspond to the scores of canopy windows co-located with field plots. The code of some plots of contrasting structure is specified (cf. table I-1). C/ loadings graph giving the proportion of total variance explained by each *PCA* axis. D-E/ circles of correlation between spatial frequencies and *PCA* axes (in cycle/km).

Texture-AGB models

K-means texture classifications were realized on the concatenated r-spectra matrix of GE1-corr and QB2 (Figure I-2). We tested classifications with one to six textural classes, and for each of the considered scenarios, an AGB prediction model was parameterized within each class. Each AGB model consisted of a multiple linear regression using some or all of the three first *PCA* axes as independent predictors and field AGB data as the model response (Table I-2). The best scenario was obtained with only three k-means groups. With more than three groups, at least one non-significant model or at least one group containing only one field plot was obtained, whereas with one or two groups, the global RSE increased. Note that the largest improvement in the model was observed when passing from one to two groups (Figure I-6), suggesting the existence of at least two main gradients in texture-structure interactions. Global AGB predictions (Table I-2) resulting from the piecewise model presented much better results (RSE=19.37%; R^2 = 0.85) than the approach without clustering (RSE=35.1%; R^2 = 0.32). In particular, AGB predictions from the piecewise model did not show any saturation up to the highest AGB levels (> 460 Mg/ha; Figure I-7). Note that the piecewise approach based on FOTO indices yielded also good results in the prediction of other forest-stand structural descriptors which are not developed in the present paper, such as the density of large trees (dbh ≥ 70 cm) and the basal area (Figure I-8).

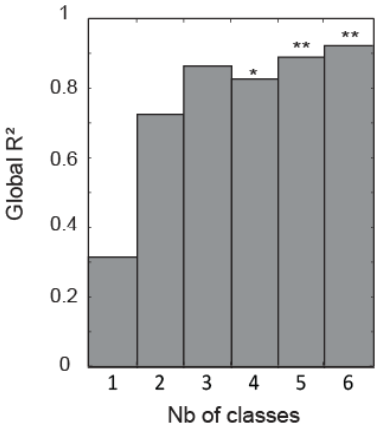

Figure I- 6. Optimizing the piecewise calibration of the biomass inversion model. Goodness of fit (R^2) obtained for different numbers of k-means classes. (*) At least one k-means group has a non-significant linear regression; (**) At least one k-means group only has less than three plot.

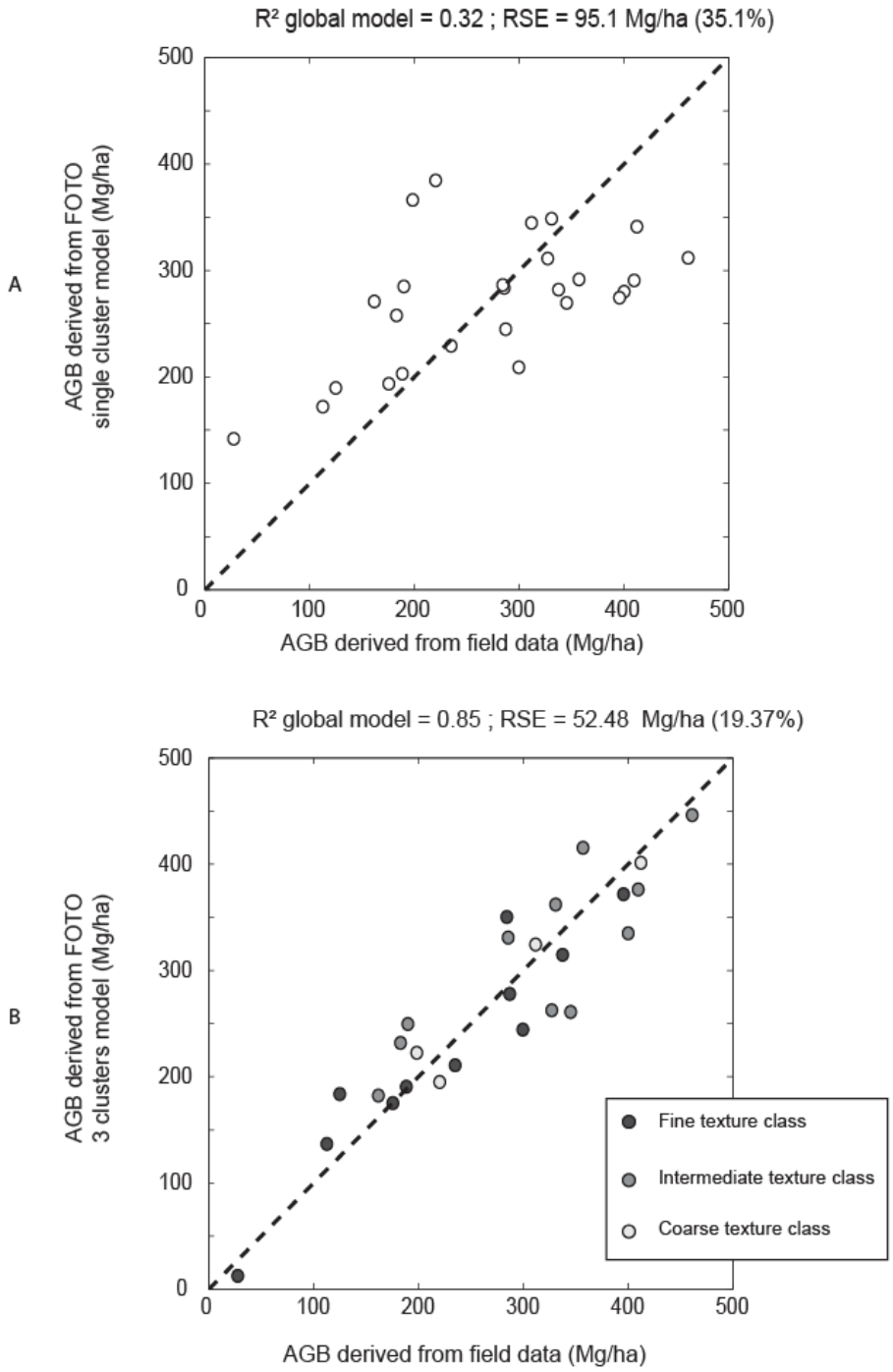

Figure I- 7. **Comparison between predicted and observed aboveground biomass** (in Mg per hectare). A/ Biomass prediction without segmentation; B/ Biomass prediction with piecewise regression on the basis of three k-means groups. Gray level of the dots indicate respective group.

Table I- 2. Parameters of aboveground biomass prediction models. α=intercept, β1=coefficient of *PCA*1, β2=coefficient of *PCA*2, β3=coefficient of *PCA*3.

		Estimate	**SE**	**tStat**	**pValue**	**RSE**	**R^2**
All (N =26)	*α*	**286.08**	**20.32**	**14.08**	**0.000**		
	β 1	-12.31	4.34	-2.83	0.001		
	β 2	-6.74	12.76	-0.53	0.6		
	β 3	23.67	23.08	1.03	0.3		
	model				*0.034*	*95.1 (%) 35.1*	*0.320*
Coarse (N=4)							
	α	234.03	16.80	13.93	0.005		
	β 2	-75.23	13.01	-5.78	0.029		
	model				*0.029*	*28.414 (%)9.9*	*0.944*
Intermediate (N=11)							
	α	315.73	22.69	13.91	0.000		
	β 1	15.27	15.15	1.01	0.348		
	β 2	-66.31	21.47	-3.09	0.018		
	β 3	78.52	26.46	2.97	0.020		
	model				*0.030*	*65.142 (%)20.8*	*0.697*
High (N=11)							
	α	363.07	24.35	14.91	0.000		
	β 1	-20.84	4.97	-4.19	0.004		
	β 2	21.47	19.69	1.09	0.312		
	β 3	102.57	37.33	2.75	0.029		
	model				*0.001*	*43.800 (%)19.5*	*0.889*
	Global model					*52.48 (%)19.37*	*0.85*

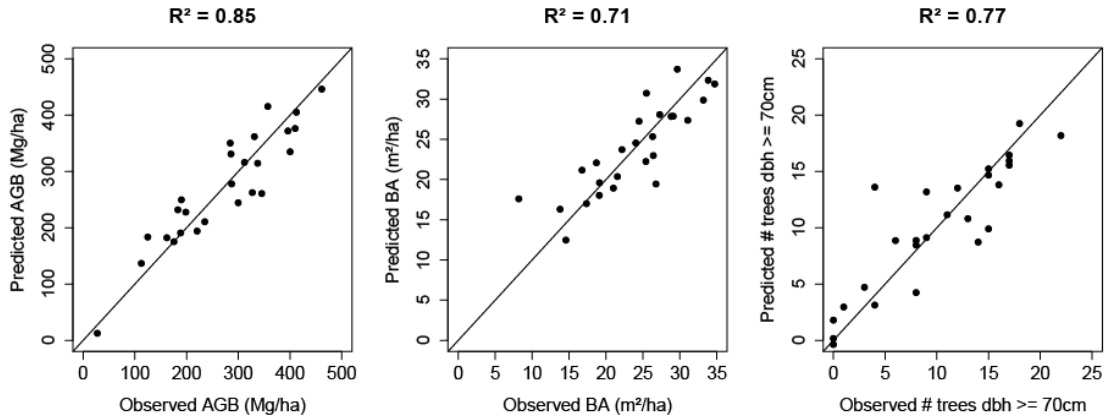

Figure I- 8. Aboveground biomass (Mg/ha; $R^2 = 0.85$) , basal area (m^2/ha; $R^2 = 0.71$) and density of large trees (count/ ha; $R^2 = 0.76$) - i.e trees with a dbh superior or equal to 70 cm- predicted from textural indices using the piecewise regression model.

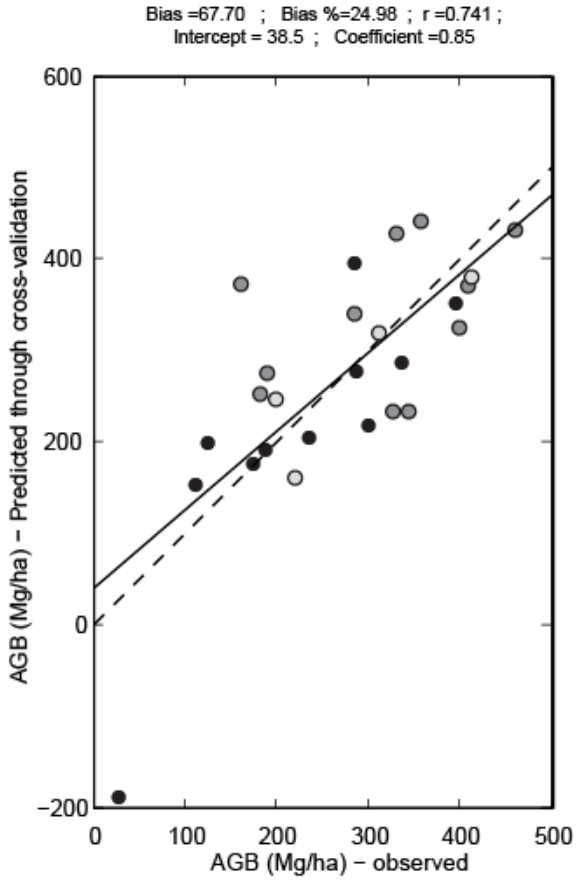

Figure I- 9. Predicted aboveground biomass (Mg/ha) values from the Leave-One-Out cross-validation performed with the piece-wise regression model and three k-means clusters.

A Leave-One-Out cross-validation was performed. The mean and standard deviations of the models parameters are summarized in Table I-3. In terms of the sensitivity of global predictions, small biases were obtained with the piecewise model (bias = 67.7 Mg/ha ; intercept = 38.5 ; slope = 0.85), whereas the model without clustering gave non-significant results. Some particular plots, such as the one in *Uapaca guineensis* secundary forest, became clear outliers when not considered in the training group, highlighting the low redundancy of plot data in our dataset (Figure I-9).

In addition, we assessed the potential risk of a biased improvement of the model quality resulting from a decrease of the sample size (Figure I-10). To this end, we analyzed the RSE distribution of AGB prediction from 999 random sub-samples of similar size as the original textural clusters (i.e. N = 4 and N = 11). The original mean RSE were always strongly below the RSE of the random samples (Figure 20) suggesting the improvement of the model cannot be attributed to a decrease of the sample size.

As final validation test, we compared the AGB map derived from either GE1-corr or QB2 images for the shared area (Figure I-11). Due to the aforementioned irreducible level of noise resulting from the different acquisition configurations, naive pixel-to-pixel comparisons at the initial resolution of 25 m produced rather low correlations (r=0.42; slope = 0.98; intercept = 24.34, Figure I-11C), despite very similar spatial structures and biomass levels between the AGB maps. To reduce the amount of noise, the maps were aggregated to a 100 m resolution and then smoothed (5 × 5 mean filter) before comparison (Figure I-11A and Figure I-11B), resulting in a much improved matching between the two predicted AGB maps (r=0.86; slope=1.03; intercept=12.01, Figure I-11D).

Table I- 3. Mean coefficient and standard deviation from Leave-One-Out cross-validation. α=intercept, *β1*=coefficient of *PCA1*, *β2*=coefficient of *PCA2*, *β3*=coefficient of *PCA3*.

Leave-One-Out	***α***	**std α**	***β 1***	**std β 1**	***β 2***	**std β 2**	***β 3***	**std β 3**
ALL (N=26)	275.18	56.34	-11.67	2.95	6.91	4.18	22.98	7.93
Coarse (N=4)	231.96	17.58	-	-	-74.64	11.66	-	-
Intermediate (N=11)	319.24	14.17	13.49	7.68	-66.53	7.36	74.20	21.43
Fine (N=11)	366.90	18.78	-21.68	3.84	22.03	8.54	102.88	15.42
Global Model RSE	51.06							
Stdev RSE	16							
Relative RSE	19.05%							

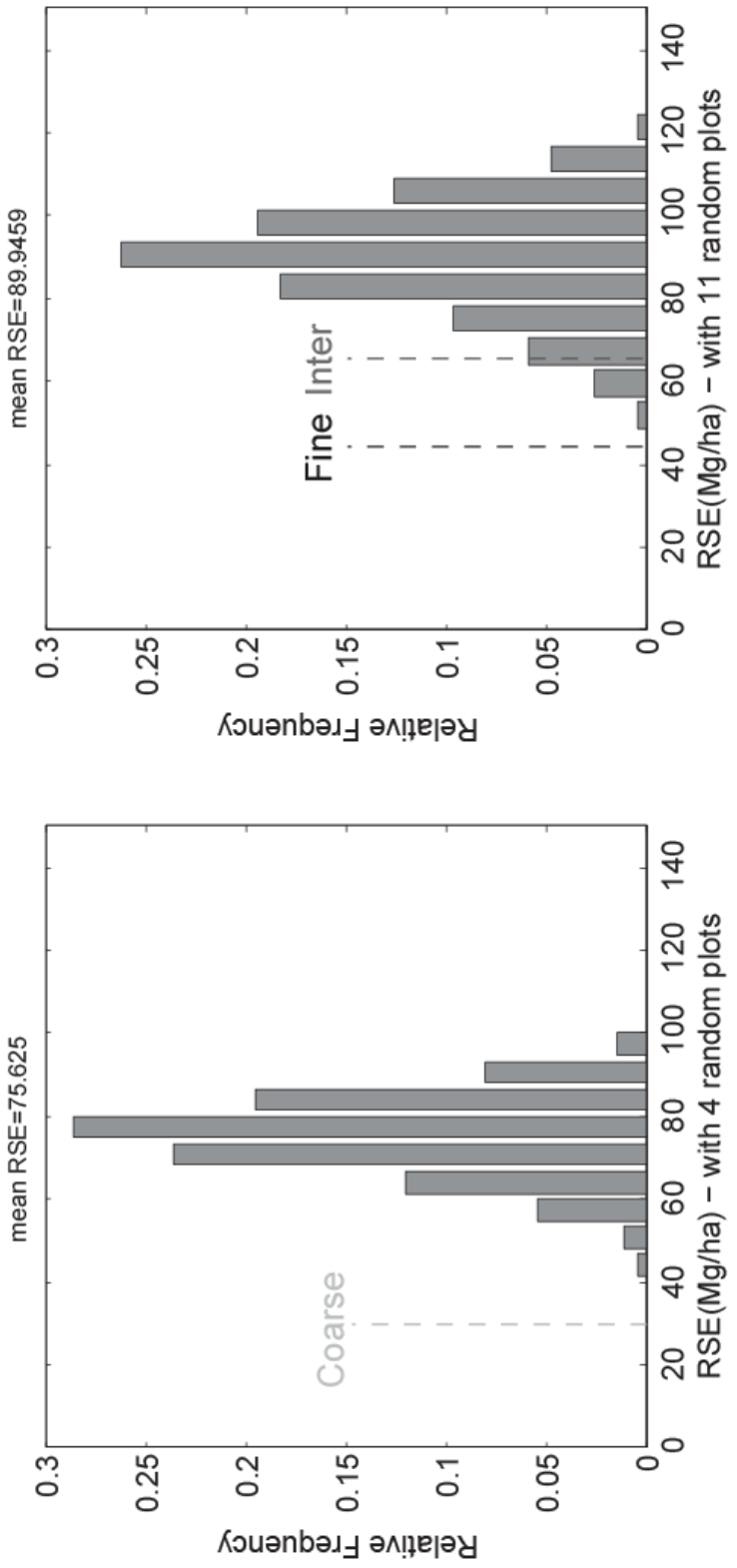

Figure I- 10. Distribution of the RSE for the prediction of AGB from textural indices resulting from 999 random clustering. The size of random clusters equal 4 (left) and 11 (right) in order to compare the simulated RSE with the RSE resulting from the k-means clustering (Coarse N=4; Inter = 11; High=11).

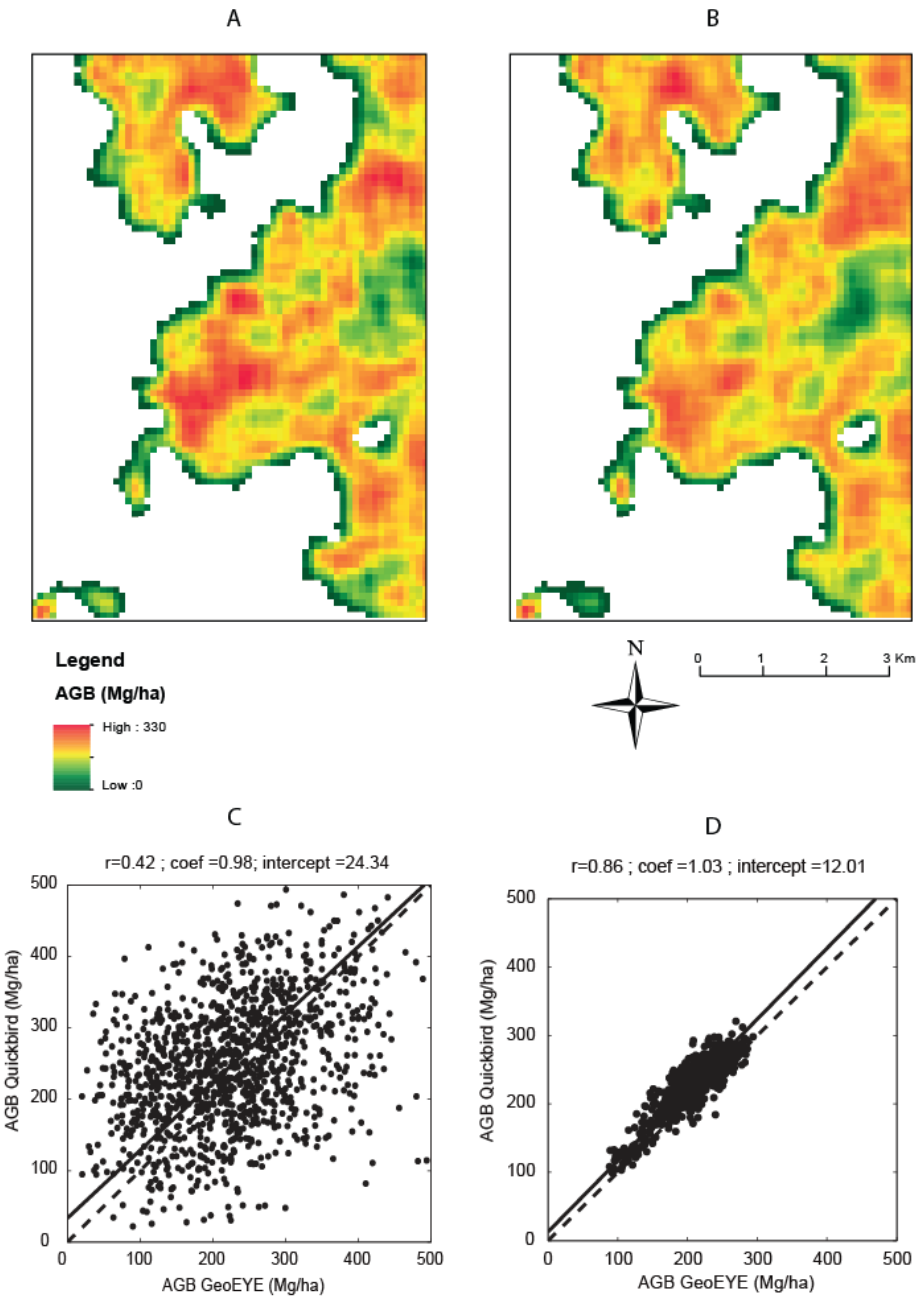

Figure I- 11. Comparison between aboveground biomass maps (in Mg per hectare) predicted (pixel resolution = 100 m) from each of the two satellite images, A/ Geoeye-1 (acquisition parameters: view zenith angle = 16.56°; sun azimuth angle = 125.3°; sun elevation = 57.2°, sun-sensor azimuth angle = 31.78) and B/ Quickbird-2 (acquisition parameters: view zenith angle = 5.4°; sun azimuth angle = 53.5°; sun-elevation = 49.4°, sun-sensor azimuth angle = 95.1°,). C/ Scattergrams from pixelwise comparisons of the biomass values predicted from each image, using C/ a pixel resolution of 25m and D/ a pixel resolution of 100m with moving average filter of order 2. C/ and D/, the dashed and continuous line stand for the 1:1 and fitted lines, respectively.

Specific texture-AGB interactions

To understand the structural information provided by our AGB models based on FOTO metrics and the practical meaning of texture classes, we described the variation of the Fourier r-spectra within each class, from low to high predicted AGB (Figure I-12). For each class, we plotted from left to right the mean r-spectrum for the set of windows corresponding respectively to percentiles 0, 25, 50, 75 and 100 of the distribution of windows scores along significant texture axes in the AGB model. In addition, an arbitrary window was randomly picked to illustrate the corresponding canopy aspect at extreme values.

In the fine texture class (Figure I-12A), i.e., the high frequency domain (Figure I-5), the predicted AGB gradient ranged from a dominance of very high frequency (F150 to FMAX, Figure 8A, left) to smoothed contributions of all frequencies with, at the end, a slight gap in low frequencies (F30-F40, Figure 8A, right). This model is mainly driven by a negative correlation with *PCA*1 and a positive one with *PCA*3 (Table I-2). Concretely, this corresponds to a transition from closed canopies dominated by small crowns (Figure I-13), i.e., pioneer forest with AGB levels as low as 50 Mg/ha, to closed canopy mature forest with larger crowns and very high AGB levels (approximately 400 Mg/ha).

For the coarse texture class (Figure I-12C), i.e., in the low frequency domain (Figure 5), the AGB model is driven primarily by *PCA*2 (Table I-2). Counter-intuitively, the highest AGB values (c.a. 360 Mg/ha) occurred for r-spectra showing a dominance of very low frequencies (Figure I-12C, right), corresponding to an open *Marantaceae* understory with a few large emergent trees (FMIN) pushing the AGB to high levels. The transition to a low AGB was caused by an increase in the contribution of intermediate frequencies (F80-F100) induced by a decrease in the abundance of large trees (F10) in favor of smaller trees with a globally lower AGB (ca. 90 Mg/ha) and a closed canopy (Figure I-14). For this group, the field plots did not cover the full range of *PCA*2 values. AGB values are likely to decrease for unsampled very coarse textures, i.e., below a certain density of large trees.

Finally, in the intermediate texture class (Figure I-12B), we observed a transition from a dominance of intermediate frequencies (F100, Figure 8B, left) with low AGB levels (ca. 85 Mg/ha) making the transition from the lower AGB situation in the coarse texture class (Figure I-12 C1), to a smoothed contribution of all frequencies with a small gap in intermediate frequencies (F100, Figure I-12 B5), matching almost perfectly with the higher AGB levels (ca. 390 Mg/ha) of the fine texture class (Figure I-12 A5). The highest AGB levels in this group were obtained for r-spectra exhibiting an increase in low frequencies induced by the effect of some large emergent trees (Figure I-15).

It is interesting to note that, although the AGB-texture models were derived independently in each group, the transition between the groups in terms of AGB prediction and the corresponding textures occurs in a continuous and coherent way when considering the transitions between the extreme spectra of adjacent texture classes.

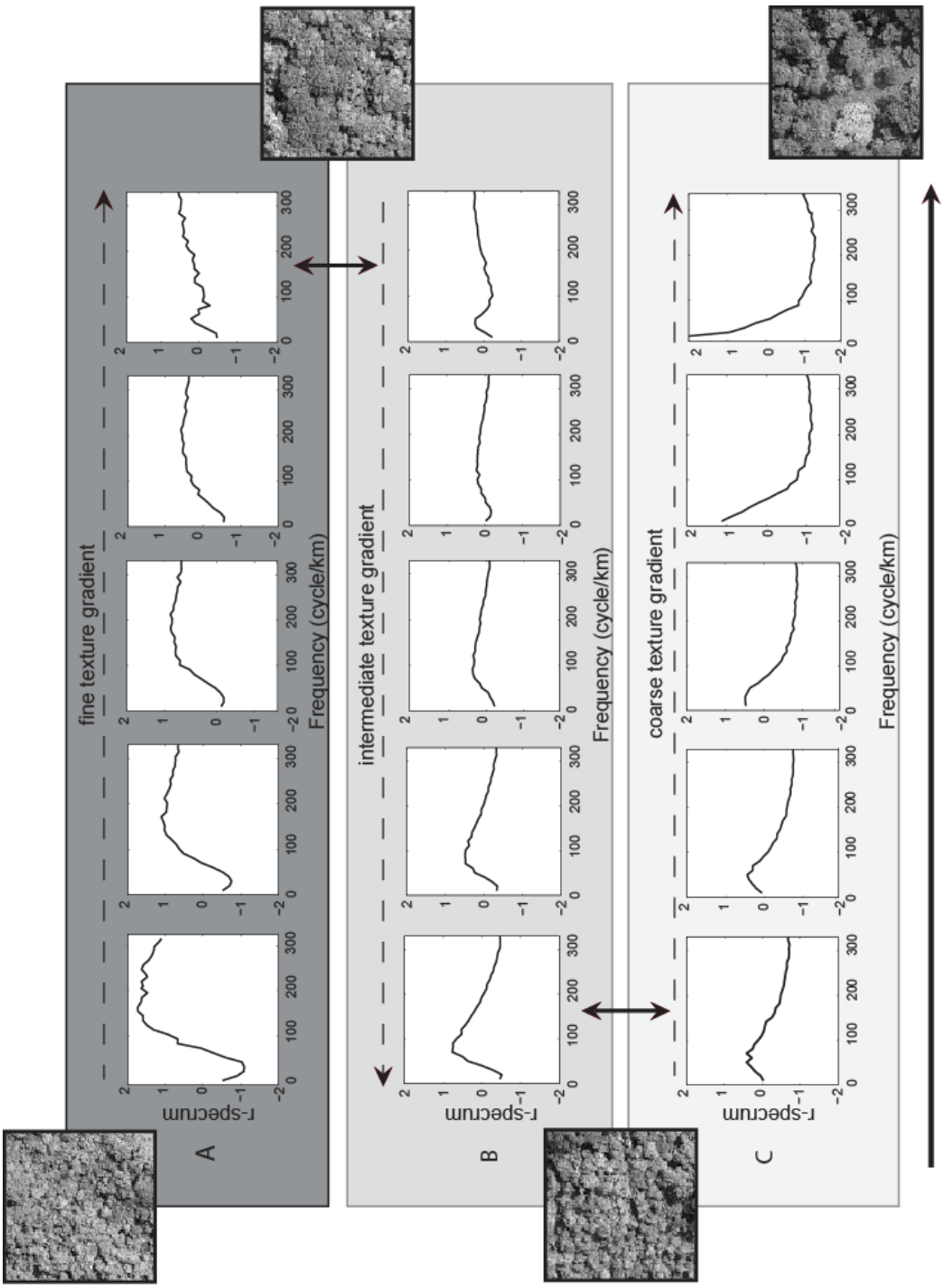

Figure I- 12. Typical examples showing the variation or Fourier r-spectra and canopy windows (Quickbird-2 scene) along the main biomass gradientin the different texture classes considered, i.e. fine (A), intermediate (B) and coarse (C) texture. From left to right, are plotted respectively the percentiles 0, 25, 50, 75 and 100 of the distribution of windows scores along the significant texture axes obtained using the 3-classes piecewise model.

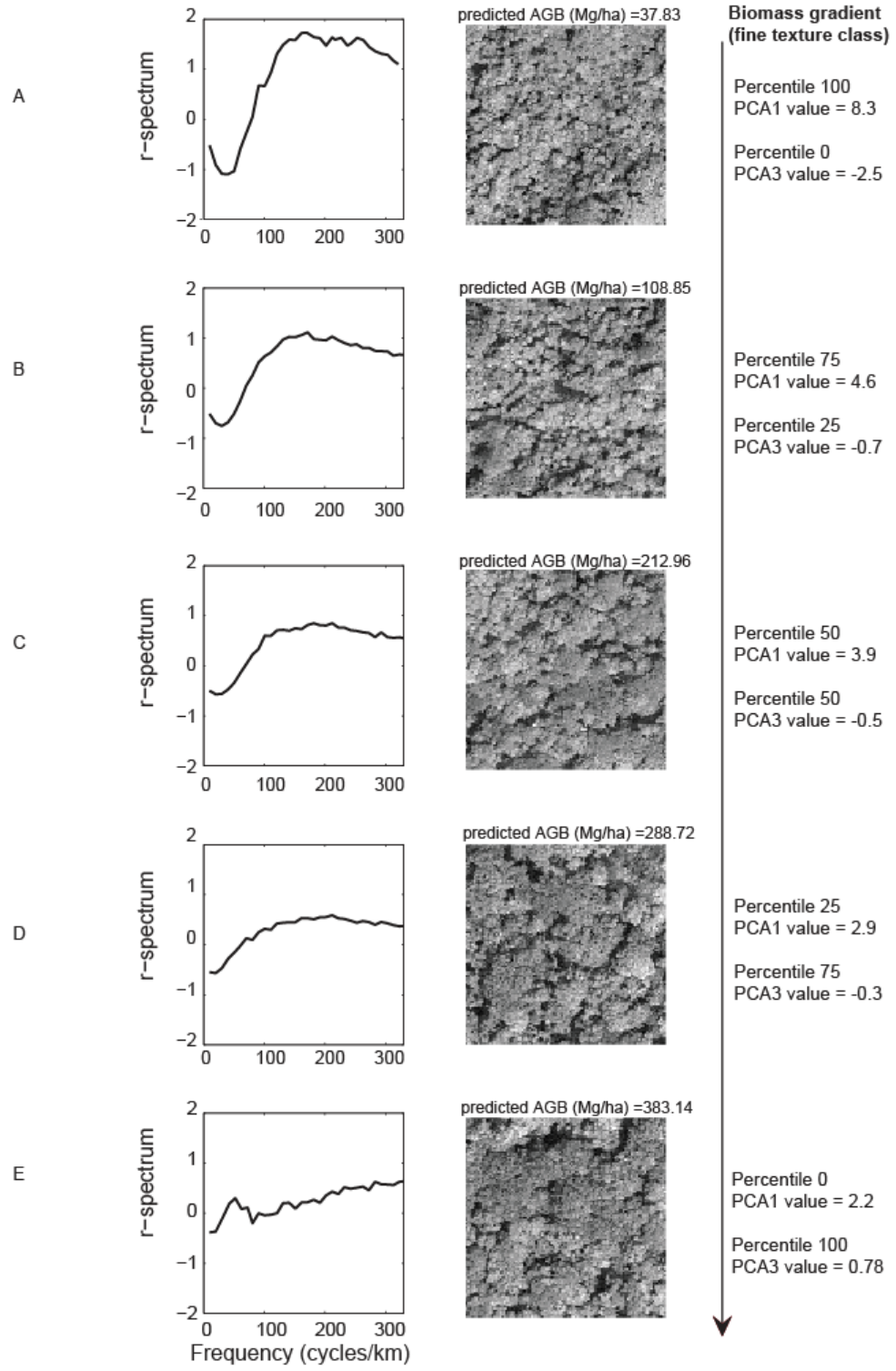

Figure I- 13. Typical examples showing the variation or Fourier r-spectra and canopy windows (Quickbird-2 scene) along the main biomass gradient in the fine texture class. A to E correspond respectively to percentiles 0, 25, 50, 75 and 100 of the distribution of windows scores along the significant texture axes obtained in that class using the 3-classes piecewise model.

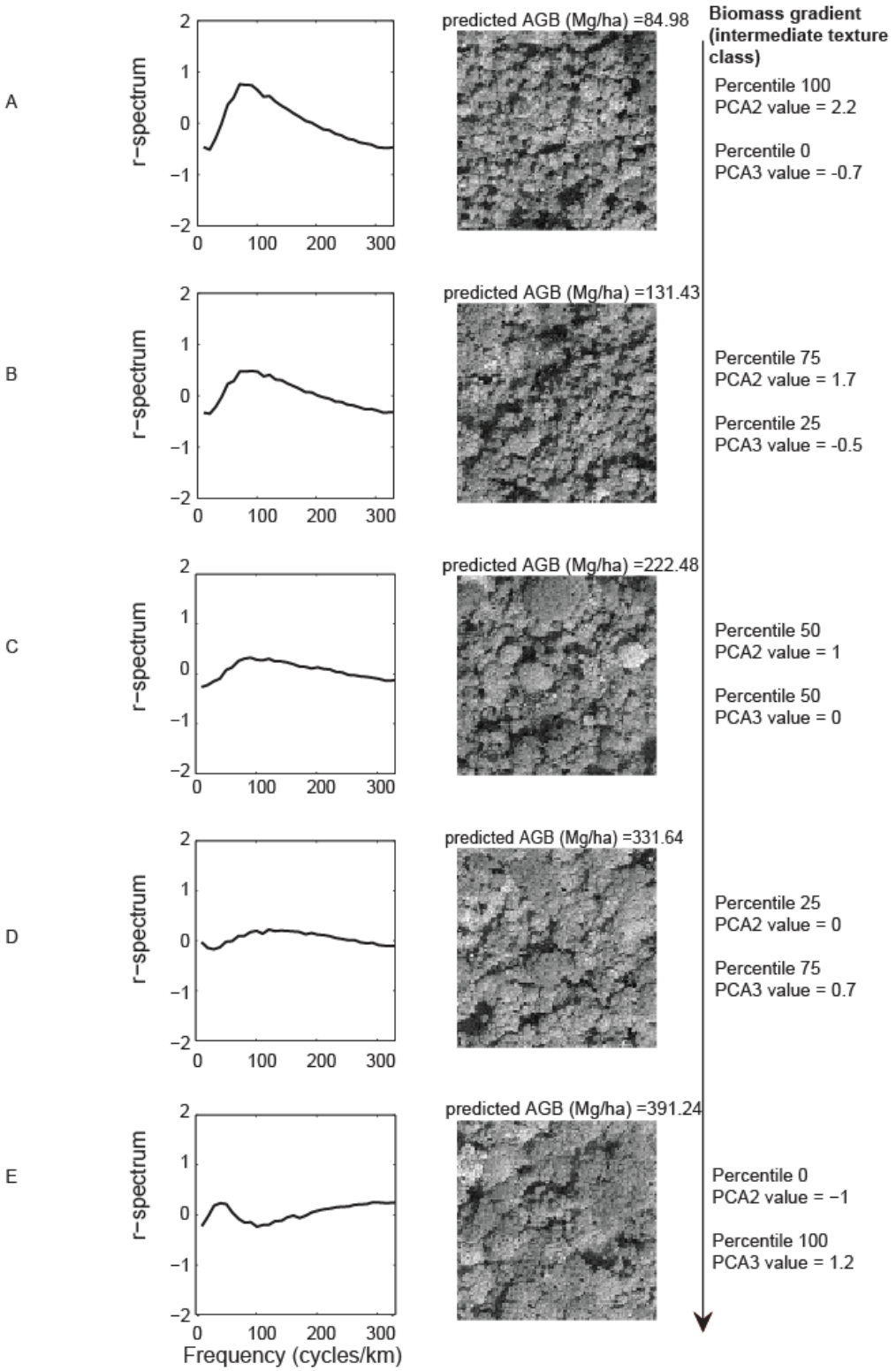

Figure I- 14. idem Figure I-13 for intermediate texture class

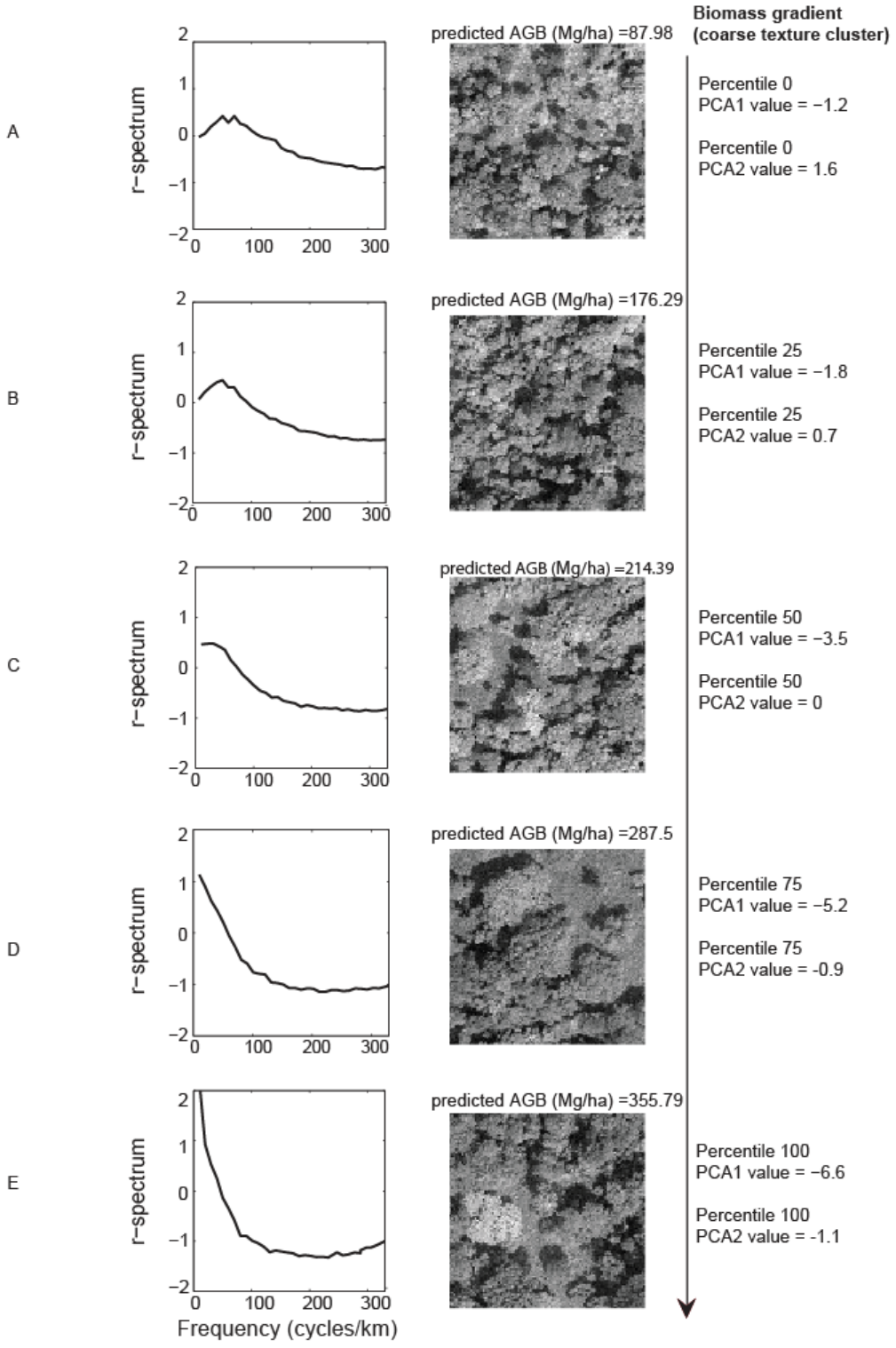

Figure I- 15. idem Figure I-13 for coarse texture class

Discussion

In the present paper, we showed that simple textural features extracted from VHR optical images offer prospects for regional and multi-temporal mapping of AGB in a wide variety of tropical forest structures.

First we demonstrated the possibility to combine VHR images acquired in contrasted instrumental conditions and, consequently, important visual differences in canopy aspect (Figure I-13 B-C) by producing equivalent AGB maps from parallel FOTO procedures. The GE1 image has a backward sun-view azimuth angle, where tree shadows are masked from the sensor, and a higher sun elevation compared to the QB2 image. Consequently, initial texture values along *PCA* axis 1 were much higher for the GE1, indicating finer textures, coherent with r-spectra with a stronger contribution of higher frequencies. This is consistent with previous studies on the sensitivity of image texture to illumination and viewing geometry (Bruniquel-Pinel and Gastellu-Etchegorry 1998, Barbier et al. 2011). In addition, the view azimuths of both images are opposed, as one image is oriented eastward and the other westward. The addition of those discrepancies introduces a maximum level of noise in the data, as different canopy features may be observed, diminishing the correspondence between the textural values of individual windows. The correction we proposed, although conditioned for the moment by the existence of a significant overlap between images, shows the feasibility of eliminating those sources of bias. Other less restrictive approaches have also been proposed (Barbier et al 2011), based, for instance, on the construction of an empirical bidirectional texture function using a large imagery dataset. Theoretical approaches are also under development using radiative transfer models (Barbier et al. 2010, 2012).

We also illustrated how FOTO indices can be applied to predict AGB without saturation from 26 up to 460 Mg/ha in very heterogeneous forest stands such as those encountered in Central Africa. In contrast with previous works on more homogenous closed canopy forests (Proisy et al. 2007, Ploton et al. 2012), variations in texture-structure relationships among forests as different as open

Marantaceae forests, young pioneer forests and monodominant *Gilbertiodendron* forests required adjusting several distinct linear regression models established for distinct parts of the textural domain (i.e., the k-means textural classes). In this study, the best AGB predictions were obtained with three textural classes, the main limit being the number of ground observations per class. In particular, despite a large dataset of 26 one-ha plots spread across a 400 km² area, only four plots were located in *Marantaceae* forests.

Predictions dramatically improved when using as few as two k-means classes, illustrating the intuitive contrast between closed canopies, in which AGB increases as canopy grain becomes coarser, and open canopies, which exhibit the opposite trend. In statistical terms, the model proposed for predicting AGB from canopy texture is analogous to piecewise linear regression (Hastie et al. 2009), except that the splits were defined *a priori* based on the textural variability in the whole image dataset. Moreover, based on the comparison of AGB prediction from random clustering and texture-based clustering, we showed that the increase of model quality was not a consequence of a random sample size decrease due to the clustering.

Although continuity was not constrained between models developed in the different classes, the resulting models did show coherent transitions between classes in terms of the AGB predicted at class limits. The choice of a non-supervised and non-hierarchical (k-means) classification method was relevant at this early exploratory stage, given that the very existence of textural groups had to be tested. Now that it has been established, a more controlled stratification procedure may be desirable. It might also be relevant to perform this pre-stratification based on independent, non-textural, information such as spectral properties or other pertinent remotely sensed signals. In the current approach, it is clear that the classes need to contain a minimal degree of textural variability if one wants to detect any useful inner gradient. It is likely that other texture-structure relationships may exist that correspond to forest types unrepresented in our sampling, especially considering other monodominant forests such as *Aucoumea klaineana* or *Musanga cecropioides*. Nevertheless, considering the diversity of forest structures already present in our study area, the complexity of

texture-structure relationships should rapidly reach its limits when generalizing the approach at the scale of Central African humid forests. To build a global map, it will be necessary to identify all typical texture classes and to take care of *PCA* gradient representativeness to define an accurate sampling design. A different approach could be to aim for more homogenous texture classes in the framework of machine learning approaches, such as regression tree or partial least square regressions (Hastie et al. 2009). However, despite expected model improvements, machine learning methods are strongly correlated to dataset specificities and may lead to a loss of clarity in model understanding and interpretation along with ecological processes.

AGB predictions were validated both by cross-validation and even more importantly by cross-checking the predictions based on each satellite image (Figure I-11). Model parameters resulting from the cross-validation were stable (Table I-3) as well as most of AGB predictions for the tested samples (Figure 19). Only some particular sites, such as the *Uapaca guineensis* colonizing forests, presented important errors. This highlights their importance in model calibration and the need to increase their representation in the sampling design.

The precision and accuracy of our predictions meets the eligibility criteria of the IPCC for a MRV method (i.e. with 20% of RSE (Houghton et al. 2009)) and are only surpassed, for equivalent areas of a few hundred km², by small footprint airborne LiDAR methods (Zolkos et al. 2013), for a price on average of a tenth of the latter, or even less (but see Barbier et al 2010, Ploton et al. 2012 for applications using free imagery from the Google Earth © digital globe). Even so, given the capacities of available satellites and weather conditions over equatorial forests, wall to wall even at a yearly time step is unconceivable. However, within current schemes in which airborne LiDAR is playing an increasing role as a mean to obtain detailed forest structural information at the landscape scale, VHR imagery texture should bring complementary quantitative and qualitative information at a moderate cost. Where LiDAR-derived AGB predictions are generally based on forest height metrics (e.g., Asner et al. 2010, Saatchi et al. 2011, Baccini et al. 2012), those coming from the FOTO method applied to VHR imagery come from the horizontal distribution of crown sizes in the canopy of dense forests,

therefore yielding a potentially complementary metric. In this respect, forest type dependency in structure-texture relationships mirrors the dependency between airborne LiDAR derived canopy height and AGB, which is constant only within forests following a given H-DBH or H-Basal Area relationship (Asner et al. 2014). Although allometries involving crown characteristics have been thus far hardly been studied in tropical dense forests, there are reasons to assume that crown-DBH relationships may be less variable across species and tree statures than crown-height correlations (Muller-Landau et al. 2006, Chave et al. 2006, Antin et al. 2013).

As variation of forest AGB results mainly from the abundance and the size of the largest canopy trees (Chave et al. 2001, Slik et al. 2013), it is obvious that canopy grain on VHR scenes should contain relevant AGB related information. However, other aspects such as canopy vertical structure, crown size frequency distribution, crown architecture, gap abundance, clumping and plasticity, or the presence of spectrally very distinct crowns such as those of large emergent leafless trees, could all play an important role on texture indices. To make progress in the identification of the structural variables conditioning canopy texture, theoretical approaches may offer a promising avenue, as it is possible to generate 3D stand models based on varying theoretical assumptions, and then simulate the radiative transfer within the scene and obtain texture images (Gastellu-Etchegorry 2008, Barbier et al. 2012, Morton et al. 2014). Such a theoretical approach could show if texture allows distinguishing between canopies produced using the perfect plasticity approximation (Purves and Pacala 2008, Purves et al. 2008, Bohlman and Pacala 2012) or a more rigid crown placement as in the TROLL (Chave 1999) or SORTIE models (Pacala et al. 1996), or to quantify the differences in canopy structure obtained using the prediction of the metabolic theory (Enquist and Niklas 2001, Enquist et al. 2009) against those of the demographic theory (Coomes et al. 2003, Muller-Landau et al. 2006).

Another important aspect to consider is the temporal hindsight provided by the available VHR optical collections. IKONOS satellite data provide 14 years of archive data, whereas in many places, airborne photographs offer more than 50 years of information, although with greatly increased challenges in terms of acquisition geometry. If visual photointerpretation has had a long and fruitful history in

forestry, it surprisingly never translated into modern, semi-automated image analysis methods. This is due to methodological impasse related to the extraction of relevant spatial statistics and the control of instrumental effects that have frustrated attempts to use VHR imagery as a tool for consistent quantitative studies of forest structure. As demonstrated here, such issues are now being overcome, offering new opportunities, notably towards REDD+ initiatives in the tropics.

Acknowledgments

We are grateful to the FRIA (FNRS) and ERAIFT for support and funding, to the WWF Belgium (Geert Lejeune, Gregory Claessens), WWF DRC (Raymond Lumbuenamo, Bruno Perodeau, Menard Mbende, Jean Mobuli) and MbouMonTour (Jean-Christophe Bokika) NGOs for logistical support, to WWF Germany for assistance with image acquisition, to Jean Lejoly (ULB, Belgium), Luc Pauwels (Meise - National Botanical Garden of Belgium, Belgium), Jean-Louis Doucet and Jean-François Gillet (ULg – Gembloux Agro-Bio Tech, Belgium) for advice and aid in botanical identifications, to the local community chiefs from Nkala and Mpelu villages for authorizations, and particularly, to Pala Eyiano, Ngamba Mongama, and Americain Mopanga for fieldwork assistance.

THESIS DISCUSSION

In this thesis, our main objective was to better understand the distribution of AGB throughout Central African forest structure. In the present section we first discuss our main results, their consequences in the REDD+ context and in particular on the different levels of measurements involved in AGB estimations. We then discuss potential perspectives in ecology, focusing on forest quantitative theories and on tropical forests species richness distribution throughout the diametric structure. Potential biases in AGB estimations related to the 'edge effect' are then discussed followed by the 'limits and perspectives' section. We then conclude by the 'key findings' as a take-home message.

1. Key findings and consequences on the “error propagation” issue of AGB estimations

- From the AGB of the tree to the AGB of the forest

We showed that largest trees hold an important share of total forest AGB (paper 2) and that the error relative to the use of WSG -the second best predictor of the AGB of the tree (Chave et al. 2005, Fayolle et al. 2013)- from global databases is negligible when compared to field measurement of WSG (paper 3). These two results bring new elements in the understanding of AGB variations both at the tree and at the forest scale.

The importance of largest trees was expected since formulas to estimate its AGB rely on tree basal area which is square-related to their DBH (e.g. Brown 1997, Clark and Clark 2000, Chave et al. 2001, an illustration for *Klainedoxa gabonensis* and *Staudtia kamerunensis* is provided in Figure D-1). In order to provide to the reader a concrete idea of the importance of largest trees in forest AGB, here are some numbers on tree AGB estimations based on our dataset in Malebo (allometric model: Chave 2005, equation for moist forests):

- The minimum AGB recorded : ~11 kg (*Xylopia aethiopica*; dbh=10 cm);
- The average AGB of trees with a DBH between 10 and 20 cm : ~93 kg;
- The average AGB of trees with a DBH superior to 50 cm : ~6900 kg;
- The maximum AGB recorded : ~68 000 kg (*Baillonella toxisperma*; dbh = 203 cm);

The average error in AGB estimation inherent to the use of allometric model is about 20 % (Chave et al. 2005), consequently this means the error on AGB estimation of the biggest tree (~13 000 kg) is greater than the sum of the AGB of a hundred trees between 10 and 20 cm (~9300 kg). Therefore, a small error on the estimation of large trees AGB has much more consequences on forest-scale AGB estimation than any errors on the estimation of small trees AGB, even when accounting small trees present a greater number of stems than large trees when regarding to the inverse relationship between the size and the frequency of trees (Morse 1985, Figure D-2). Consequently, to decrease the risks of error propagation between AGB estimation at the tree scale and AGB estimation at the forest scale, here we suggest more attention and more effort should be put in the assessment of the AGB of largest trees. For example, the use of allometric models with more predictors than classical models, e.g. considering tree tapering and crown characteristics (Goodman et al. 2014) and the increase of field sampling measurement on largest trees (multiple measurement of total height, particular care on buttresses) should both decrease the error on AGB forest-scale estimations. Furthermore, as we showed that about 1.5 % of species hold 50 % of the AGB of 9 sites widespread in Central Africa, i.e. the BHD species (paper 2), another possibility to decrease existing errors could be to consider the use of mono-specific allometric models (18 species for the 9 sites investigated) to estimate AGB of BHD species and multi-species models for the remaining 98.5 % species.

Among the predictors commonly used in allometric models, the WSG has often been questioned because WSG values from global wood database (e.g. Dryad, Zanne et al. 2009) are often preferred to actual field measurement (Clark and Kellner 2012). Such approximation completely neglects potential intra-specific variation in WSG and potential site dependency. However, we showed in paper 3 that species-average WSG measured in our site did not differ significantly from species-average WSG extracted from global databases when considering the entire pool of species at the forest-scale. This confirms previous results obtained by Fayolle and colleagues (2013) and Chave and colleagues (2014). As a consequence, we suggest that the use of species-average WSG extracted from wood databases is a minor source of error in the estimation of forest AGB.

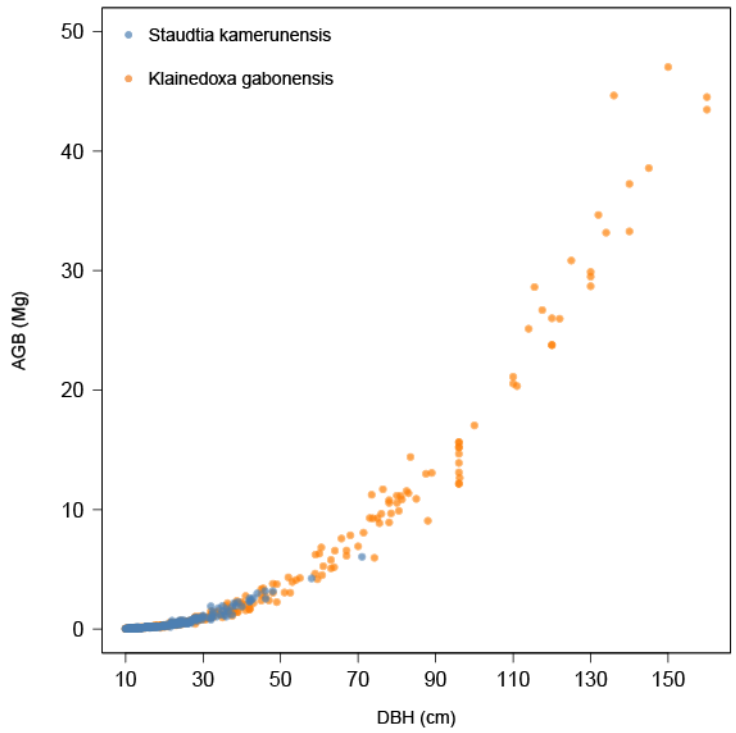

Figure D- 1. Evolution of the AGB of trees with their DBH. The figure is illustrated for *Staudtia kamerunensis* (blue) and for *Klainedoxa gabonensis* (orange).

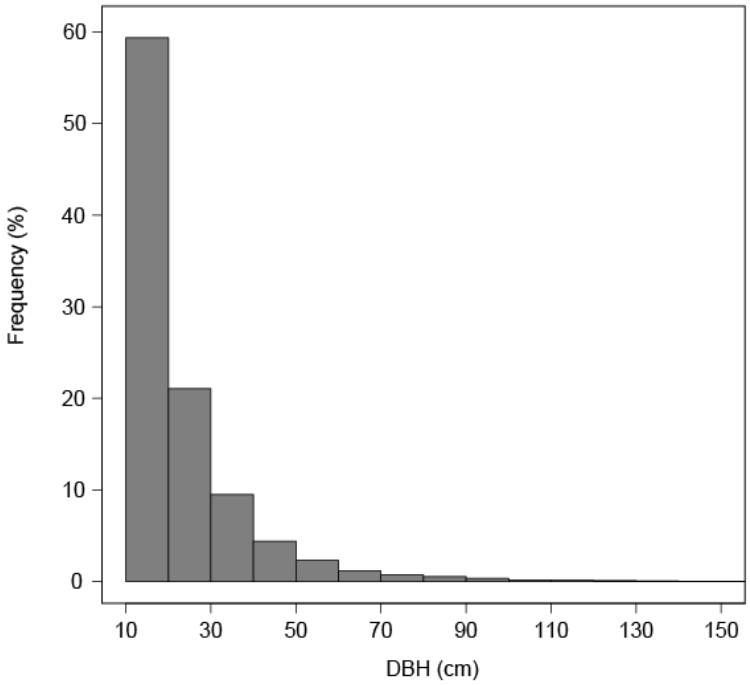

Figure D- 2. Histrogram of the size-frequency distribution of all the stems recorded in Malebo.

- From the AGB of the forest to AGB mapping of the region

In the present thesis, we established a model allowing to assess forest AGB from varying number of largest trees for Central Africa (paper 2). In particular, we showed that by measuring only 5 % of the largest stems with a DBH ≥ to 10 cm of a given 1-ha plot, the error on the estimation of the entire plot AGB is only about 14 %. These results provide the opportunity to investigate the development of cost-effective methods to survey tropical forest AGB. Lower cost of forest survey should open perspective to increase the current sampling cover of tropical forest. This should decrease the uncertainties of current regional maps of AGB prediction (e.g. Saatchi et al. 2011, Baccini et al. 2012) since the lack of ground dataset (Mitchard et al. 2013, 2014) presenting the appropriated size for remote-sensing products (Réjou-Méchain et al. 2014) has recently been reported as one of the most important issue in AGB mapping. The development of new methods to survey tropical forest AGB should therefore focus on the trade-off between field cost (plot size, number of plots per area unit, number trees per area unit) and AGB prediction quality (error of the "largest tree" model, error related to the pixel-to-ground relationship). In practice, we suggest to develop such tool on the basis of large existing sampling designs for which the coordinates of each single tree are recorded (e.g., CTFS sampling designs of Korup 50-ha; or Ituri 4*10-ha). In each site, several sampling scenario must be tested which allow to assess the sampling effort vs. errors in AGB estimations. Such tool would allow REDD+ managers and scientists to adapt their strategy according to their objectives, their financial budget and their priorities in terms of prediction accuracy and precision.

The quality of AGB prediction in our paper 1, presenting an error of 15 %, rely on the specificity of the remote-sensing method developed, i.e. the FOTO method, but also on a fair ground sampling effort, i.e. with 26 1-ha plots over an area of about 400 km². This corresponds to 0,065 % of the area sampled. Assessing the relationship between the relative area sampled and the error in AGB prediction from any remote-sensing product could provide interesting information about the minimum sampling effort required for each existing remote-sensing product. Such relationship should present an asymptotical trend from varying shape depending on the remote-sensing product which facilitates the identification of potential critical threshold.

The main results discussed in the present section are summarized in Figure D-3, which is based on the thesis framework developed in the Introduction part. Regarding to the error propagation issue, we show that we have to account at least for a combination of 20 % of error inherent to the allometric model when estimating the AGB of the tree, 14 % of error using largest trees model with the 20 largest trees when estimating the AGB of the forest with 1-ha plots and 15 % of error in AGB mapping due to uncertainties related to the FOTO method. Others sources of error exist but are not accounted here: issues in tree height measurement or the use of DBH-H allometries, the impact of the plot size on field estimation accuracy and on remote-sensing product geolocation and pixel correspondence issue.

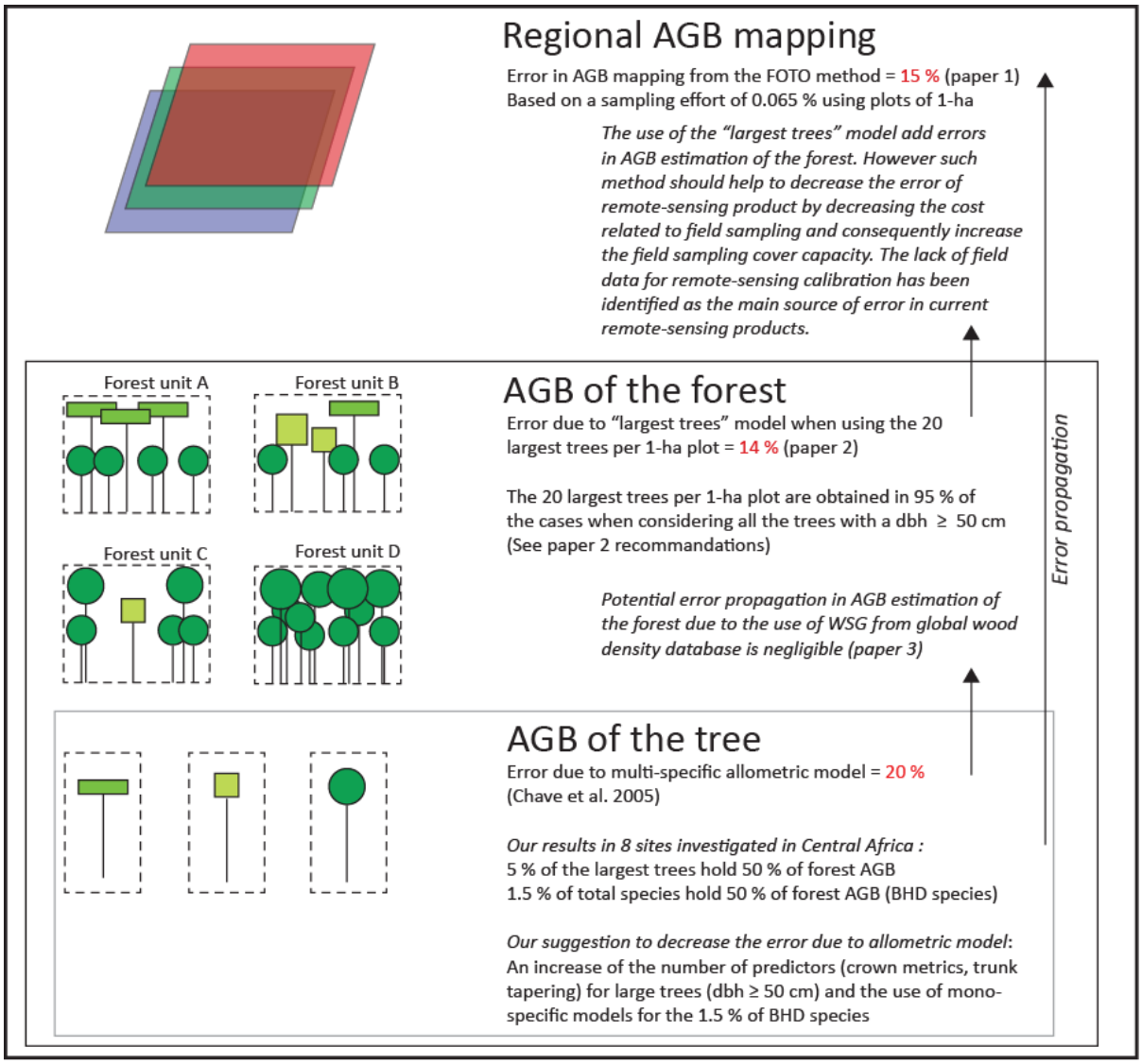

Figure D- 3 : Summary of the key findings related to the error propagation issue, illustrated in the original thesis framework.

2. Perspectives in Ecology

2.1. Forest quantitative theories

Another opportunity to investigate the importance of the largest trees might be to consider quantitative theories. One of the most interesting theory developed is the so-called West-Brown-Enquist (WBE) metabolic scaling theory (Enquist and Niklas 2001, West et al. 2009, Enquist et al. 2009). This theory is based on the assumption that the body size of a given biological organism affects its rates of biological structures and processes from cellular metabolism to population dynamics (West et al. 1997). From this assumption, one of the most prevalent allometric pattern can be characterized: the inverse relationship between the body mass and the abundance of a given organism (Enquist and Niklas 2001). Therefore, such theory might be applied to describe the size-frequency distribution of trees of natural forests. Among the simplifying assumptions made by the theory to describe the forest-stand structure (see West et al. (2009) for details), one in particular draws our attention : the inverse relationship between size and abundance of trees is invariant in a natural forest (Enquist and Niklas 2001). Based on this assumption, the whole forest structure might be approximated from the abundance of trees in a given size class. Both theoretical and empirical works (Coomes et al. 2003, Muller-Landau et al. 2006, Enquist et al. 2009) showed, however, that non-competitive induced mortality (Enquist et al. 2009) leads to an overestimation of the density of the largest trees by the metabolic scaling model predictions. Non-competitive induced mortality are attributed to exogenous causes of mortality which particularly hit the largest trees (Enquist et al. 2009). Among those, we can list droughts, winds, repeated wildfires, competition with invasive plants, air pollution, disease, herbivory and insect attack (Anderegg et al. 2012, Lindenmayer et al. 2012).

Different assumptions have been made to understand this overestimation but its explanation is still debating. On the one hand, the WBE theory considers that the overestimation is part of the theory as it appears to be systematic (Enquist et al. 2009). On the other hand, Coomes and colleagues (2003) suggest that the frequency of the largest trees is overestimated due to the combination of the

increase trees mortality rate with age and random exogenous parameters. Because this last assumption implies that stochastic events also drive the frequency of large trees, this would prevent any prediction of the forest-stand structure from the largest trees.

Therefore, the successful prediction of the entire forest-stand AGB from the AGB of largest trees obtained in paper 2 argue in favor of the WBE theory and meets conclusions of Rutishauser and colleagues (2010) suggesting forest structure is mainly driven by endogenous factors (e.g., competition for resources) and not external forcing.

In practice, the WBE theory uses an inverse power-law to characterize, on a logarithmic scale, an invariant size-frequency distribution of trees (Enquist and Niklas 2001). Derived from the results of paper 2, we plotted here the cumulated frequency of trees for each field plot according to an inferior DBH limit from our dataset in Malebo (Figure D-4). We compare the WBE theory (red dotted line) to the observed trajectories of each plot (black to grey dots). The gradient of plot AGB is represented in grey levels, from dark grey (low AGB) to light grey (high AGB). We observe that the distance between plots trajectories and the WBE theory (roughly estimated here as the difference between expected frequency and observed frequency at each DBH value) increases with the limit of the considered tree size (DBH). This emphasizes the statement on the overestimation of the frequency of largest trees in the WBE theory (Coomes et al. 2003, Muller-Landau et al. 2006, Enquist et al. 2009). However, as mentioned by Enquist and colleagues (2009) and as suggested by our results in Paper 2, this deviation appears to be systematic. Interestingly, it also appears to be systematically related to the variation of the AGB of the plot. All the plots deviate from the theory similarly, with high AGB plots showing the latest deviations (i.e. a deviation occurring for larger DBH sizes; Figure D-4).

The parameterization of these cumulated distributions would be particularly interesting for future research in tropical forest ecology as it might allow describing precisely the entire forest-stand structure (e.g; the frequency of trees in each class size) from a few indicators (e.g. largest trees). This might help us to better describe the structural differences between forests and to better understand their dynamics and their interactions with bio-climatic determinants. However, the non-linearity of

the pattern makes it difficult to interpret. Therefore, here we provide several suggestions which might overcome this issue:

- We could consider the distribution of the cumulated AGB of trees per plot instead of the distribution of the DBH. This may potentially correct the overestimation coming from exponential relationship between DBH and AGB of trees;
- Assuming the light is the main driver of forest-stand structure, it may be more appropriate to account for the distribution of tree crown size instead of the DBH;
- As the deviation to the model appears to be relatively abrupt, we could make the assumption of the existence of two different structures: the structure of trees belonging to the canopy (in full light exposure) and the structure of the understory (in the shadow). We may further model them separately.

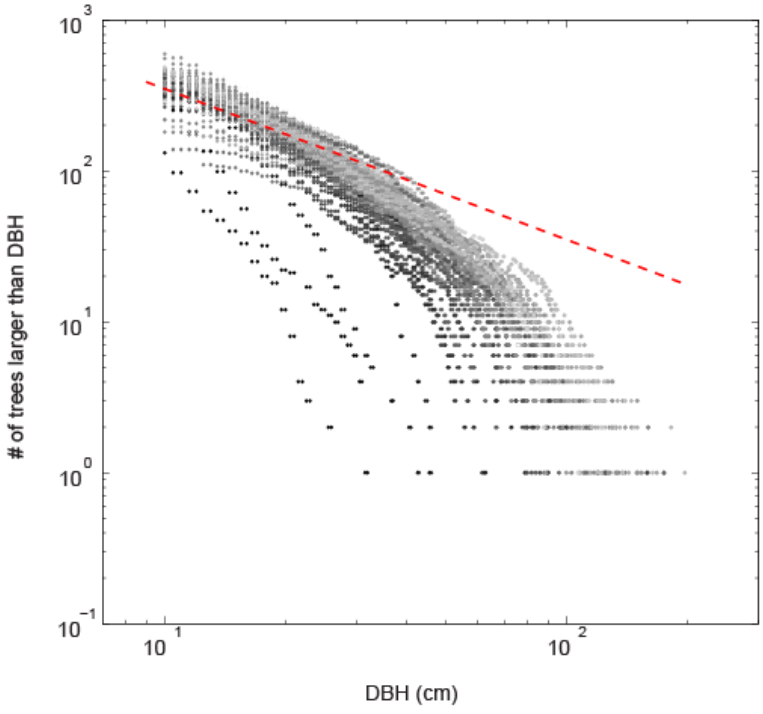

Figure D- 4. Inverse cumulated number of trees presenting a size superior or equal to DBH. The red dotted line represent the prediction from the WBE theory, grey dotted trajectories represent the observed values in 32 1-ha plots (low AGB: dark grey; high AGB: light grey).

2.2. Forest species richness

The opportunity to use the species richness within the largest trees as an indicator of the global species richness (see paper 2) of the forest was not expected and leads to new perspectives in the understanding of the species richness distribution within tropical forests.

Considering the trees of the understory have a non-null probability to reach the canopy, basically depending on growth and mortality rate (Coomes et al. 2003, Muller-Landau et al. 2006), largest trees species richness may be expected to be a good indicator of total species richness. Interestingly, using simple linear regression models, different prediction quality (R^2) and coefficients estimates (slope and intercept) were observed depending on the site and on forest type considered (paper 2, Figure II-2). Such variations could be related to forests guilds composition, in terms of light-demanding and shade-tolerant percentage, which must influences growth and mortality rates and consequently the recruitment of understory species in larger size classes (Wright et al. 2003). Here we observed that *Gilbertiodendron dewevrei* monodominant forests presented the biggest slope and the best coefficient of determination ($R^2 = 0.7$). These forests are known as old-growth successions (White 2001b, Makana et al. 2011, Gillet and Doucet 2012), most of their species consequently belong to shade-tolerant guild. Shade-tolerant species of the understory trying to reach the canopy may be assumed to suffer less from the inter-specific competition than light-demanding species. Such hypothesis has to be considered with caution and deserves further investigations on the distribution of species richness across the diametric structure of the forest.

In parallel of paper 2, in order to show whether large tree species are a random subset of the whole species pool or whether they represent a specific species richness distribution, we constructed null models where individual trees were selected randomly, independently of their size (n=999 iteration). We then compared random accumulation of species diversity with the species accumulation obtained when ranking the trees by decreasing size. This method, which has never been investigated to our knowledge, allowed us to characterize contrasted patterns in the distribution of the diversity. For instance, we illustrate on Figure D-5 the difference between a plot of Korup site (a dense mixed-

species forest) and a plot of Ituri (a monodominant *Gilbertiodendron dewevrei* forest). We can observe that the 'so-called' mono-dominant forest-stands may present lots of species in one plot (~50) but present less than 20 % of the total number of species in the 100 largest trees. Furthermore, species richness accumulation from the largest to the smallest tree presents a very different pattern than expected with random selection. Such "sigmoid" shape illustrates the dominance of *Gilbertiodendron dewevrei* in the largest size classes of trees. In contrast, more than 50 % of the total number of species is found in the 100 largest trees in the Korup plot displayed. Here, species richness accumulation from the largest to the smallest tree presents higher saturation level than expected with random selection. Indeed, we find more than 50 % of total species richness in the 100 largest trees while about 40 % were expected with the random selection. These results stress out that species richness is not randomly distributed through the diametric structure and appears related to forest typology and/or successional forest stage.

These results offer interesting perspectives to better understand forest ecosystems by quantifying and dissecting the vertical distribution (i.e. through the diametric structure of the forest) of species richness across the different size classes of a forest.

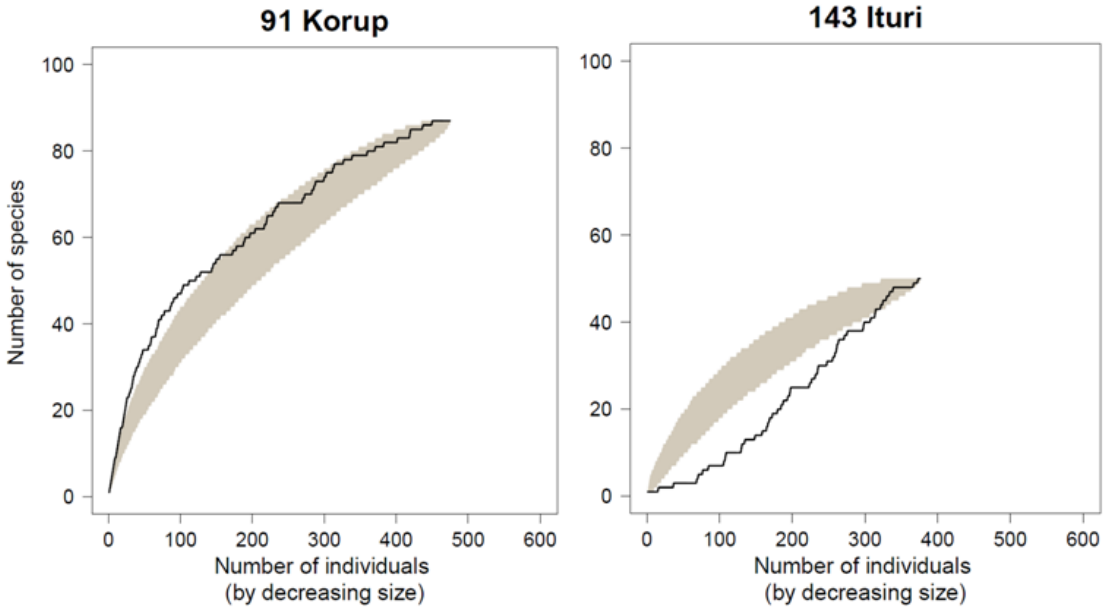

Figure D-5. Species richness distribution across the diametric structure. Comparison between ranked by decreasing size (balck line) and random curve (grey surface)

3. The 'edge effect'

In the present PhD thesis we initially considered to study the impact of an 'edge effect' on the distribution of AGB within tropical forest, and more particularly to investigate the potential error occurring when bypassing such process. The 'edge' is a central element in Landscape Ecology and is defined as the zone located at the intersection of two different patch types (Farina 2000), e.g. the savannah and the forest. This zone often presents different species composition and abundance since it contains species from both vegetations involved and is influenced by both micro-environmental properties (Forman 1995, Farina 2000).

In practice, following recommendations of Gibbs et al. (2007) and Picard and Gourlet-Fleury (2008) to study the distribution of AGB within tropical forest, we established a systematic sampling design (grid 1 km²), which is partly represented on Figure I-1 (edge plots where excluded in Paper 1). The locations of the plots were selected randomly in order to maximize the representativeness of the landscape and to avoid any statistical issues. To investigate the potential impact of an 'edge effect', the sampling design was divided in two sets of plots:

- 40 Plots of 0.25 ha at the edge of the forest (from 0 to 200 m of the forest-savannah limit);
- 15 Plots of 1 ha (further than 400 m from the forest-savannah limit).

Note 400 m were considered as a minimum to avoid the main known edge effects affecting tropical forests according to Laurance (2008).

Based on these datasets, no significant differences were found between the AGB at the core and at the edge of the forest. In addition, they presented both a wide range of AGB values (from less than 100 Mg/ha to more than 300 Mg/ha). Here we suggest this may be due to the important heterogeneity of tropical forest structure and composition, both in the core and in the edge of the forest. On the field, we observed several contrasted situations that may argue in favor of such assumption:

- Recent and old field (regrowth forest) from villagers are generally small (~1-ha) and can often be found more than 1000 meter from forest edge;

- Where the savannah is regularly burned, specific tree species are often found in the first meters of forest edges (e.g. *Pentaclethra eetveldeana*). However, such trees are quite common in the core of the forest and may present important dimensions both in the edge and in forest core (dbh ≥ 70 cm, H ≥ 25 m);
- The transition from savannah to forest is sometimes related to topography. A vertical decrease of 20 to 30 meters on the first 50 meters from the savannah often led us into dense tropical forests. For instance, plot M2P5 of Paper 1 corresponds to this situation and is dominated by *Gilbertiodendron dewevrei*, i.e. the species characteristic of Old growth monodominant forests in Central Africa. Such forest are generally related to high AGB values (cf. Paper 1 and 2);
- Marantacean forests are common in the investigated area and may be present from the edge to several kilometers within the forest. Such forest type can present various values of AGB depending on the number of remaining large trees (cf. Paper 1).

Consequently, forest cores and forest edges appear to present a large panel of structure and compositions which is reflected by a high variability of AGB in both situations. In such heterogeneous environment, no global or homogeneous 'edge effect' could be identified on forest AGB.

Therefore, we suggest this has an important consequence for studies aiming at characterizing forest AGB variations or local 'edge effects': AGB predictions methods must account for the heterogeneity of tropical forest and the spatial variability of AGB. Considering the forest core or the forest edge as a single homogenous unit could lead to important errors in AGB estimations. We showed in paper 2 that forest AGB is a question of largest trees. As a consequence, remote-sensing methods able to intercept forest largest trees metrics on each coordinates of a given raster (optical image, radar or lidar datasets) may predict forest AGB whether the coordinates considered are in the edge or in the core of the forest. The corresponding field sampling design must consequently maximize the gradient of the metric considered by the remote-sensing product and the gradient of AGB. However, when no

remote-sensing products are available prior to fieldwork, a systematic and randomized sampling design will ensure to maximize the representativeness of forest heterogeneity.

4. Limits and perspectives

4.1. Fourier Textural Ordination

The successful mapping of forest AGB from the FOTO method (paper 1), is very promising and encourages the development of a regional approach in Central Africa. However, in the first attempts recently performed in that direction, some problems in the stability and the consistency of the results have been observed (pers.comm.Barbier). This type of issue is generally attributed to the large amount and variety of VHR remote-sensing products which need to be combined for a regional approach. This leads to potential important differences in terms of sensors and acquisition conditions, which are complex to correct when there is no overlaps between the scenes (differences in sun-view-sensor geometries). In addition, using a large amount of scenes requires a large amount of field datasets for calibration and validation.

Here we suggest other sources of bias which need to be investigated and addressed to solve the lack of stability and of consistency of the results:

- We should define properly the textural clusters (i.e. the group in which we develop each prediction model of AGB). We propose to use a supervised classification method instead of a k-means classification. Because with a k-means method, the identified clusters depend on the properties of the scene investigated. Therefore, such clusters may vary from one scene to another;
- We should properly identify the influence of acquisition parameters on texture and on the potential AGB prediction. We suggest to simulate forest plots based on two different entries : (i) the number of large trees and (ii) the understory cover.

4.2. Wood density profiles

Two main limits can be identified in our study on WSG profiles: the lack of representativeness in the radial intra-individual variation of wood density and the lack of representativeness in the vertical intra- and inter-individual variation. In the framework of the impact WSG variation on the AGB of the tree, such parameters must be further investigated, at least for BHD species.

However, our results open great perspectives when considering the understanding of the decreasing trends of wood density from pith-to-bark which appear consistent within our samples. As discussed in paper 3 and in opposition to what is generally believed, we showed that the species presenting a decrease of WSG from pith-to-bark are frequent in Africa, especially considering biomass hyperdominant species (see paper 2). In paper 3, we observed that the species concerned by this decrease of WSG from pith-to-bark are mainly composed of hardwood species but not always of shade-tolerant species as sometimes mentioned in the literature (Woodcock and Shier 2002, Henry et al. 2010). While an increase in WSG from pith-to-bark makes a consensus by being attributed to light-demanding species (Wiemann and Williamson 1988), our result show that no consensus seems to be found for decreasing trends. Therefore, we suggest that further investigations should be conducted in the two following directions:

- A full characterization of the wood anatomy : an anatomical interpretation of the radial variation of WSG from pith-to-bark could provide interesting elements to understand the decreasing pattern;
- A better understanding of tree ontogeny (plant establishment, fructification, crown development,…) and its relationship with its habitat could help to formulate appropriate assumption to identify the determinant of such variations in the WSG profiles.

5. Key findings

The main results obtained in the present thesis are the following:

a. The canopy structure mirrors an important share of forest-stand structure (paper 1);
b. The distribution of AGB through the forest-stand is conserved within and between the investigated locations from western Cameroon to eastern DRC (paper 2), therefore forest-stand structure is very stable across Central Africa;
c. The 5 % largest stems AGB explain more than 90 % of total AGB variation in the investigated locations from western Cameroon to eastern DRC;
d. Largest trees convey important shares of forest-stand AGB and species richness variance in Central African forests (paper 2);
e. Only 18 species on 1194 (~1.5 %) hold 50 % of total AGB in the sites investigated in Central Africa. These are referenced as biomass hyperdominant (BHD) species. (paper 2);
f. Wood specific gravity (WSG) extracted from global database do not differ significantly from WSG estimated in the field when AGB is estimated at the forest-scale (paper 3).

These results provide concrete progress in our understanding of tropical forest ecology and carbon storage at the scale of the tree, of the forest and the Central African region. In particular, they emphasize the key role played by largest trees, and consequently highlight the importance of the canopy layer (a, c, d) in the understanding of tropical forest complexity.

In the REDD+ context, we believe our results offer new perspectives to develop cost-effective sampling strategies, which should decrease the effort and the cost of current methods, and increase the sampling cover capacity of participating countries.

BIBLIOGRAPHY

Ablain, M., A. Cazenave, G. Valladeau, and S. Guinehut. 2009. A new assessment of the error budget of global mean sea level rate estimated by satellite altimetry over 1993–2008. Ocean Science 5:193–201.

Ackerly, D. D. 1996. Canopy structure and dynamics:Intergration of growth processes in Tropical pioneer trees. Pages 619–658 *in* S. S. Mulkey, R. L. Chazdon, and A. P. Smith, editors. Tropical Forest Plant Ecophysiology. Springer US, Boston, MA.

Agrawal, A., D. Nepstad, and A. Chhatre. 2011. Reducing Emissions from Deforestation and Forest Degradation. Annual Review of Environment and Resources 36:373–396.

Anderegg, W. R. L., J. M. Kane, and L. D. L. Anderegg. 2012. Consequences of widespread tree mortality triggered by drought and temperature stress.

Antin, C., R. Pélissier, G. Vincent, and P. Couteron. 2013. Crown allometries are less responsive than stem allometry to tree size and habitat variations in an Indian monsoon forest. Trees 5:1485–1495.

Antonarakis, A. S., S. S. Saatchi, R. L. Chazdon, and P. R. Moorcroft. 2011. Using Lidar and Radar measurements to constrain predictions of forest ecosystem structure and function. Ecological applications 21:1120–37.

Asner, G. P., C. B. Anderson, R. E. Martin, D. E. Knapp, R. Tupayachi, F. Sinca, and Y. Malhi. 2014. Landscape-scale changes in forest structure and functional traits along an Andes-to-Amazon elevation gradient. Biogeosciences 11:843–856.

Asner, G. P., G. V. N. Powell, J. Mascaro, D. E. Knapp, J. K. Clark, J. Jacobson, T. Kennedy-Bowdoin, A. Balaji, G. Paez-Acosta, E. Victoria, L. Secada, M. Valqui, and R. F. Hughes. 2010. High-resolution forest carbon stocks and emissions in the Amazon. Proceedings of the National Academy of Sciences of the United States of America 107:16738–42.

Asner, G. P., and A. Warner. 2003. Canopy shadow in IKONOS satellite observations of tropical forests and savannas. Remote Sensing of Environment 87:521–533.

Baccini, a., M. a. Friedl, C. E. Woodcock, and Z. Zhu. 2007. Scaling Field Data to Calibrate and Validate Moderate Spatial Resolution Remote Sensing Models. Photogrammetric Engineering & Remote Sensing 73:945–954.

Baccini, A., and G. P. Asner. 2013. Improving pantropical forest carbon maps with airborne LiDAR sampling. Carbon Management 4:591–600.

Baccini, A., S. J. Goetz, W. S. Walker, N. T. Laporte, M. Sun, D. Sulla-Menashe, J. Hackler, P. S. A. Beck, R. Dubayah, M. A. Friedl, S. Samanta, and R. A. Houghton. 2012. Estimated carbon dioxide emissions from tropical deforestation improved by carbon-density maps. Nature Climate Change 2:182–185.

Bagchi, R., T. Swinfield, R. E. Gallery, O. T. Lewis, S. Gripenberg, L. Narayan, and R. P. Freckleton. 2010. Testing the Janzen-Connell mechanism: pathogens cause overcompensating density dependence in a tropical tree. Ecology letters 13:1262–9.

Baker, T. R., O. L. Phillips, W. F. Laurance, N. C. A. Pitman, S. Almeida, L. Arroyo, A. Difiore, T. Erwin, M. Paraense, and E. Goeldi. 2009. Do species traits determine patterns of wood production in Amazonian forests ?297–307.

Baker, T. R., O. L. Phillips, Y. Malhi, S. Almeida, L. Arroyo, A. Di Fiore, T. Erwin, T. J. Killeen, S. G. Laurance, W. F. Laurance, S. Lewis, J. Lloyd, A. Monteagudo, D. Neill, S. Patino, N. C. A. Pitman, N. Silva, and R. V. Martinez. 2004. Variation in wood density determines spatial patterns in Amazonian forest biomass. Global Change Biology 10:545–562.

Balzter, H., C. Rowland, and P. Saich. 2007. Forest canopy height and carbon estimation at Monks Wood National Nature Reserve, UK, using dual-wavelength SAR interferometry. Remote Sensing of Environment 108:224–239.

Banin, L., T. R. Feldpausch, O. L. Phillips, T. R. Baker, J. Lloyd, K. Affum-Baffoe, E. J. M. M. Arets, N. J. Berry, M. Bradford, R. J. W. Brienen, S. Davies, M. Drescher, N. Higuchi, D. W. Hilbert, a. Hladik, Y. Iida, K. A. Salim, a. R. Kassim, D. a. King, G. Lopez-Gonzalez, D. Metcalfe, R. Nilus, K. S.-H. Peh, J. M. Reitsma, B. Sonké, H. Taedoumg, S. Tan, L. White, H. Wöll, and S. L. Lewis. 2012. What controls tropical forest architecture? Testing environmental, structural and floristic drivers. Global Ecology and Biogeography 21:1179–1190.

Baraloto, C., Q. Molto, S. Rabaud, B. Hérault, R. Valencia, L. Blanc, P. V. a. Fine, and J. Thompson. 2013. Rapid Simultaneous Estimation of Aboveground Biomass and Tree Diversity Across Neotropical Forests: A Comparison of Field Inventory Methods. Biotropica 45:288–298.

Baraloto, C., C. E. Timothy Paine, L. Poorter, J. Beauchene, D. Bonal, A.-M. Domenach, B. Hérault, S. Patiño, J.-C. Roggy, and J. Chave. 2010. Decoupled leaf and stem economics in rain forest trees. Ecology letters 13:1338–47.

Barbier, N., P. Couteron, J.-P. Gastelly-Etchegorry, and C. Proisy. 2012. Linking canopy images to forest structural parameters: potential of a modeling framework. Annals of Forest Science 69:305–311.

Barbier, N., P. Couteron, J. Lejoly, V. Deblauwe, and O. Lejeune. 2006. Self-organized vegetation patterning as a fingerprint of climate and human impact on semi-arid ecosystems. Journal of Ecology 94:537–547.

Barbier, N., P. Couteron, C. Proisy, Y. Malhi, and J.-P. Gastellu-Etchegorry. 2010. The variation of apparent crown size and canopy heterogeneity across lowland Amazonian forests. Global Ecology and Biogeography 19:72–84.

Barbier, N., C. Proisy, C. Véga, D. Sabatier, and P. Couteron. 2011. Bidirectional texture function of high resolution optical images of tropical forest: An approach using LiDAR hillshade simulations. Remote Sensing of Environment 115:167–179.

Bastin, J.-F, N. Barbier, P. Couteron, B. Adams, A. Shapiro, J. Bogaert, and C. De Cannière. 2014. Aboveground biomass mapping of African forest mosaics using canopy texture analysis: toward a regional approach. Ecological Applications 24:1984–2001.

Bastin, J. F., J. P. Djibu, F. Havyarimana, S. Alongo, S. Kumba, C. Shalukoma, A. Motondo, V. Joiris, P. Duez, and J. Bogaert. 2011. Multiscalar analysis of the spatial pattern of forest ecosystems in Central Africa justified by the pattern/process paradigm: two case studies. Pages 79–98 *in* D. A.Boehm, editor. Forestry: Research, Ecology and Policies. Nova science publishers, Inc., New York.

Bates, D. 2005. Fitting linear mixed models in R. R News 5:27–30.

Beeckman, H. 2003. A xylarium for the sustainable management of biodiversity: the wood collection of the Royal Museum for Central Africa, Tervuren, Belgium. Bulletin de l'APAD.

Beer, C., M. Reichstein, E. Tomelleri, P. Ciais, M. Jung, N. Carvalhais, C. Rödenbeck, M. A. Arain, D. Baldocchi, G. B. Bonan, A. Bondeau, A. Cescatti, G. Lasslop, A. Lindroth, M. Lomas, S. Luyssaert, H. Margolis, K. W. Oleson, O. Roupsard, E. Veenendaal, N. Viovy, C. Williams, F. I. Woodward, and D. Papale. 2010. Terrestrial gross carbon dioxide uptake: global distribution and covariation with climate. Science (New York, N.Y.) 329:834–8.

Betbeder, J., V. Gond, F. Frappart, N. N. Baghdadi, G. Briant, and E. Bartholome. 2014. Mapping of Central Africa Forested Wetlands Using Remote Sensing. IEEE Journal of Selected Topics in Applied Earth Observations and Remote Sensing 7:531–542.

Bohlman, S., and S. Pacala. 2012. A forest structure model that determines crown layers and partitions growth and mortality rates for landscape-scale applications of tropical forests. Journal of Ecology 100:508–518.

Bonan, G. B. 2008. Forests and climate change: forcings, feedbacks, and the climate benefits of forests. Science (New York, N.Y.) 320:1444–9.

Bouillenne, R., J. Moureau, and P. Deuse. 1955. Esquisse écologique des faciès forestiers et marécageux des bords du lac Tumba. Page 44. Duculot, J. Institut Royal Colonial Belge, Bruxelles.

Breiman, L., J. H. Friedman, R. A. Olshen, and C. J. Stone. 1984. Classification and Regression Trees. Page 368 (C. Hall Crc, Ed.) The Wadsworth statisticsprobability series. Wadsworth, Monterey.

Brown, S. 1997. Estimating biomass and biomass change of tropical forests: a primer. Page 55 FAO Forestry Paper. Food and Agriculture Organization of the United Nations.

Brown, S. L., and P. E. Schroeder. 1999. Spatial patterns of aboveground production and mortality of woody biomass for eastern U.S. forests. Ecological Applications 9:968–980.

Bruniquel-Pinel, V., and J. P. Gastellu-Etchegorry. 1998. Sensitivity of Texture of High Resolution Images of Forest to Biophysical and Acquisition Parameters. Remote Sensing of Environment 65:61–85.

Burnham, K. P., and D. R. Anderson. 2002. Model selection and multimodel inference: a practical information-theoretic approach. Page 488 Ecological Modelling. Springer.

Cavalieri, D. J., P. Gloersen, and W. J. Campbell. 1984. Determination of sea ice parameters with the NIMBUS 7 SMMR. Journal of Geophysical Research: Atmospheres 89:5355–5369.

Cavalieri, D. J., and C. L. Parkinson. 2008. Antarctic sea ice variability and trends, 1979–2006. Journal of Geophysical Research 113:C07004.

CBFP. 2012. The forests of the Congo Basin: state of the forest 2010. Page 276 (D. P. and E. A. R. de Wasseige C., de Marcken P., Bayol N., Hiol Hiol F., Mayaux Ph., Desclée B., Nasi R., Billand A., Ed.). Publications Office of the European Union, Luxembourg.

Chao, K.-J., O. L. Phillips, E. Gloor, A. Monteagudo, A. Torres-Lezama, and R. V. Martínez. 2008. Growth and wood density predict tree mortality in Amazon forests. Journal of Ecology 96:281–292.

Chave, J. 1999. Study of structural, successional and spatial patterns in tropical rain forests using TROLL, a spatially explicit forest model. Ecological Modelling 124:233–254.

Chave, J., C. Andalo, S. Brown, M. a Cairns, J. Q. Chambers, D. Eamus, H. Fölster, F. Fromard, N. Higuchi, T. Kira, J.-P. Lescure, B. W. Nelson, H. Ogawa, H. Puig, B. Riéra, and T. Yamakura. 2005. Tree allometry and improved estimation of carbon stocks and balance in tropical forests. Oecologia 145:87–99.

Chave, J., R. Condit, S. Aguilar, A. Hernandez, S. Lao, and R. Perez. 2004. Error propagation and scaling for tropical forest biomass estimates. Philosophical transactions of the Royal Society of London. Series B, Biological sciences 359:409–20.

Chave, J., D. Coomes, S. Jansen, S. L. Lewis, N. G. Swenson, and A. E. Zanne. 2009. Towards a worldwide wood economics spectrum. Ecology letters 12:351–66.

Chave, J., H. C. Muller-Landau, T. R. Baker, T. a Easdale, H. ter Steege, and C. O. Webb. 2006. Regional and phylogenetic variation of wood density across 2456 Neotropical tree species. Ecological applications 16:2356–67.

Chave, J., M. Réjou-Méchain, A. Búrquez, E. Chidumayo, M. S. Colgan, W. B. Delitti, A. Duque, T. Eid, P. M. Fearnside, R. C. Goodman, M. Henry, A. Martínez-Yrízar, W. a Mugasha, H. C. Muller-Landau, M. Mencuccini, B. W. Nelson, A. Ngomanda, E. M. Nogueira, E. Ortiz-Malavassi, R. Pélissier, P. Ploton, C. M. Ryan, J. G. Saldarriaga, and G. Vieilledent. 2014.

Improved allometric models to estimate the aboveground biomass of tropical trees. Global Change Biology:n/a–n/a.

Chave, J., B. Riera, M.-A. Dubois, and B. Riéra. 2001. Estimation of biomass in a neotropical forest of French Guiana : spatial and temporal variability. Journal of Tropical Ecology 17:79–96.

Chavez, P. S. 1996. Image-based atmospheric corrections: revised and improved. Photogrammetric Engineering and Remote Sensing 62:1025–1036.

Chisholm, R. A., H. C. Muller-Landau, K. Abdul Rahman, D. P. Bebber, Y. Bin, S. A. Bohlman, N. A. Bourg, J. Brinks, S. Bunyavejchewin, N. Butt, H. Cao, M. Cao, D. Cárdenas, L.-W. Chang, J.-M. Chiang, G. Chuyong, R. Condit, H. S. Dattaraja, S. Davies, A. Duque, C. Fletcher, N. Gunatilleke, S. Gunatilleke, Z. Hao, R. D. Harrison, R. Howe, C.-F. Hsieh, S. P. Hubbell, A. Itoh, D. Kenfack, S. Kiratiprayoon, A. J. Larson, J. Lian, D. Lin, H. Liu, J. A. Lutz, K. Ma, Y. Malhi, S. McMahon, W. McShea, M. Meegaskumbura, S. Mohd. Razman, M. D. Morecroft, C. J. Nytch, A. Oliveira, G. G. Parker, S. Pulla, R. Punchi-Manage, H. Romero-Saltos, W. Sang, J. Schurman, S.-H. Su, R. Sukumar, I.-F. Sun, H. S. Suresh, S. Tan, D. Thomas, S. Thomas, J. Thompson, R. Valencia, A. Wolf, S. Yap, W. Ye, Z. Yuan, and J. K. Zimmerman. 2013. Scale-dependent relationships between tree species richness and ecosystem function in forests. Journal of Ecology 101:1214–1224.

Church, J. A., and N. J. White. 2011. Sea-Level Rise from the Late 19th to the Early 21st Century. Surveys in Geophysics 32:585–602.

Clark, D. B., and D. A. Clark. 2000. Landscape-scale variation in forest structure and biomass in a tropical rain forest. Forest Ecology and Management 137:185–198.

Clark, D. B., and J. R. Kellner. 2012. Tropical forest biomass estimation and the fallacy of misplaced concreteness. Journal of Vegetation Science 23:1191–1196.

Comiso, J. C., and F. Nishio. 2008. Trends in the sea ice cover using enhanced and compatible AMSR-E, SSM/I, and SMMR data. Journal of Geophysical Research 113:C02S07.

Coomes, D. A., R. P. Duncan, R. B. Allen, and J. Truscott. 2003. Disturbances prevent stem size-density distributions in natural forests from following scaling relationships. Ecology Letters 6:980–989.

Couteron, P. 2002. Quantifying change in patterned semi-arid vegetation by Fourier analysis of digitized aerial photographs. International Journal of Remote Sensing 23:3407–3425.

Couteron, P., R. Pelissier, E. A. Nicolini, and D. Paget. 2005. Predicting tropical forest stand structure parameters from Fourier transform of very high-resolution remotely sensed canopy images. Journal of Applied Ecology 42:1121–1128.

Deblauwe, V., N. Barbier, P. Couteron, O. Lejeune, and J. Bogaert. 2008. The global biogeography of semi-arid periodic vegetation patterns. Global Ecology and Biogeography 17:715–723.

DeFries, R., F. Achard, S. Brown, M. Herold, D. Murdiyarso, B. Schlamadinger, and C. de Souza. 2007. Earth observations for estimating greenhouse gas emissions from deforestation in developing countries. Environmental Science & Policy 10:385–394.

Détienne, P., and B. Chanson. 1996. L'éventail de la densité du bois des feuillus : Comparaison entre différentes régions du monde. Bois et forêts des tropiques:19–30.

Djomo, A. N., A. Ibrahima, J. Saborowski, and G. Gravenhorst. 2010. Allometric equations for biomass estimations in Cameroon and pan moist tropical equations including biomass data from Africa. Forest Ecology and Management 260:1873–1885.

Dlugokencky, E., and P. Tans. 2014. Recent CO2, NOAA, ESRS. www.esrl.noaa.gov/gmd/ccgg/trends/global.html.

Drake, J. B., R. G. Knox, R. O. Dubayah, D. B. Clark, R. Condit, J. B. Blair, and M. Hofton. 2003. Above-ground biomass estimation in closed canopy Neotropical forests using lidar remote sensing: factors affecting the generality of relationships. Global Ecology and Biogeography 12:147–159.

Dubayah, R. O., and J. B. Drake. 2000. Lidar Remote Sensing for Forestry. Journal of Forestry 98:44–46.

Duveiller, G., P. Defourny, B. Desclée, and P. Mayaux. 2008. Deforestation in Central Africa: Estimates at regional, national and landscape levels by advanced processing of systematically-distributed Landsat extracts. Remote Sensing of Environment 112:1969–1981.

Enquist, B. J., and K. J. Niklas. 2001. Invariant scaling relations across tree-dominated communities. Nature 410:655–660.

Enquist, B. J., G. B. West, and J. H. Brown. 2009. Extensions and evaluations of a general quantitative theory of forest structure and dynamics. Proceedings of the National Academy of Sciences of the United States of America 106:7046–51.

Evrard, C. 1968. Recherches écologiques sur le peuplement forestier des sols hydromorphes de la Cuvette centrale congolaise. Page 295 Série scientifique INEAC. Institut pour l'étude agronomique du Congo, Bruxelles.

FAO. 2007. Digital soil map of the world. Rome.

Farina, A. 2000. Principles and Methods in Landscape Ecology: Towards a Science of the Landscape. Page 434. Springer Science & Business Media.

Fauset, S., O. . Johnson, M. Gloor, T. R. Baker, A. Monteagudo, R. J. W. Brienen, T. R. Feldpausch, G. Lopez-Gonzalez, Y. Malhi, H. ter Steege, N. C. A. Pitman, C. Baraloto, J. Engel, P. Pertonelli, A. Andrade, J. L. Camargo, G. W. S. Laurance, W. F. Laurance, J. Chave, E. Allie, P. N. Vargas, J. Terborgh, K. Ruokolainen, M. Silveira C., G. A. Aymard, L. Arroyo, D. Bonal, H. Ramirez-Angulo, A. Araujo-Murakami, D. Neill, B. Herault, B. S.

Armando Torres-Lezama, Marimon, R. P. Salomão, J. Comiskey, M. Réjou-Méchain, M. Toledo, A. Prieto, P. van der Mee, T. J. Killeen, B.-H. M. Jr., L. Poorter, R. G. A. . Boo, E. V. Torre, Maria Cristina Peñuela-, Mora, F. R. C. Costa, C. Levis, J. Schietti, P. Souza, Nikée Groot, E. Arets, V. C. Moscoso, W. Castro, E. N. Honorio, Coronado, M. Pena-Claros, C. Stahl, J. Barroso, J. Talbot, I. C. G. Vieira, G. van der Heijden, R. Thomas, V. Vos, E. Almeida, E. A. Davila, L. E. O. C. Aragão, T. Erwin, P. S. Morandi, E. A. de Oliveira, M. B. X. Valadão, R. Zagt, P. van de Hout, P. A. Loayza, O. Wang, M. Alexiades, C. Cerón, I. Huamantupa-Chuquimaco, A. Di Fiore, J. Peacock, N. C. P. Camacho, R. K. Umetsu, R. Burnham, R. H. Fernandez, C. A. Quesada, J. Stropp, S. A. Vieira, M. Steininger, C. R. Rodriguez, Z. Restrepo, A. Esquivel, S. Lewis, G. Pickavance, R. V. Martinez, and O. Phillips. (n.d.). Hyperdominance in Amazonian forest carbon cycling. Nature Climate Change.

Fayolle, A., J.-L. Doucet, J.-F. Gillet, N. Bourland, and P. Lejeune. 2013. Tree allometry in Central Africa: Testing the validity of pantropical multi-species allometric equations for estimating biomass and carbon stocks. Forest Ecology and Management 305:29–37.

Fayolle, A., N. Picard, J.-L. Doucet, M. Swaine, N. Bayol, F. Bénédet, and S. Gourlet-Fleury. 2014a. A new insight in the structure, composition and functioning of central African moist forests. Forest Ecology and Management 329:195–205.

Fayolle, A., M. D. Swaine, J.-F. Bastin, N. Bourland, J. A. Comiskey, G. Dauby, J.-L. Doucet, J.-F. Gillet, S. Gourlet-Fleury, O. J. Hardy, B. Kirunda, F. N. Kouamé, and A. J. Plumptre. 2014b. Patterns of tree species composition across tropical African forests. Journal of Biogeography 41:2320–2331.

Fearnside, P. M. 1997. Wood density for estimating forest biomass in Brazilian Amazonia. Forest Ecology and Management 90:59–87.

Feldpausch, T. R., L. Banin, O. L. Phillips, T. R. Baker, S. L. Lewis, C. a. Quesada, K. Affum-Baffoe, E. J. M. M. Arets, N. J. Berry, M. Bird, E. S. Brondizio, P. de Camargo, J. Chave, G. Djagbletey, T. F. Domingues, M. Drescher, P. M. Fearnside, M. B. França, N. M. Fyllas, G. Lopez-Gonzalez, a. Hladik, N. Higuchi, M. O. Hunter, Y. Iida, K. a. Salim, a. R. Kassim, M. Keller, J. Kemp, D. a. King, J. C. Lovett, B. S. Marimon, B. H. Marimon-Junior, E. Lenza, a. R. Marshall, D. J. Metcalfe, E. T. a. Mitchard, E. F. Moran, B. W. Nelson, R. Nilus, E. M. Nogueira, M. Palace, S. Patiño, K. S.-H. Peh, M. T. Raventos, J. M. Reitsma, G. Saiz, F. Schrodt, B. Sonké, H. E. Taedoumg, S. Tan, L. White, H. Wöll, and J. Lloyd. 2011. Height-diameter allometry of tropical forest trees. Biogeosciences 8:1081–1106.

Foody, G. M., M. E. Cutler, J. Mcmorrow, D. Pelz, and H. Tangki. 2001. Mapping the Biomass of Bornean Tropical Rain Forest from Remotely Sensed Data. Global Ecology and Biogeography 10:379–387.

Forman, R. T. T. 1995. Land Mosaics: The Ecology of Landscapes and Regions. Page 632. Cambridge University Press.

Frazer, G. W., M. A. Wulder, and K. O. Niemann. 2005. Simulation and quantification of the fine-scale spatial pattern and heterogeneity of forest canopy structure: A lacunarity-

based method designed for analysis of continuous canopy heights. Forest Ecology and Management 214:65–90.

Gastellu-Etchegorry, J. P. 2008. 3D modeling of satellite spectral images, radiation budget and energy budget of urban landscapes. Meteorology and Atmospheric Physics 102:187–207.

Gastellu-Etchegorry, J. P., P. Guillevic, F. Zagolski, V. Demarez, V. Trichon, D. Deering, and M. Leroy. 1999. Modeling BRF and Radiation Regime of Boreal and Tropical Forests : I . BRF. Remote Sensing of Environment 68:281–316.

GEA. 2006. Energy resources and potentials. Pages 425–512 Global Energy Assessment—Toward a Sustainable Future. Cambridge University Press, Cambridge, United Kingdom, and New York, NY, USA.

Gerard, F. F., and P. R. J. North. 1997. Analyzing the effect of structural variability and canopy gaps on forest BRDF using a geometric-optical model. Remote Sensing of Environment 62:46–62.

Gibbs, H. K., S. Brown, J. O. Niles, and J. a Foley. 2007. Monitoring and estimating tropical forest carbon stocks: making REDD a reality. Environmental Research Letters 2:1–13.

Gillet, J.-F., and J.-L. Doucet. 2012. A commented checklist of woody plants in the Northern Republic of Congo. Plant Ecology and Evolution:1–14.

Goetz, S., and R. Dubayah. 2011. Advances in remote sensing technology and implications for measuring and monitoring forest carbon stocks and change.

Gond, V., A. Fayolle, A. Pennec, G. Cornu, P. Mayaux, P. Camberlin, C. Doumenge, N. Fauvet, and S. Gourlet-Fleury. 2013. Vegetation structure and greenness in Central Africa from Modis multi-temporal data. Philosophical transactions of the Royal Society of London. Series B, Biological sciences 368:20120309.

Goodman, R. C., O. L. O. L. Phillips, and T. R. Baker. 2014. The importance of crown dimensions to improve tropical tree biomass estimates. Ecological Applications 24:680–698.

Gourlet-Fleury, S., V. Rossi, M. Rejou-Mechain, V. Freycon, A. Fayolle, L. Saint-André, G. Cornu, J. Gérard, J.-M. Sarrailh, O. Flores, F. Baya, A. Billand, N. Fauvet, M. Gally, M. Henry, D. Hubert, A. Pasquier, and N. Picard. 2011. Environmental filtering of dense-wooded species controls above-ground biomass stored in African moist forests. Journal of Ecology 99:981–990.

Grime, J. 1998a. Benefits of plant diversity to ecosystems: immediate, filter and founder effects. Journal of Ecology:891–899.

Grime, J. 1998b. Benefits of plant diversity to ecosystems: immediate, filter and founder effects. Journal of Ecology:891–899.

Grime, J. P. 1998c. Benefits of plant diversity to ecosystems: immediate, filter and founder effects. Journal of Ecology 86:902–910.

Hall, P., P. S. Ashton, R. Condit, N. Manokaran, S. P. Hubbell, F. Dallmeier, and J. A. Comiskey. 1998. Signal and noise in sampling tropical forest structure and dynamics. Pages 63–77 Forest biodiversity research, monitoring and modeling. Conceptual background and Old World case studies. Parthenon Publishing Group.

Hallé, F., R. A. A. Oldeman, and P. B. Tomlinson. 1978. Tropical trees and forests: an architectural analysis. Page 441 Tropical trees and forests an architectural analysis. Springer, Berlin. Germany.

Hansell, D. A., C. A. Carlson, D. J. Repeta, and R. Schlitzer. 2009, December 1. Dissolved organic matter in the ocean : a controversy stimulates new insights. Oceanography Society.

Hansen, J., R. Ruedy, M. Sato, and K. Lo. 2010. GLOBAL SURFACE TEMPERATURE CHANGE. Reviews of Geophysics 48:RG4004.

Harms, K. E., S. J. Wright, O. Calderón, a Hernández, and E. a Herre. 2000. Pervasive density-dependent recruitment enhances seedling diversity in a tropical forest. Nature 404:493–5.

Harris, N. L., S. Brown, S. C. Hagen, S. S. Saatchi, S. Petrova, W. Salas, M. C. Hansen, P. V Potapov, and A. Lotsch. 2012. Baseline map of carbon emissions from deforestation in tropical regions. Science (New York, N.Y.) 336:1573–6.

Hastie, T., R. Tibshirani, and J. Friedman. 2009. The Elements of Statistical Learning: Data Mining, Inference, and Prediction, Second Edition. Page 768 Springer Series in Statistics. Springer.

Hawthorne, W. D. 1995. Ecological Profiles of Ghanaian Forest Trees. Page 345. Oxford Forestry Institute, Department of Plant Sciences, University of Oxford.

Henry, M., A. Besnard, W. A. Asante, J. Eshun, S. Adu-Bredu, R. Valentini, M. Bernoux, and L. Saint-André. 2010. Wood density, phytomass variations within and among trees, and allometric equations in a tropical rainforest of Africa. Forest Ecology and Management 260:1375–1388.

Hietz, P., R. Valencia, and S. Joseph Wright. 2013. Strong radial variation in wood density follows a uniform pattern in two neotropical rain forests. Functional Ecology 27:684–692.

Houghton, R. A. 2005. Aboveground Forest Biomass and the Global Carbon Balance. Global Change Biology 11:945–958.

Houghton, R. A., F. Hall, and S. J. Goetz. 2009. Importance of biomass in the global carbon cycle. Journal of Geophysical Research 114:G00E03.

Houghton, R. A., J. L. Lawrence, J. L. Hackler, and S. Brown. 2001. The Spatial Distribution of Forest Biomass in the Brazilian Amazon: A Comparison of Estimates. Global Change Biology 7:731–746.

Imhoff, M. L. 1995. Radar backscatter and biomass saturation: ramifications for global biomass inventory. IEEE Transactions on Geoscience and Remote Sensing 33:511–518.

Inogwabini, B., M. Bewa, M. Longwango, M. Abokome, and M. Vuvu. 2008. The Bonobos of the Lake Tumba – Lake Maindombe Hinterland : Threats and Opportunities for Population Conservation. Pages 273–290 *in* T. Furuichi and J. Thompson, editors. The bonobos: Behavior; Ecology, and Conservation. Springer-US, New York.

IPCC. 2006. 2006 IPCC Guidelines for National Greenhouse Gas Inventories, Prepared by the National Greenhouse Gas Inventories Programme. (H. S. Eggleston, L. Buendia, K. Miwa, T. Ngara, and K. Tanabe, Eds.). IGES. Japan, Japan.

IPCC. 2013. Climate Change 2013:The physical science basis. Contribution of Working Group I to the Fifth Assessment Report of the Intergovernmental Panel on Climate Change. Cambridge, UK.

Jevrejeva, S., J. C. Moore, A. Grinsted, and P. L. Woodworth. 2008. Recent global sea level acceleration started over 200 years ago? Geophysical Research Letters 35:L08715.

Jones, P. D., D. H. Lister, T. J. Osborn, C. Harpham, M. Salmon, and C. P. Morice. 2012. Hemispheric and large-scale land-surface air temperature variations: An extensive revision and an update to 2010. Journal of Geophysical Research 117:D05127.

Joos, F., R. Roth, J. S. Fuglestvedt, G. P. Peters, I. G. Enting, W. von Bloh, V. Brovkin, E. J. Burke, M. Eby, N. R. Edwards, T. Friedrich, T. L. Frölicher, P. R. Halloran, P. B. Holden, C. Jones, T. Kleinen, F. T. Mackenzie, K. Matsumoto, M. Meinshausen, G.-K. Plattner, A. Reisinger, J. Segschneider, G. Shaffer, M. Steinacher, K. Strassmann, K. Tanaka, A. Timmermann, and A. J. Weaver. 2013. Carbon dioxide and climate impulse response functions for the computation of greenhouse gas metrics: a multi-model analysis. Atmospheric Chemistry and Physics 13:2793–2825.

Joos, F., and R. Spahni. 2008. Rates of change in natural and anthropogenic radiative forcing over the past 20,000 years. Proceedings of the National Academy of Sciences of the United States of America 105:1425–30.

Justice, C., D. Wilkie, Q. Zhang, J. Brunner, and C. Donohogue. 2001. Central African forests, carbon and climate change. Climate Research 17:229–246.

Keller, M., G. P. Asner, M. Palace, R. Pereira, J. N. M. Silva, and J. C. Zweede. 2002. Estimating Canopy Structure in an Amazon Forest from Laser Range Finder and IKONOS Satellite Observations. Biotropica 34:483–492.

Kellner, J., and G. Asner. 2014. Winners and losers in the competition for space in tropical forest canopies. Ecology Letters.

Kimes, D. S. 1983. Dynamics of directional reflectance factor distributions for vegetation canopies. Applied Optics 22:1364.

King, D. A., S. J. Davies, M. N. N. Supardi, and S. Tan. 2005. Tree growth is related to light interception and wood density in two mixed dipterocarp forests of Malaysia. Functional Ecology 19:445–453.

King, D. A., S. J. Davies, S. Tan, and N. S. M. Noor. 2006. The role of wood density and stem support costs in the growth and mortality of tropical trees. Journal of Ecology 94:670–680.

Köhler, P., G. Knorr, D. Buiron, A. Lourantou, and J. Chappellaz. 2011, April 13. Abrupt rise in atmospheric CO2 at the onset of the Bølling/Allerød: in-situ ice core data versus true atmospheric signal.

Lagmouch, M., and B. Hardy. 2008. Carte de l'occupation du sol de la République Démocratique du Congo. Tervuren.

Laporte, N. T., J. Stabach, R. Grosch, T. Lin, and S. Goetz. 2007. Expansion of industrial logging in Central Africa. Science (New York, N.Y.) 316:1451.

Laskar, J., P. Robutel, F. Joutel, M. Gastineau, A. C. M. Correia, and B. Levrard. 2004. A long-term numerical solution for the insolation quantities of the Earth. Astronomy & Astrophysics, 428:261–285.

Laurance, W. 2008. Theory meets reality: How habitat fragmentation research has transcended island biogeographic theory. Biological Conservation 141:1731–1744.

Lawrimore, J. H., M. J. Menne, B. E. Gleason, C. N. Williams, D. B. Wuertz, R. S. Vose, and J. Rennie. 2011. An overview of the Global Historical Climatology Network monthly mean temperature data set, version 3. Journal of Geophysical Research 116:D19121.

Lebrun, J., and G. Gilbert. 1954. Une classification écologique des forêts du Congo. Publication INEAC série scientifique 63.

Lefsky, M. A., W. B. Cohen, and T. A. Spies. 2001. An evaluation of alternate remote sensing products for forest inventory, monitoring, and mapping of Douglas-fir forests in western Oregon. Canadian Journal of Forest Research 31:78–87.

Leuliette, E. W., and R. Scharroo. 2010. Integrating Jason-2 into a Multiple-Altimeter Climate Data Record. Marine Geodesy 33:504–517.

Lewis, S. L., G. Lopez-Gonzalez, B. Sonké, K. Affum-Baffoe, T. R. Baker, L. O. Ojo, O. L. Phillips, J. M. Reitsma, L. White, J. a Comiskey, M.-N. Djuikouo K, C. E. N. Ewango, T. R. Feldpausch, A. C. Hamilton, M. Gloor, T. Hart, A. Hladik, J. Lloyd, J. C. Lovett, J.-R. Makana, Y. Malhi, F. M. Mbago, H. J. Ndangalasi, J. Peacock, K. S.-H. Peh, D. Sheil, T. Sunderland, M. D. Swaine, J. Taplin, D. Taylor, S. C. Thomas, R. Votere, and H. Wöll. 2009. Increasing carbon storage in intact African tropical forests. Nature 457:1003–6.

Lewis, S. L., B. Sonké, T. Sunderland, S. K. Begne, G. Lopez-gonzalez, G. M. F. Van Der Heijden, O. L. Phillips, K. Affum-Baffoe, T. R. Baker, L. Banin, J.-F. Bastin, H. Beeckman, P. Boeckx, J. Bogaert, C. De Cannière, V. Chezeaux, C. J. Clark, M. Collins, G. Djagbletey, V. Droissart, J.-L. Doucet, C. E. N. Ewango, S. Fauset, T. R. Feldpausch, E. G. Foli, J.-F. Gillet, A. C. Hamilton, D. J. Harris, T. B. Hart, T. de Haulleville, A. Hladik, K. Hufkens, D. Huygens, P. Jeanmart, K. Jeffery, M.-N. D. Kamdem, E. Kearlsey, M. E. Leal, J. Lloyd, J. C. Lovett, J.-R. Makana, Y. Malhi, A. R. Marshall, L. Ojo, K. S.-H. Peh, G. Pickavance, J. R. Poulsen, M. Reitsma, D. Sheil, M. Simo, K. Steppe, H. E. Taedoumg, J. Talbot, J. Taplin, D. Taylor, S. C. Thomas, B. Toirambe, H. Verbeeck, J. Vleminckx, L. J. T. White, S. Willcock, H. Woell, and L. Zemagho. 2013. Above-ground biomass and structure of 260 African tropical forests. Philosophical transactions of the Royal Society of London. Series B, Biological sciences.

Lindenmayer, D. B., W. F. Laurance, and J. F. Franklin. 2012. Global decline in large old trees. Science 338:1305–1306.

Lu, D. 2006. The potential and challenge of remote sensing-based biomass estimation. International Journal of Remote Sensing 27:1297–1328.

Lubini, A., and K. Kusehuluka. 1991. La forêt ombrophile semi-sempervirente à Celtis mildbraedii et Gambeya lacourtiana dans la région de Kikwit (Zaïre). Bulletin du Jardin Botantique National de Belgique 61:305–334.

Lubini, A., and A. Mandango. 1981. Etude phytosociologique et écologique des forêts à Uapaca guineensis dans le nord-est du districti forestier central (Zaïre). Bulletin du Jardin botanique national de Belgique 51:231–254.

Lutz, J. A., A. J. Larson, M. E. Swanson, and J. A. Freund. 2012. Ecological importance of large-diameter trees in a temperate mixed-conifer forest. PloS one 7:e36131.

Makana, J.-R., C. N. Ewango, S. M. McMahon, S. C. Thomas, T. B. Hart, and R. Condit. 2011. Demography and biomass change in monodominant and mixed old-growth forest of the Congo. Journal of Tropical Ecology 27:447–461.

Maley, J. 2002. Destruction of African Forests Years Ago Still Exerts a Major Influence on Present Vegetation Formations 33:13–30.

Malhi, Y., S. Adu-Bredu, R. A. Asare, S. L. Lewis, and P. Mayaux. 2013. The past, present and future of Africa's rainforests. Philosophical transactions of the Royal Society of London. Series B, Biological sciences 368:20120293.

Malhi, Y., and J. Wright. 2004. Spatial patterns and recent trends in the climate of tropical rainforest regions. Philosophical transactions of the Royal Society of London. Series B, Biological sciences 359:311–29.

Maniatis, D., L. Saint André, M. Temmerman, Y. Malhi, and H. Beeckman. 2011a. The potential of using xylarium wood samples for wood density calculations: a comparison

of approaches for volume measurement. iForest - Biogeosciences and Forestry 4:150–159.

Maniatis, D., Y. Malhi, L. Saint André, D. Mollicone, N. Barbier, S. Saatchi, M. Henry, L. Tellier, M. Schwartzenberg, and L. White. 2011b. Evaluating the Potential of Commercial Forest Inventory Data to Report on Forest Carbon Stock and Forest Carbon Stock Changes for REDD+ under the UNFCCC. International Journal of Forestry Research 2011:1–13.

Maniatis, D., and D. Mollicone. 2010. Options for sampling and stratification for national forest inventories to implement REDD+ under the UNFCCC. Carbon balance and management 5:9.

Markus, T., and D. J. Cavalieri. 2000. An enhancement of the NASA Team sea ice algorithm. IEEE Transactions on Geoscience and Remote Sensing 38:1387–1398.

Mascaro, J., G. P. Asner, D. H. Dent, S. J. DeWalt, and J. S. Denslow. 2012. Scale-dependence of aboveground carbon accumulation in secondary forests of Panama: A test of the intermediate peak hypothesis. Forest Ecology and Management 276:62–70.

Mascaro, J., M. Detto, G. P. Asner, and H. C. Muller-Landau. 2011. Evaluating uncertainty in mapping forest carbon with airborne LiDAR. Remote Sensing of Environment 115:3770–3774.

Mitchard, E. T. A., T. R. Feldpausch, R. J. W. Brienen, G. Lopez-Gonzalez, A. Monteagudo, T. R. Baker, S. L. Lewis, J. Lloyd, C. A. Quesada, M. Gloor, H. ter Steege, P. Meir, E. Alvarez, A. Araujo-Murakami, L. E. O. C. Aragão, L. Arroyo, G. Aymard, O. Banki, D. Bonal, S. Brown, F. I. Brown, C. E. Cerón, V. Chama Moscoso, J. Chave, J. A. Comiskey, F. Cornejo, M. Corrales Medina, L. Da Costa, F. R. C. Costa, A. Di Fiore, T. F. Domingues, T. L. Erwin, T. Frederickson, N. Higuchi, E. N. Honorio Coronado, T. J. Killeen, W. F. Laurance, C. Levis, W. E. Magnusson, B. S. Marimon, B. H. Marimon Junior, I. Mendoza Polo, P. Mishra, M. T. Nascimento, D. Neill, M. P. Núñez Vargas, W. A. Palacios, A. Parada, G. Pardo Molina, M. Peña-Claros, N. Pitman, C. A. Peres, L. Poorter, A. Prieto, H. Ramirez-Angulo, Z. Restrepo Correa, A. Roopsind, K. H. Roucoux, A. Rudas, R. P. Salomão, J. Schietti, M. Silveira, P. F. de Souza, M. K. Steininger, J. Stropp, J. Terborgh, R. Thomas, M. Toledo, A. Torres-Lezama, T. R. van Andel, G. M. F. van der Heijden, I. C. G. Vieira, S. Vieira, E. Vilanova-Torre, V. A. Vos, O. Wang, C. E. Zartman, Y. Malhi, and O. L. Phillips. 2014. Markedly divergent estimates of Amazon forest carbon density from ground plots and satellites. Global Ecology and Biogeography:n/a–n/a.

Mitchard, E. T. A., S. S. Saatchi, G. P. Asner, and A. Baccini. 2013. Uncertainty in the spatial distribution of tropical forest biomass: a comparison of pan-tropical maps. Carbon balance and management 8:1–13.

Mitchard, E. T. A., S. S. Saatchi, L. J. T. White, K. A. Abernethy, K. J. Jeffery, S. L. Lewis, M. Collins, M. A. Lefsky, M. E. Leal, I. H. Woodhouse, and P. Meir. 2012. Mapping tropical forest biomass with radar and spaceborne LiDAR in Lopé National Park, Gabon: overcoming problems of high biomass and persistent cloud. Biogeosciences 9:179–191.

Molto, Q., V. Rossi, and L. Blanc. 2013. Error propagation in biomass estimation in tropical forests. Methods in Ecology and Evolution 4:175–183.

Morse, D. R., J. H. Lawton, M. M. Dodson, and M. H. Williamson. 1985. Fractal dimension of vegetation and the distribution of arthropod body lengths. Nature 314:731–733.

Morton, D. D. C., J. Nagol, C. C. C. Carabajal, J. Rosette, M. Palace, B. D. Cook, E. F. Vermote, D. J. Harding, and P. R. J. North. 2014. Amazon forests maintain consistent canopy structure and greenness during the dry season. Nature 506:221–4.

Mosango, M., and J. Lejoly. 1990. La forêt dense humide à Piptadeniastrum africanum et Celtis mildbraedii des environs de Kisangani (Zaïre). Pages 853–870 *in* H. Baijnath, M. Cheek, H. F.N., J. Lejoly, G. L. Lucas, F. P. Malaisse, C. R. Peters, and D. C. J. Wessels, editors. Comptes rendus de la douzième réunion plénière de l'AETFAT (Hambourg, 4-10 Septembre 1988). Hubert & C. Göttingen.

Mougin, E., C. Proisy, G. Marty, F. Fromard, H. Puig, J. L. Betoulle, and J. P. Rudant. 1999. Multifrequency and multipolarization radar backscattering from mangrove forests. IEEE Transactions on Geoscience and Remote Sensing 37:94–102.

Mugglestone, M. A., and E. Renshaw. 1998. Detection of geological lineations on aerial photographs using two-dimensional spectral analysis. Computers & Geosciences 24:771–784.

Muller-Landau, H. C. 2004. Interspecific and Inter-site Variation in Wood Specific Gravity of Tropical Trees. Biotropica 36:20–32.

Muller-Landau, H. C., R. S. Condit, K. E. Harms, C. O. Marks, S. C. Thomas, S. Bunyavejchewin, G. Chuyong, L. Co, S. Davies, R. Foster, S. Gunatilleke, N. Gunatilleke, T. Hart, S. P. Hubbell, A. Itoh, A. R. Kassim, D. Kenfack, J. V LaFrankie, D. Lagunzad, H. S. Lee, E. Losos, J.-R. Makana, T. Ohkubo, C. Samper, R. Sukumar, I.-F. Sun, M. N. Nur Supardi, S. Tan, D. Thomas, J. Thompson, R. Valencia, M. I. Vallejo, G. V. Muñoz, T. Yamakura, J. K. Zimmerman, H. S. Dattaraja, S. Esufali, P. Hall, F. He, C. Hernandez, S. Kiratiprayoon, H. S. Suresh, C. Wills, and P. Ashton. 2006. Comparing tropical forest tree size distributions with the predictions of metabolic ecology and equilibrium models. Ecology letters 9:589–602.

Myhre, G., E. J. Highwood, K. P. Shine, and F. Stordal. 1998. New estimates of radiative forcing due to well mixed greenhouse gases. Geophysical Research Letters 25:2715–2718.

Nerem, R. S., D. P. Chambers, C. Choe, and G. T. Mitchum. 2010. Estimating Mean Sea Level Change from the TOPEX and Jason Altimeter Missions. Marine Geodesy 33:435–446.

Ngomanda, A., N. L. Engone Obiang, J. Lebamba, Q. Moundounga Mavouroulou, H. Gomat, G. S. Mankou, J. Loumeto, D. Midoko Iponga, F. Kossi Ditsouga, R. Zinga Koumba, K. H. Botsika Bobé, C. Mikala Okouyi, R. Nyangadouma, N. Lépengué, B. Mbatchi, and N. Picard. 2014. Site-specific versus pantropical allometric equations: Which option to

estimate the biomass of a moist central African forest? Forest Ecology and Management 312:1–9.

Nicodemus, F. E. 1965. Directional Reflectance and Emissivity of an Opaque Surface. Applied Optics 4:767.

Niklas, K. 1995. Size-dependent Allometry of Tree Height, Diameter and Trunk-taper. Annals of Botany 75:217–227.

Nock, C. A., D. Geihofer, M. Grabner, P. J. Baker, S. Bunyavejchewin, and P. Hietz. 2009. Wood density and its radial variation in six canopy tree species differing in shade-tolerance in western Thailand. Annals of botany 104:297–306.

Onoda, Y., A. E. Richards, and M. Westoby. 2010. The relationship between stem biomechanics and wood density is modified by rainfall in 32 Australian woody plant species. The New phytologist 185:493–501.

Osazuwa-Peters, O. L., S. J. Wright, and A. E. Zanne. 2014. Radial variation in wood specific gravity of tropical tree species differing in growth-mortality strategies. American journal of botany:ajb.1400040–.

Pacala, S. W., C. D. Canham, J. Saponara, J. A. S. Jr., R. K. Kobe, and E. Ribbens. 1996. Forest Models Defined by Field Measurements: Estimation, Error Analysis and Dynamics. Ecological Monographs 66:1.

Palace, M., M. Keller, G. P. Asner, S. Hagen, and B. Braswell. 2008. Amazon Forest Structure from IKONOS Satellite Data and the Automated Characterization of Forest Canopy Properties. Biotropica 40:141–150.

Pan, Y., R. A. Birdsey, J. Fang, R. Houghton, P. E. Kauppi, W. A. Kurz, O. L. Phillips, A. Shvidenko, S. L. Lewis, J. G. Canadell, P. Ciais, R. B. Jackson, S. W. Pacala, A. D. McGuire, S. Piao, A. Rautiainen, S. Sitch, and D. Hayes. 2011. A large and persistent carbon sink in the world's forests. Science (New York, N.Y.) 333:988–993.

Panshin, A. J., and C. de Zeeuw. 1980. textbook of wood technology. McGraw-Hill Book Co.

Parkinson, C. L., and D. J. Cavalieri. 2012. Antarctic sea ice variability and trends, 1979–2010. The Cryosphere Discussions 6:931–956.

Patenaude, G., R. Milne, and T. P. Dawson. 2005. Synthesis of remote sensing approaches for forest carbon estimation: reporting to the Kyoto Protocol. Environmental Science & Policy 8:161–178.

Phillips, O. L., P. Hall, A. H. Gentry, S. A. Sawyer, and R. Vasquez. 1994. Dynamics and species richness of tropical rain forests. Proceedings of the National Academy of Sciences 91:2805–2809.

Picard, N., and S. Gourlet-Fleury. 2008. Manuel de référence pour l'installation de dispositifs permanents en Forêt de production dans le Bassin du Congo. Page 270 (CIRAD, Ed.). Commission des forêts d'afrique centrale, Yaounde.

Pinheiro, J., and D. Bates. 2000. Mixed-Effects Models in S and S-PLUS. Page 530. Springer-V. New York.

Plana, V. 2004. Mechanisms and tempo of evolution in the African Guineo–Congolian rainforest. Philosophical Transactions of the Royal Society of London. Series B: Biological Sciences 359:1585–1594.

Ploton, P., R. Pélissier, N. Barbier, C. Proisy, B. R. Ramesh, and P. Couteron. 2013. Canopy texture analysis for large-scale assessments of rainforest stand structure and biomass. Page 444 *in* M. Lowman, S. Devy, and T. Ganesh, editors. Treetops at Risk. Springer. New York.

Ploton, P., R. Pélissier, and C. Proisy. 2012. Assessing aboveground tropical forest biomass using Google Earth canopy images. Ecological Applications 22:993–1003.

Poorter, L. 2008. The relationships of wood-, gas- and water fractions of tree stems to performance and life history variation in tropical trees. Annals of botany 102:367–75.

Prather, M. J., C. D. Holmes, and J. Hsu. 2012. Reactive greenhouse gas scenarios: Systematic exploration of uncertainties and the role of atmospheric chemistry. Geophysical Research Letters 39:n/a–n/a.

Proisy, C., N. Barbier, M. Guéroult, R. Pélissier, J.-P. Gastelly-Etchegorry, E. Grau, and P. Couteron. 2012. Biomass Prediction in Tropical Forests: The Canopy Grain Approach. Pages 59–76 *in* L. Fatoyinbo, editor. Remote Sensing of Biomass - Priniciples and Applications. InTech Open Access Publisher, Croatia.

Proisy, C., P. Couteron, and F. Fromard. 2007. Predicting and mapping mangrove biomass from canopy grain analysis using Fourier-based textural ordination of IKONOS images. Remote Sensing of Environment 109:379–392.

Purves, D., and S. Pacala. 2008. Predictive models of forest dynamics. Science (New York, N.Y.) 320:1452–3.

Purves, D. W., J. W. Lichstein, N. Strigul, and S. W. Pacala. 2008. Predicting and understanding forest dynamics using a simple tractable model. Proceedings of the National Academy of Sciences of the United States of America 105:17018–22.

Ray, R. D., and B. C. Douglas. 2011. Experiments in reconstructing twentieth-century sea levels. Progress in Oceanography 91:496–515.

Rayner, N. A. 2003. Global analyses of sea surface temperature, sea ice, and night marine air temperature since the late nineteenth century. Journal of Geophysical Research 108:4407.

Reich, P. B. 2014. The world-wide “fast-slow” plant economics spectrum: a traits manifesto. Journal of Ecology 102:275–301.

Réjou-Méchain, M., H. C. Muller-Landau, M. Detto, S. C. Thomas, T. Le Toan, S. S. Saatchi, J. S. Barreto-Silva, N. A. Bourg, S. Bunyavejchewin, N. Butt, W. Y. Brockelman, M. Cao, D. Cárdenas, J.-M. Chiang, G. B. Chuyong, K. Clay, R. Condit, H. S. Dattaraja, S. J. Davies, A. Duque, S. Esufali, C. Ewango, R. H. S. Fernando, C. D. Fletcher, I. A. U. N. Gunatilleke, Z. Hao, K. E. Harms, T. B. Hart, B. Hérault, R. W. Howe, S. P. Hubbell, D. J. Johnson, D. Kenfack, A. J. Larson, L. Lin, Y. Lin, J. A. Lutz, J.-R. Makana, Y. Malhi, T. R. Marthews, R. W. McEwan, S. M. McMahon, W. J. McShea, R. Muscarella, A. Nathalang, N. S. M. Noor, C. J. Nytch, A. A. Oliveira, R. P. Phillips, N. Pongpattananurak, R. Punchi-Manage, R. Salim, J. Schurman, R. Sukumar, H. S. Suresh, U. Suwanvecho, D. W. Thomas, J. Thompson, M. Uríarte, R. Valencia, A. Vicentini, A. T. Wolf, S. Yap, Z. Yuan, C. E. Zartman, J. K. Zimmerman, and J. Chave. 2014. Local spatial structure of forest biomass and its consequences for remote sensing of carbon stocks. Biogeosciences Discussions 11:5711–5742.

Réjou-Méchain, M., R. Pélissier, S. Gourlet-Fleury, P. Couteron, R. Nasi, and J. D. Thompson. 2008. Regional variation in tropical forest tree species composition in the Central African Republic: an assessment based on inventories by forest companies. Journal of Tropical Ecology 24:663.

Remm, J., and A. Lõhmus. 2011. Tree cavities in forests – The broad distribution pattern of a keystone structure for biodiversity. Forest Ecology and Management 262:579–585.

De Ridder, M., J. Van den Bulcke, D. Vansteenkiste, D. Van Loo, M. Dierick, B. Masschaele, Y. De Witte, D. Mannes, E. Lehmann, H. Beeckman, L. Van Hoorebeke, and J. Van Acker. 2011. High-resolution proxies for wood density variations in Terminalia superba. Annals of botany 107:293–302.

Rohde, R. A., S. Mosher, and Z. Hausfather. 2013. Comparison of Historical CMIP5 Surface Temperatures to the Berkeley Earth Gridded Observational Temperature Field. AGU Fall Meeting Abstracts -1:1091.

Rondeux, J. 1999. La mesure des arbres et des peuplements forestiers. Page 522. Les Presse. Belgique, Gembloux.

Royer, P. D., N. S. Cobb, M. J. Clifford, C.-Y. Huang, D. D. Breshears, H. D. Adams, and J. C. Villegas. 2011. Extreme climatic event-triggered overstorey vegetation loss increases understorey solar input regionally: primary and secondary ecological implications. Journal of Ecology 99:714–723.

Rutishauser, E., F. Wagner, B. Herault, E.-A. Nicolini, and L. Blanc. 2010. Contrasting above-ground biomass balance in a Neotropical rain forest. Journal of Vegetation Science:672–682.

Ryan, R., B. Baldridge, R. A. Schowengerdt, T. Choi, D. L. Helder, and S. Blonski. 2003. IKONOS spatial resolution and image interpretability characterization. Remote Sensing of Environment 88:37–52.

Saatchi, S. S., N. L. Harris, S. Brown, M. Lefsky, E. T. a Mitchard, W. Salas, B. R. Zutta, W. Buermann, S. L. Lewis, S. Hagen, S. Petrova, L. White, M. Silman, and A. Morel. 2011. Benchmark map of forest carbon stocks in tropical regions across three continents. Proceedings of the National Academy of Sciences of the United States of America 108:9899–904.

Sallenave, P. 1955. Propriétés Physiques et Mécaniques des Bois Tropicaux de l'Union Française. CTFT. Nogent sur Marn, France.

Sallenave, P. 1964. Propriétés Physiques et Mécaniques des Bois Tropicaux. Premier Supplément. CTFT. Nogent sur Marne, France.

Sallenave, P. 1971. Propriétés Physiques et Mécaniques des Bois Tropicaux. Deuxième Supplément. CTFT. Nogent sur Marne, France.

Sarker, L. R., J. E. Nichol, B. Ahmad, I. Busu, and A. A. Rahman. 2011. Improved forest biomass estimates using ALOS AVNIR-2 texture indices. Remote Sensing of Environment 115:968–977.

Schumacher, F., and F. Hall. 1933. Logarithmic expression of timbertree volume. Journal of Agricultural Research 47:719–734.

Serckx, A., M.-C. Huynen, J.-F. Bastin, A. Hambuckers, R. C. Beudels-Jamar, M. Vimond, E. Raynaud, and H. S. Kühl. 2014. Nest grouping patterns of bonobos (Pan paniscus) in relation to fruit availability in a forest-savannah mosaic. PloS one 9:e93742.

Sist, P., L. Mazzei, L. Blanc, and E. Rutishauser. 2014. Large trees as key elements of carbon storage and dynamics after selective logging in the Eastern Amazon. Forest Ecology and Management 318:103–109.

Slik, J. W. F. 2006. Estimating species-specific wood density from the genus average in Indonesian trees. Journal of Tropical Ecology 22:481.

Slik, J. W. F., G. Paoli, K. McGuire, I. Amaral, J. Barroso, M. Bastian, L. Blanc, F. Bongers, P. Boundja, C. Clark, M. Collins, G. Dauby, Y. Ding, J.-L. Doucet, E. Eler, L. Ferreira, O. Forshed, G. Fredriksson, J.-F. Gillet, D. Harris, M. Leal, Y. Laumonier, Y. Malhi, A. Mansor, E. Martin, K. Miyamoto, A. Araujo-Murakami, H. Nagamasu, R. Nilus, E. Nurtjahya, Á. Oliveira, O. Onrizal, A. Parada-Gutierrez, A. Permana, L. Poorter, J. Poulsen, H. Ramirez-Angulo, J. Reitsma, F. Rovero, A. Rozak, D. Sheil, J. Silva-Espejo, M. Silveira, W. Spironelo, H. ter Steege, T. Stevart, G. E. Navarro-Aguilar, T. Sunderland, E. Suzuki, J. Tang, I. Theilade, G. van der Heijden, J. van Valkenburg, T. Van Do, E. Vilanova, V. Vos, S. Wich, H. Wöll, T. Yoneda, R. Zang, M.-G. Zhang, and N. Zweifel. 2013. Large trees drive forest aboveground biomass variation in moist lowland forests across the tropics. Global Ecology and Biogeography:n/a–n/a.

Sokal, R. R., and F. J. Rohlf. 1995. Biometry: the principles and practice of statistics in biological research. Page 887 (W. H. Freeman, Ed.) New York. W. H. Freeman and Company.

Ter Steege, H., N. C. A. Pitman, D. Sabatier, C. Baraloto, R. P. Salomão, J. E. Guevara, O. L. Phillips, C. V Castilho, W. E. Magnusson, J.-F. Molino, A. Monteagudo, P. Núñez Vargas, J. C. Montero, T. R. Feldpausch, E. N. H. Coronado, T. J. Killeen, B. Mostacedo, R. Vasquez, R. L. Assis, J. Terborgh, F. Wittmann, A. Andrade, W. F. Laurance, S. G. W. Laurance, B. S. Marimon, B.-H. Marimon, I. C. Guimarães Vieira, I. L. Amaral, R. Brienen, H. Castellanos, D. Cárdenas López, J. F. Duivenvoorden, H. F. Mogollón, F. D. de A. Matos, N. Dávila, R. García-Villacorta, P. R. Stevenson Diaz, F. Costa, T. Emilio, C. Levis, J. Schietti, P. Souza, A. Alonso, F. Dallmeier, A. J. D. Montoya, M. T. Fernandez Piedade, A. Araujo-Murakami, L. Arroyo, R. Gribel, P. V. A. Fine, C. A. Peres, M. Toledo, G. A. Aymard C, T. R. Baker, C. Cerón, J. Engel, T. W. Henkel, P. Maas, P. Petronelli, J. Stropp, C. E. Zartman, D. Daly, D. Neill, M. Silveira, M. R. Paredes, J. Chave, D. de A. Lima Filho, P. M. Jørgensen, A. Fuentes, J. Schöngart, F. Cornejo Valverde, A. Di Fiore, E. M. Jimenez, M. C. Peñuela Mora, J. F. Phillips, G. Rivas, T. R. van Andel, P. von Hildebrand, B. Hoffman, E. L. Zent, Y. Malhi, A. Prieto, A. Rudas, A. R. Ruschell, N. Silva, V. Vos, S. Zent, A. A. Oliveira, A. C. Schutz, T. Gonzales, M. Trindade Nascimento, H. Ramirez-Angulo, R. Sierra, M. Tirado, M. N. Umaña Medina, G. van der Heijden, C. I. A. Vela, E. Vilanova Torre, C. Vriesendorp, O. Wang, K. R. Young, C. Baider, H. Balslev, C. Ferreira, I. Mesones, A. Torres-Lezama, L. E. Urrego Giraldo, R. Zagt, M. N. Alexiades, L. Hernandez, I. Huamantupa-Chuquimaco, W. Milliken, W. Palacios Cuenca, D. Pauletto, E. Valderrama Sandoval, L. Valenzuela Gamarra, K. G. Dexter, K. Feeley, G. Lopez-Gonzalez, and M. R. Silman. 2013. Hyperdominance in the Amazonian tree flora. Science 342:1243092.

Stephenson, N. L., A. J. Das, R. Condit, S. E. Russo, P. J. Baker, N. G. Beckman, D. A. Coomes, E. R. Lines, W. K. Morris, N. Rüger, E. Alvarez, C. Blundo, S. Bunyavejchewin, G. Chuyong, S. J. Davies, A. Duque, C. N. Ewango, O. Flores, J. F. Franklin, H. R. Grau, Z. Hao, M. E. Harmon, S. P. Hubbell, D. Kenfack, Y. Lin, J.-R. Makana, A. Malizia, L. R. Malizia, R. J. Pabst, N. Pongpattananurak, S.-H. Su, I.-F. Sun, S. Tan, D. Thomas, P. J. van Mantgem, X. Wang, S. K. Wiser, and M. A. Zavala. 2014. Rate of tree carbon accumulation increases continuously with tree size. Nature.

Stöckli, R., E. Vermote, N. Saleous, R. Simmon, and D. Herring. 2005. The Blue Marble Next Generation - A true color earth dataset including seasonal dynamics from MODIS.

Swenson, N. G., and B. J. Enquist. 2007. Ecological and evolutionary determinants of a key plant functional trait: wood density and its community-wide variation across latitude and elevation. American journal of botany 94:451–9.

Tarnocai, C., J. G. Canadell, E. A. G. Schuur, P. Kuhry, G. Mazhitova, and S. Zimov. 2009. Soil organic carbon pools in the northern circumpolar permafrost region. Global Biogeochemical Cycles 23:n/a–n/a.

Turner, I. M. 2001. The Ecology of Trees in the Tropical Rain Forest. Page 298. Cambridge University Press, Cambridge.

UNFCCC. 2010. Appendix 1: Guidance and safeguards for policy approaches and positive incentives on issues relating to reducing emissions from deforestation and forest degradation in developing countries; and the role of conservation, sustainable management of forests a. Pages 26–27.

Valbuena, R., F. Mauro, and J. A. Manzanera. 2010. Accuracy and precision of GPS receivers under forest canopies in a mountainous environment. Spanish Journal of Agricultural Research 8:1047–1057.

Vancutsem, C., J. Pekel, L. Kibambe, X. Blaes, C. de Waseige, and F. Defourny. 2006. République démocratique du Congo - occupation du sol. Carte Géographique. Presses Universitaire de Louvain. Bruxelles, Belgique.

Vermote, E. F., N. Z. El Saleous, and C. O. Justice. 2002. Atmospheric correction of MODIS data in the visible to middle infrared: first results. Remote Sensing of Environment 83:97–111.

Vieilledent, G., R. Vaudry, S. F. D. Andriamanohisoa, O. S. Rakotonarivo, H. Z. Randrianasolo, H. N. Razafindrabe, C. B. Rakotoarivony, J. Ebeling, and M. Rasamoelina. 2012. A universal approach to estimate biomass and carbon stock in tropical forests using generic allometric models. Ecological Applications 22:572–83.

Viennois, G., N. Barbier, I. Fabre, and P. Couteron. 2013. Multiresolution quantification of deciduousness in West Central African forests. Biogeosciences Discussions 10:7171–7200.

Violle, C., M.-L. Navas, D. Vile, E. Kazakou, C. Fortunel, I. Hummel, and E. Garnier. 2007. Let the concept of trait be functional! Oikos 116:882–892.

Wagner, F., E. Rutishauser, L. Blanc, and B. Herault. 2010. Effects of Plot Size and Census Interval on Descriptors of Forest Structure and Dynamics. Biotropica 42:664–671.

Walsh, J. E., and W. L. Chapman. 2001. 20th-century sea-ice variations from observational data. Annals of Glaciology 33:444–448.

Van der Werf, G. R., D. C. Morton, R. S. DeFries, J. G. J. Olivier, P. S. Kasibhatla, R. B. Jackson, G. J. Collatz, and J. T. Randerson. 2009. CO2 emissions from forest loss. Nature Geoscience 2:737–738.

West, G. B., J. H. Brown, and B. J. Enquist. 1997. A general model for the origin of allometric scaling laws in biology. Science (New York, N.Y.) 276:122–6.

West, G. B., B. J. Enquist, and J. H. Brown. 2009. A general quantitative theory of forest structure and dynamics. Proceedings of the National Academy of Sciences of the United States of America 106:7040–7045.

White, F. 1983. The vegetation of Africa: A descriptive memoir to accompany the UNESCO/AETFAT/UNSO vegetation map of Africa. Natural Resources Research 20.

White, L. 2001a. Forest-savanna dynamics and the origins of Marantaceae forest in central Gabon. Pages 165–182 *in* N.-T. WeberW, WhiteLJT, VedderA, editor. African rain forest ecology and conservation: Interdisciplinary Perspective. Yale University Press, New Haven, London.

White, L. J. T. 2001b. The African rain forest: climate and vegetation. Pages 3–29 *in* W. Weber, A. Veder, H. Simons Morland, L. J. T. White, and T. B. Hart, editors. African Rain Forest Ecology and Conservation An Interdisciplinary Perspective. Yale University Press.

Wiemann, M., and G. Williamson. 1988. Extreme Radial Changes in Wood Specific Gravity in Some Tropical Pioneers. Wood and Fiber Science 20:344–349.

Williamson, G. B., and M. C. Wiemann. 2011. Age versus size determination of radial variation in wood specific gravity: lessons from eccentrics. Trees 25:585–591.

Williamson, G. B., and M. C. M. Wiemann. 2010. Measuring wood specific gravity correctly. American Journal of Botany 97:519–524.

Woodcock, D. W., and a. D. Shier. 2002. Wood specific gravity and its radial variations: the many ways to make a tree. Trees 16:437–443.

Wright, S. J., H. C. Muller-Landau, R. Condit, and S. P. Hubbell. 2003. GAP-DEPENDENT RECRUITMENT, REALIZED VITAL RATES, AND SIZE DISTRIBUTIONS OF TROPICAL TREES. Ecology 84:3174–3185.

Yoshimura, T., and H. Hasegawa. 2003. Comparing the precision and accuracy of GPS positioning in forested areas. Journal of Forest Research 8:147–152.

Zanne, A. E., G. Lopez-Gonzalez, D. A. Coomes, J. Ilic, S. Jansen, S. L. Lewis, R. B. Miller, N. G. Swenson, M. C. Wiemann, and J. Chave. 2009. Global wood density database. Dryad 235:33.

Zheng, D., J. Rademacher, J. Chen, T. Crow, M. Bresee, J. Le Moine, and S.-R. Ryu. 2004. Estimating aboveground biomass using Landsat 7 ETM+ data across a managed landscape in northern Wisconsin, USA. Remote Sensing of Environment 93:402–411.

Zhou, J., C. Proisy, X. Descombes, I. Hedhli, N. Barbier, J. Zerubia, J. P. Gastellu-Etchegorry, and P. Couteron. 2010. Tree crown detection in high resolution optical and LiDAR images of tropical forest. *in* Christopher M. U. Neale; Antonino Maltese, editor. Remote Sensing for Agriculture Ecosystems and Hydrology XII. The International Society for Optical Engineering, Toulouse.

Zolkos, S. G., S. J. Goetz, and R. Dubayah. 2013. A meta-analysis of terrestrial aboveground biomass estimation using lidar remote sensing. Remote Sensing of Environment 128:289–298.

Zuur, A., E. Ieno, N. Walker, A. Saveliev, and G. Smith. 2009. Mixed effects models and extensions in ecology with R. Page 596 Survival Analysis, Edition …. Springer Science & Business Media.

APPENDIX A

SPECIES LIST – VERNACULAR - SCIENTIFIC

Vernacular name	*Family*	Species
Ba	Arecaceae	Elais guineensis
Banziani	Asparagaceae	Dracaena mannii
Biontere	Annonaceae	Xylopia hypolampra Mildbr.
Biontere2	Annonaceae	Xylopia cupularis
Bobfu	Fabaceae (Mimosoideae)	Piptadeniastrum africanum (Hook.f.) Brenan
Bolu	Clusiaceae/ guttiferaceae	Symphonia globulifera L.f.
Bonkolo_grandes_feuilles	Malvaceae	Cola ballayi Cornu ex Heckel
Bonkolo_petites_feuilles	Malvaceae	Cola griseiflora De Wild.
Boparu	Fabaceae (caesalpinoideae)	Copaifera spp.
Boparu_grandes_feuilles	Meliaceae	Guarea cedrata (A.Chev.) Pellegr.
Bopili1	Fabaceae (caesalpinoideae)	Scorodophloeus zenkeri Harms
Bopili2	Huaceae	Afrostyrax lepidophyllus Mildbr.
Bopili3	Fabaceae (caesalpinoideae)	Cynometra sp1
Boyabi	Sapotaceae	Baillonella toxisperma Pierre
BoyabiBlanc	Sapotaceae	Tieghemella africana Pierre
Buu	Myristicaceae	Staudtia kamerunensis var. gabonensis (Warb.) Fouilloy
Bwamoti	Rutaceae	Zanthoxylum gilletii (De Wild.) P.G.Waterman
Ebabi	Fabaceae (Papilionoideae)	Millettia laurentii De Wild.
Ebabi-arbuste	Fabaceae (Papilionoideae)	Millettia drastica
Ebie	Flacourtiaceae	Oncoba mannii Oliv.
Ebunu	Rubiaceae	Nauclea latifolia
Elolo	Annonaceae	Annona senegalensis Pers.
Elumbuli	Apocynaceae	Rauvolfia vomitoria
Emein1Jaune	Olacaceae	Strombosia pustulata Oliv.
Emein2	Olacaceae	Heisteria parvifolia Sm.
Emein_rouge_lignes	Olacaceae	Strombosia grandifolia Hook.f.
Emein_sève_rouge	Olacaceae	Strombosiopsis tetrandra Engl.
Emein_ya_boutons	Olacaceae	Diogoa zenkeri (Engl.) Exell & Mendonça
Enama	Moraceae	Ficus spp.
Endi1	Euphorbiaceae	Plagiostyles africana (Müll.Arg.) Prain
Endi2	Euphorbiaceae	Duvigneaudia inopinata (Prain) J.Léonard
Entuemofuru	Moraceae	Myrianthus arboreus P.Beauv.
Epu	Passifloraceae	Paropsia guineensis
Esau	Fabaceae (Mimosoideae)	Tetrapleura tetraptera (Schumach. & Thonn.) Taub.
Esia-sia - ya esoba - petits fruits	Euphorbiaceae	Uapaca guineensis Müll.Arg.
Esiemofuru	Verbenaceae	Vitex ferruginea Schumach. & Thonn.
Esiemofuru2	Verbenaceae	Vitex congolense
Esili	Fabaceae (Mimosoideae)	Pentaclethra eetveldeana De Wild. & T.Durand
Esiye	Euphorbiaceae	Maprounea africana Müll.Arg.
Esoyili	Verbenaceae	Vitex congolense
Esusou	Hypericeae	Psorospermum febrifugum Spach
Etionsa_esobe	Euphorbiaceae	Chaetocarpus africanus
Ewere	Euphorbiaceae	Hymenocardia spp.
Eweremofuru	Combretaceae	Combretum lokele Liben
Kwero1	Fabaceae (caesalpinoideae)	Dialium zenkeri
Kwero2	Chrysobalanaceae	Parinari excelsa Sabine.

Vernacular name	*Family*	Species
Lebain1	Ebenaceae	Diospyros ferrea (Willd.) Bakh.
Lebain2	Ebenaceae	Diospyros sp1
Lebeilenzo	Melastomataceae	Warneckea sp1
Lebu	Arecaceae	Borassus aethiopum
Lefaki	Meliaceae	Lovoa trichilioides
Lefaki_noir	Meliaceae	Entandrophragma angolense (Welw.) C.DC. (cf. congoense)
Lefaki-médicament (odeur de vicks)	Sapindaceae	Ganophyllum giganteum (A.Chev.) Hauman
Lempia	Moraceae	Ficus sp2
Lepipa_grandes_feuilles	Irvigiaceae	Irvingia grandifolia (Engl.) Engl.
Lepipa_petites_feuilles	Irvigiaceae	Irvingia gabonensis (Aubry-LeComte ex O'Rorke) Baill.
Lepoene	Apocynaceae	Rauvolfia macrophylla
Luo1	Clusiaceae	Garcinia kola
Luo2	Apocynaceae	Picralima nitida Stapf.
Mbulbabfuba	Thymelaceae	Dicranolepis baertsiana
Mobala	Fabaceae (Mimosoideae)	Pentaclethra macrophylla Benth.
Mobamu	Sapotaceae	Chrysophyllum lacourtianum De Wild.
Mobamu2	Sapotaceae	Chrysophyllum africanum
Mobamu3	Sapotaceae	Chrysophyllum beguei
Mobe	Annonaceae	Anonidium mannii Oliv.
Mobeon	Rubiaceae	Massularia acuminata (G.Don) Bullock ex Hoyle
Mobfuma	Bombacaceae	Ceiba pentandra (L.) Gaertn.
Mobilankeon1	Malvaceae	Cola diversifolia De Wild. & T.Durand
Mobilankeon2	Malvaceae	Cola gigantea A.Chev.
Mobilu 3 - Mobao (amer)	Malvaceae	Cola spp.
Mobilu1	Malvaceae	Cola acuminata (P.Beauv.) Schott & Endl.
Mobilu2	Malvaceae	Cola cf. ballayi
Mobolo	Annonaceae	Isolona hexaloba Engl. & Diels
Moboro	Fabaceae (Papillonoideae)	Milletia sp1
Mofwu	Apocynaceae	Alstonia congensis Engl.
Mogbafu	Ochnaceae	Campylospermum cf. bukobense (Gilg)
Mokakuma	Sapotaceae	Omphalocarpum elatum Miers
Mokakuma2	Sapotaceae	Omphalocarpum lecomteanum Pierre ex Engl.
Mokakuma3	Sapotaceae	Omphamlocarpum procerum
Mokaru	Anacardiaceae	Sorindeia africana Engl.
Mokaunkaun savane	Rubiaceae	Gaertnera paniculata
Mokaunkaun	Guttiferaceae / Clusiaceae	Allanblackia ?
Mokie	Euphorbiaceae	Macaranga barteri Müll.Arg.
Mokie avec feuilles dentées	Euphorbiaceae	Macaranga monandra Müll.Arg.
Mokie ya mai	Euphorbiaceae	Macaranga staudtii Pax
Mokilankima	Myristicaceae	Pycnanthus angolensis (Welw.) Warb.
Mokinkaa1	Rubiaceae	Rytigynia sp1.
Mokinkaa2	Rubiaceae	Rytigynia sp2.
Mokoli	Annoncaceae	Cleistopholis glauca Pierre ex Engl. & Diels
Mokonkaun	Sapindaceae	Pancovia laurentii (De Wild.) Gilg ex De Wild.
Mokuon	Acanthaceae	Thomendersia hensii
Molieme_grandes_feuilles	Fabaceae (caesalpinoideae)	Brachystegia laurentii (De Wild.) Louis ex Hoyle

Vernacular name	*Family*	Species
Molieme_petites_feuilles	Fabaceae (caesalpinoideae)	Bikinia evrardii
Molili	Euphorbiaceae	Tetrorchidium didymostemon
Molondo	Moraceae	Milicia excelsa (Welw.) C.C.Berg
Molondo2	Boraginaceae	Cordia platythyrsa
Molu	Fabaceae (Mimosoideae)	Albizia gummifera
Molurumoba	Clusiaceae	Garcinia punctata Oliv.
Mombiene2	Rubiaceae	Colletoecema dewevrei
Mombimbili	Fabaceae (caesalpinoideae)	Erythrophleum suaveolens (Guill. & Perr.) Brenan
Momeon	Fabaceae (caesalpinoideae)	Daniellia pynaertii De Wild.
Momeon ya mai	Fabaceae (caesalpinoideae)	Hylodendron gabunense
Mompei	Fabaceae (caesalpinoideae)	Quassia africana (Steyaert) Mendonça & Torre
Mompini	Fabaceae (caesalpinoideae)	Aphanocalyx microphyllus
Mondiri	Fabaceae (caesalpinoideae)	Gilbertiodendron dewevrei (De Wild.) J.Léonard
Mongaangaa	Euphorbiaceae	Sclerocroton cornutus (Pax) Kruijt & Roebers / Sapium cornutum
Mongele	Euphorbiaceae	Ricinodendron heudelotii (Baill.) Pierre ex Heckel subsp. Heudelotii
Monkama	Flacourtiaceae	Oncoba welwitschii Oliv.
Monkee	Fabaceae (caesalpinoideae)	Erythrophleum suaveolens (Guill. & Perr.) Brenan
MonkeeJ	Fabaceae (caesalpinoideae)	Afzelia bipindensis Harms
Monkuma	Meliaceae	Trichilia martineaoui
MonkumaGF	Meliaceae	Trichilia sp1
Monkumankuma	Passifloraceae	Barteria fistulosa Mast.
Monkwinkweu	Fabaceae (caesalpinoideae)	Berlinia (congolensis - confusa)
Monsia	Ochnaceae	Rhabdophyllum arnoldianum (De Wild. & T.Durand) Tiegh.
Monsia2	Ochnaceae	Rhabdophyllum sp.
Monsia3	Ochnaceae	Rhabdophyllum sp.
Montimonsuo	Fabaceae (caesalpinoideae)	Dialium sp1
Motimontala	Annonaceae	Uvaria? Mischogyne?
Montuna	Hypericaceae	Harungana madagascariensis Lam. ex Poir.
Mopapu	Fabaceae (Mimosoideae)	Fillaeopsis discophora Harms
Mopounamueli	Rubiaceae	Hallea stipulosa (DC.) Leroy
Mopounansio	Gentianaceae	Anthocleista liebrechtsiana De Wild. & T.Durand
Mosa	Lecythidiaceae	Petersianthus macrocarpus (P.Beauv.) Liben
Mosauamofuru1	Burseraceae	Dacryodes edulis
Mosauamofuru2	Burseraceae	Santiria trimera (Oliv.) Aubrév.
Moseon	Euphorbiaceae	Maprounea membranorea
Mosio	Urticaceae	Musanga cecropioides R.Br.
Motiamfuamfu	Malvaceae	Grewia oligoneura Sprague
Motimanku1	Pandaceae	Microdesmis cf. puberula
Motimanku2a	Flacourtiaceae	Scottellia klaineana
Motimanku2b	Violaceae	Rinorea oblongifolia (C.H.Wright) Marquand ex Chipp
Motimanku2c	Violaceae	Rinorea brachypetala (Turcz.) Kuntze
Moyempani	Fabaceae (Papillonoideae)	Millettia cf. drastica
Moyili	Olacaceae	Ongokea gore (Hua) Pierre
Mpaba	Fabaceae (caesalpinoideae)	Guibourtia pellegriana/Aphalocalyx
Mukulungu	Sapotaceae	Autranella congolensis (De Wild.) A.Chev.

Vernacular name	*Family*	Species
Munzoni	Bignonaceae	Markhamia tomentosa
Ndaliba	Euphorbiaceae	Drypetes sp1. (Drypetes chevalieri Beille ex Hutch. & Dalziel)
Ngabebalu	Myristicaceae	Coelocaryon preussii Warb.
Nguimbere	Fabaceae (caesalpinoideae)	Dialium pachyphyllum
Nguogni noir	Fabaceae (caesalpinoideae)	Celtis tessmannii Rendle
Nguogni tronc fissuré	Fabaceae (caesalpinoideae)	Tessmannia africana Harms
Nguogni tronc flisse	Fabaceae (caesalpinoideae)	Tessmannia anomala (Micheli) Harms
Nkuri	Irvigiaceae	Klainedoxa gabonensis Pierre ex Engl.
Nkuribedzu	Chrysobalanaceae	Marantes glabra
Nsalbain_rugueux	Dichapetalaceae	Dichapetalum sp1
Nsalbain_lisse1	Ebenaceae	Diospyros iturensis
Nsalbain_lisse2	Ebenaceae	Diospyros dendo
Nsia	Annonaceae	Xylopia aethiopica (Dunal) A.Rich.
Nsia ya mai - racines aériennes	Annoncaceae	Xylopia staudtii - rubescens
Nsiabanduu	Dichapetalaceae	Tapura sp1
Nsiabonkono	Meliaceae	Trichilia cf. rubescens
Nziali	Clusiaceae	Garcinia sp1
Nzini1	Annonaceae	Polyalthia suaveolens Engl. & Diels
Nzini2	Annonaceae	Annickia chlorantha Oliv.
Nzini3	Annonaceae	Piptostigma fasciculatum De Wild.
Nzini3-smalltree	Annonaceae	Polyceratocarpus gossweileri
Sii	Olacaceae	Olax spp.
Siu	Tiliaceae	Desplatsia dewevrei (De Wild. & T.Durand) Burret
Tsii	Burseraceae	Canarium schweinfurthii Engl.
Zuu	Sapindaceae	Eriocoelum microspermum Gilg ex Radlk.

APPENDIX B

PUBLICATIONS

Ecological Applications, 00(0), 0000, pp. 000–000

Aboveground biomass mapping of African forest mosaics using canopy texture analysis: toward a regional approach

JEAN-FRANÇOIS BASTIN,[1,2,3,6] NICOLAS BARBIER,[4] PIERRE COUTERON,[4] BENOÎT ADAMS,[1] AURÉLIE SHAPIRO,[5] JAN BOGAERT,[2] AND CHARLES DE CANNIÈRE[1]

[1]*Landscape Ecology and Plant Production Systems Unit, Université Libre de Bruxelles, Brussels, Belgium*
[2]*Biodiversity and Landscape Unit, Gembloux Agro-Bio Tech, Université de Liège, Gembloux, Belgium*
[3]*Ecole Régionale Post-universitaire d'Aménagement et de Gestion Intégrés des Forêts et Territoires Tropicaux, Kinshasa, the Democratic Republic of the Congo*
[4]*IRD, UMR AMAP, F-34000 Montpellier, France*
[5]*World Wide Fund for Nature (WWF)-Germany, Berlin, Germany*

Abstract. In the context of the reduction of greenhouse gas emissions caused by deforestation and forest degradation (the REDD+ program), optical very high resolution (VHR) satellite images provide an opportunity to characterize forest canopy structure and to quantify aboveground biomass (AGB) at less expense than methods based on airborne remote sensing data. Among the methods for processing these VHR images, Fourier textural ordination (FOTO) presents a good method to detect forest canopy structural heterogeneity and therefore to predict AGB variations. Notably, the method does not saturate at intermediate AGB values as do pixelwise processing of available space borne optical and radar signals. However, a regional-scale application requires overcoming two difficulties: (1) instrumental effects due to variations in sun–scene–sensor geometry or sensor-specific responses that preclude the use of wide arrays of images acquired under heterogeneous conditions and (2) forest structural diversity including monodominant or open canopy forests, which are of particular importance in Central Africa. In this study, we demonstrate the feasibility of a rigorous regional study of canopy texture by harmonizing FOTO indices of images acquired from two different sensors (Geoeye-1 and QuickBird-2) and different sun–scene–sensor geometries and by calibrating a piecewise biomass inversion model using 26 inventory plots (1 ha) sampled across very heterogeneous forest types. A good agreement was found between observed and predicted AGB (residual standard error [RSE] = 15%; $R^2 = 0.85$; $P < 0.001$) across a wide range of AGB levels from 26 Mg/ha to 460 Mg/ha, and was confirmed by cross validation. A high-resolution biomass map (100-m pixels) was produced for a 400-km^2 area, and predictions obtained from both imagery sources were consistent with each other ($r = 0.86$; slope = 1.03; intercept = 12.01 Mg/ha). These results highlight the horizontal structure of forest canopy as a powerful descriptor of the entire forest stand structure and heterogeneity. In particular, we show that quantitative metrics resulting from such textural analysis offer new opportunities to characterize the spatial and temporal variation of the structure of dense forests and may complement the toolbox used by tropical forest ecologists, managers or REDD+ national monitoring, reporting and verification bodies.

Key words: aboveground biomass; canopy structure; canopy texture analysis; central Africa; Congo Basin forest; forest classification; forest-stand structure; Fourier transform; remote sensing; very high resolution imagery.

In: Forestry: Research, Ecology and Policies
Editor: Diane A. Boehm, pp. 79-98

ISBN:978-1-61209-824-1

Chapter 5

MULTISCALAR ANALYSIS OF THE SPATIAL PATTERN OF FOREST ECOSYSTEMS IN CENTRAL AFRICA JUSTIFIED BY THE PATTERN/PROCESS PARADIGM: TWO CASE STUDIES

J. F. Bastin[1], J. P. Djibu[1], F. Havyarimana[1], S. Alongo[1], S. Kumba[1], C. Shalukoma[1], A. Motondo[2], V. Joiris[3], C. Stévigny[4], P. Duez[4], C. De Cannière[1] and J. Bogaert[1]*

[1]Université Libre de Bruxelles, Ecole Interfacultaire de Bioingénieurs, Service d'Ecologie du Paysage et Systèmes de Production Végétale, Bruxelles, Belgique
[2]Institut Facultaire des Sciences Agronomiques de Yangambi, Yangambi/Kisangani, République Démocratique du Congo
[3]Université Libre de Bruxelles, Institut de Sociologie, Bruxelles, Belgique.
[4]Université Libre de Bruxelles, Laboratoire de Pharmacognosie, Bromatologie et Nutrition humaine, Bruxelles, Belgique

ABSTRACT

The pattern/process paradigm justifies the focus of ecological studies on spatial pattern. Two case studies are discussed in which spatial pattern is put forward. The first study analyzes the impact of the definition of forest as a land cover class on the quantification of the spatial pattern of the forest. For the Katanga Province in the Democratic Republic of the Congo, it is shown that the interplay of two factors determines the outcome of a fragmentation analysis: the area considered as forested, and the landscape metrics used. The second study disentangles the relation between tree density and understory diversity in the Bururi Forest Nature Reserve in Burundi. The intermediate disturbance hypothesis is used to explain the nonlinear relationship between understory diversity and tree density. Cluster analysis and comparisons of understory vegetations from environments with different tree densities, confirmed this link between tree density and understory development.

* Corresponding author (jan.bogaert@ulb.ac.be)

PHILOSOPHICAL TRANSACTIONS OF THE ROYAL SOCIETY B

rstb.royalsocietypublishing.org

Research

Cite this article: Lewis SL *et al.* 2013 Above-ground biomass and structure of 260 African tropical forests. Phil Trans R Soc B 368: 20120295.
http://dx.doi.org/10.1098/rstb.2012.0295

One contribution of 18 to a Theme Issue 'Change in African rainforests: past, present and future'.

Subject Areas:
ecology, environmental science, plant science

Keywords:
climate, soil, wood density, Congo Basin, east Africa, west Africa

Author for correspondence:
Simon L. Lewis
e-mail: s.l.lewis@leeds.ac.uk

Electronic supplementary material is available at http://dx.doi.org/10.1098/rstb.2012.0295 or via http://rstb.royalsocietypublishing.org.

Royal Society Publishing
Informing the science of the future

Above-ground biomass and structure of 260 African tropical forests

Simon L. Lewis[1,2], Bonaventure Sonké[3], Terry Sunderland[4], Serge K. Begne[2,3], Gabriela Lopez-Gonzalez[2], Geertje M. F. van der Heijden[5,6], Oliver L. Phillips[2], Kofi Affum-Baffoe[7], Timothy R. Baker[2], Lindsay Banin[8], Jean-François Bastin[9,10,11], Hans Beeckman[12], Pascal Boeckx[13], Jan Bogaert[10], Charles De Cannière[9], Eric Chezeaux[14], Connie J. Clark[15], Murray Collins[16], Gloria Djagbletey[17], Marie Noël K. Djuikouo[3,18], Vincent Droissart[19], Jean-Louis Doucet[20,21], Cornielle E. N. Ewango[22,23], Sophie Fauset[2], Ted R. Feldpausch[2], Ernest G. Foli[17], Jean-François Gillet[21], Alan C. Hamilton[24], David J. Harris[25], Terese B. Hart[26,27], Thales de Haulleville[10,12], Annette Hladik[28], Koen Hufkens[13], Dries Huygens[13,29], Philippe Jeanmart[30], Kathryn J. Jeffery[31,32,33], Elizabeth Kearsley[12,13,34], Miguel E. Leal[35], Jon Lloyd[2,36], Jon C. Lovett[2], Jean-Remy Makana[22], Yadvinder Malhi[37], Andrew R. Marshall[38,39], Lucas Ojo[40], Kelvin S.-H. Peh[2,41], Georgia Pickavance[2], John R. Poulsen[15], Jan M. Reitsma[42], Douglas Sheil[4,43,44], Murielle Simo[3], Kathy Steppe[34], Hermann E. Taedoumg[3], Joey Talbot[2], James R. D. Taplin[45], David Taylor[46], Sean C. Thomas[47], Benjamin Toirambe[12], Hans Verbeeck[34], Jason Vleminckx[48], Lee J. T. White[31,32,33], Simon Willcock[2,49], Hannsjorg Woell[50] and Lise Zemagho[3]

[1]Department of Geography, University College London, London WC1E 6BT, UK
[2]School of Geography, University of Leeds, Leeds LS2 9JT, UK
[3]Plant Systematic and Ecology Laboratory, Department of Biology, Higher Teachers' Training College, University of Yaounde I, PO Box 047, Yaounde, Cameroon
[4]Center for International Forestry Research, Bogor, Indonesia
[5]University of Wisconsin-Milwaukee, PO Box 413, Milwaukee, WI 53201, USA
[6]Smithsonian Tropical Research Institute, Apartado Postal 0843-03092, Panama
[7]Mensuration Unit, Forestry Commission of Ghana, Kumasi, Ghana
[8]Centre for Ecology and Hydrology, Bush Estate, Penicuik, Midlothian EH26 0QB, UK
[9]Landscape Ecology and Vegetal Production Systems Unit, Université Libre de Bruxelles, Brussels, Belgium
[10]Biodiversity and Landscape Unit, Gembloux Agro-Bio Tech, Université de Liège, Gembloux, Belgium
[11]Ecole Régionale post-universitaire d'Aménagement et de gestion Intégrés des Forêts et Territoires tropicaux, Kinshasa, Republic Democratic of Congo
[12]Laboratory for Wood Biology and Xylarium, Royal Museum for Central Africa, Tervuren, Belgium
[13]Isotope Bioscience Laboratory-ISOFYS, Department of Applied Analytical and Physical Chemistry, Faculty of Bioscience Engineering, Ghent University, Ghent, Belgium
[14]Rougier-Gabon, Oloumi Industrial Estate, PO Box 130, Libreville, Gabon
[15]Nicholas School of the Environment, Duke University, PO Box 90328, Durham, NC 27708, USA
[16]Grantham Research Institute on Climate Change and the Environment, London School of Economics, Tower 3, Clements Inn Passage, London WC2A 2AZ, UK
[17]Forestry Research Institute of Ghana (FORIG), UP Box 63, KNUST, Kumasi, Ghana
[18]Department of Botany and Plant Physiology, Faculty of Science, University of Buea, PO Box 63 Buea-Cameroon
[19]Institut de Recherche pour le Développement (IRD), Unité Mixte de Recherche AMAP (Botanique et Bioinformatique de l'Architecture des Plantes), Boulevard de la Lironde, Montpellier, France
[20]Laboratory of Tropical and Subtropical Forest Regions, Unit of Forest and Nature Management, University of Liège, Gembloux, Belgium
[21]Nature +, c/o Gembloux Agro-Bio Tech, University of Liège, Gembloux, Belgium
[22]Wildlife Conservation Society-DR Congo, PO Box 240, Kinshasa I, DR Congo
[23]Centre de Formation et de Recherche en Conservation Forestiere (CEFRECOF), Democratic Republic of Congo
[24]128 Busbridge Lane, Godalming, Surrey GU7 1QJ, UK
[25]Royal Botanic Garden Edinburgh, 20A Inverleith Row, Edinburgh EH3 5LR, UK

Journal of Biogeography (J. Biogeogr.) (2014)

ORIGINAL ARTICLE

Patterns of tree species composition across tropical African forests

Adeline Fayolle[1]*, Michael D. Swaine[2†], Jean-François Bastin[3,4,5], Nils Bourland[1], James A. Comiskey[6], Gilles Dauby[7], Jean-Louis Doucet[1], Jean-François Gillet[1], Sylvie Gourlet-Fleury[8], Olivier J. Hardy[7], Ben Kirunda[9], François N. Kouamé[10] and Andrew J. Plumptre[9]

[1]Unité de Gestion des Ressources Forestières et des Milieux Naturels, Gembloux Agro-Bio Tech, Université de Liège, 2 Passage des Déportés, 5030 Gembloux, Belgium, [2]Institute of Biological and Environmental Sciences, University of Aberdeen, Aberdeen AB24 3UU, UK, [3]Service d'Ecologie du paysage et systèmes de production végétale, Université Libre de Bruxelles, CP264/2, Boulevard du Triomphe, 1050 Bruxelles, Belgium, [4]Unité Biodiversité et Paysage, Gembloux Agro-Bio Tech, Université de Liège, 2 Passage des Déportés, 5030 Gembloux, Belgium, [5]Ecole Régionale post-universitaire d'Aménagement et de gestion Intégrés des Forêts et Territoires tropicaux, Kinshasa, République Democratique du Congo, [6]Inventory and Monitoring Program, National Park Service, 120 Chatham Lane, Fredericksburg, VA 22405, USA, [7]Evolutionary Biology and Ecology – CP160/12, Faculté des Sciences, Université Libre de Bruxelles, 50 Avenue F. Roosevelt, 1050 Bruxelles, Belgium, [8]Unité de Recherche Biens et Services des Ecosystèmes Forestiers tropicaux, Département Environnements et Sociétés du CIRAD, TA C-105/D/Campus International de Baillarguet, 34398 Montpellier Cedex 5, France, [9]Albertine Rift Program, Wildlife Conservation Society, Kampala, Uganda, [10]Laboratoire de Botanique, Université Félix Houphouët-Boigny, 31 BP 165 Abidjan, République de la Côte d'Ivoire

*Correspondence: Adeline Fayolle, Unité de Gestion des Ressources Forestières et des Milieux Naturels, Gembloux Agro-Bio Tech, Université de Liège, 2 Passage des Déportés, 5030 Gembloux, Belgium.

ABSTRACT

Aim In this study we identified large-scale variation in tree species composition across tropical African forests and determined the underlying environmental and historical factors.

Location Tropical forests from Senegal to Mozambique.

Methods Distribution data were gathered for 1175 tree species in 455 sample sites scattered across tropical Africa, including all types of tropical forests (wet, moist, dry, and lowland to moderate elevation montane forests). The value of elevation and 19 climatic variables extracted from the BIOCLIM data set were assigned to each sample site. We determined the variation in species composition using correspondence analysis and identified the environmental correlates. We defined floristic clusters according to species composition and identified the characteristic species using indicator analysis.

Results We identified a major floristic discontinuity located at the Albertine rift that separated the dry, moist and wet forests of West and Central Africa (the entire Guineo-Congolian Region) from the upland and coastal forests of East Africa. Except for the Albertine Rift, we found no evidence to support the other proposed floristic discontinuities (Dahomey Gap etc.). We detected two main environmental gradients across tropical African forests. The rainfall gradient was strongly correlated with the variation in tree species composition in West and Central Africa. The elevation/temperature gradient highlighted the major floristic differences within East Africa and between East Africa and the Guineo-Congolian Region, the latter being most probably due to the geological disruption and associated climatic history of the East African uplift.

Main conclusions We found floristic evidence for three main biogeographical regions across the tropical African forests, and described six floristic clusters with particular environmental conditions within these regions: Coastal and Upland for East Africa, Dry and Wet-Moist for West Africa, and Moist and Wet for Central Africa.

Keywords

Albertine Rift, African tropical forests, biogeographical analysis, correspondence analysis, East African uplift, environmental gradients, floristic discontinuities, indicator species, Pleistocene climatic oscillations.

TROPICULTURA, 2013, 1, 75-81

Influence de l'effet de lisière sur la productivité du teck (*Tectona grandis* L.f.): étude de cas des teckeraies privées du Sud-Bénin

M. S. Toyi[1*], J.-F. Bastin[2,3], Marie André[3], C. De Cannière[2], B. Sinsin[1] & J. Bogaert[3]

Mots clés : Production du bois en lisière- Ecologie du paysage- Modèle de plantation- Sud-Bénin

Keywords : *Tectona grandis* L.f.- Landscape ecology- Edge effect- Private teak plantation- Southern Benin

Résumé

*La présente étude vise à améliorer la production du bois de teck (*Tectona grandis *L.f.) à l'échelle des plantations privées du Sud-Bénin à travers l'application d'un concept central de l'écologie du paysage: l'effet de lisière. Le teck étant une espèce héliophile, l'hypothèse d'une plus forte production de bois en lisière a été testée. Ainsi, 62 teckeraies privées ont été parcourues et 10667 arbres ont été mesurés. L'échantillonnage stratifié en 3 zones distinctes pour chaque plantation : le centre, la lisière et les sommets (coins des plantations), a permis de mettre en évidence l'effet de lisière sur la production de bois. Dans chaque zone, une placette a été installée et le diamètre à 130 cm du sol (dbh) a été mesuré pour tous les arbres. La différence de surface foliaire par individu entre la lisière et le centre des plantations a également été mesurée. Enfin, l'influence de la configuration spatiale des plantations et de l'orientation de chaque coté des plantations sur la production de bois a été testée. Les résultats montrent que l'effet de lisière sur la production du bois de teck touche 4 lignes de plantations, la première présentant une production de l'ordre de 150% par rapport au centre. On note également une influence significative de la lisière sur la surface foliaire, (production de l'ordre de 218% en lisière par rapport au centre). Aucune influence de l'orientation des côtés de la plantation n'a été observée. La forme des plantations présente une influence significative sur la production de bois. Ainsi, les plantations ayant une forme maximisant leur périmètre par rapport à leur surface, présentent une production de bois plus importante. Ces résultats ont permis de proposer un modèle de plantation inclus dans un système agroforestier qui optimise la production de bois par unité de surface et présentant une succession de 2 lignes de plantation entrecoupées de champs.*

Summary

Influence of Edge Effect on Productivity of Teak (*Tectona grandis* L.f.): a Case Study of Private Teak Plantations in Southern Benin

*The present study aims to improve the production of teak wood (*Tectona grandis *L.f.) on private plantations in southern Benin through the application of a central concept in landscape ecology: the edge effect. As teak is an heliophilous species, the hypothesis of a higher wood production in edges was tested on the basis of the basal area G. 62 private teak plantations were investigated and 10,667 trees were measured. The stratified sampling scheme in 3 distinct parts for each plantation (the centre, the edge and the summits) permitted to highlight the edge effect on wood production. For each part, a plot was installed and the diameter at breast height (dbh) was measured for all trees. The leaf area between the edge and the centre of plantations was measured. Finally, the influence of the spatial configuration of plantations and the direction of each side of these plantations on the production of wood was tested. Results show that the edge effect on the production of teak wood affects 4 planting line, the first presenting a production on the order of 150% relative to the centre. We notice meaningful influence of the edge on the leaf area (a production on the order of 218% in the edge relative to the centre). No influence of the direction of the sides of the plantation was observed. The shape of the plantations presents a meaningful influence on the wood production. These results permitted to propose a planting model included in an agroforestry system that optimizes the production of wood per area and having a succession of 2 planting line interrupted by fields.*

1 Université d'Abomey-Calavi, Faculté des Sciences Agronomiques, Laboratoire d'Ecologie Appliquée, 01 BP 526, Cotonou, Bénin.
2 Université Libre de Bruxelles, Ecole Interfacultaire de Bioingénieurs, Service d'Ecologie du Paysage et Systèmes de Production Végétale, CP 169, 50 Avenue F. Roosevelt, 1050 Bruxelles, Belgique.
3 Université de Liège, Gembloux Agro-Bio Tech, Unité Biodiversité et Paysage, 02 Passage des Déportés, B-5030 Gembloux, Belgique.
* Auteur pour correspondances E-mail: mireille.toyi@gmail.com; 02 BP 1181 Porto-Novo, Bénin. Tel: (229) 97 89 58 02.

TROPICULTURA, 2013, 1, 62-70

Tree Plantation Will Not Compensate Natural Woody Vegetation Cover Loss in the Atlantic Department of Southern Benin

M.S. Toyi[1*], Y.S.S. Barima[2], A. Mama[1,3], M. André[4], J.-F. Bastin[3,4], C. De Cannière[3], B. Sinsin[1] & J. Bogaert[4]

Keywords: Land use and land cover change- Probability matrix- First-order Markov model- Tree plantation- Benin

Mots clés: Changement d'occupation et d'utilisation du sol- Matrice de probabilité- Modèle de Markov de premier ordre- Plantation forestière- Bénin

Summary

This study deals with land use and land cover changes for a 33 years period. We assessed these changes for eight land cover classes in the south of Benin by using an integrated multi-temporal analysis using three Landsat images (1972 Landsat MSS, 1986 Landsat TM and 2005 Landsat ETM+). Three scenarios for the future were simulated using a first-order Markovian model based on annual probability matrices. The contribution of tree plantations to compensate forest loss was assessed. The results show a strong loss of forest and savanna, mainly due to increased agricultural land. Natural woody vegetation ("forest", "wooded savanna" and "tree and shrub savanna") will seriously decrease by 2025 due to the expansion of agricultural activities and the increase of settlements. Tree plantations are expected to double by 2025, but they will not compensate for the loss of natural woody vegetation cover. Consequently, we assist to a continuing woody vegetation area decrease. Policies regarding reforestation and forest conservation must be initiated to reverse the currently projected tendencies.

Résumé

Les plantations forestières ne compenseront pas les pertes de végétations naturelles boisées dans le Département de l'Atlantique au sud du Bénin

La présente étude traite des processus de changements d'occupation et d'utilisation du sol sur une durée de 33 années. Ces changements ont été évalués pour huit classes d'occupation du sol au sud de Bénin à partir d'une analyse multi-temporelle de trois images satellitaires de type Landsat MSS 1972, Landsat TM 1986 et Landsat ETM+2005. Trois scénarii ont été simulés à partir d'une chaîne de Markov de premier ordre basée sur des matrices de probabilité. La contribution des plantations forestières en vue de compenser les pertes de végétation naturelle a été évaluée. Les résultats indiquent une perte importante des végétations naturelles boisées ("forêt", "savane boisée" et "savanes arborée et arbustive"), principalement due à une augmentation des superficies agricoles. Les végétations naturelles boisées seront drastiquement réduites jusqu'en 2025 au profit des exploitations agricoles et des habitations. Les plantations forestières pourraient doubler leur superficie en 2025, mais elles ne pourront pas compenser les pertes de végétation naturelle boisée. Par conséquent, on assistera à une dégradation constante des végétations naturelles boisées. Des politiques de développement durable basées sur le reboisement et la conservation des forêts doivent être initiées en vue d'inverser les tendances actuelles.

1 Université d'Abomey-Calavi, Faculté des Sciences Agronomiques, Laboratoire d'Ecologie Appliquée, Cotonou, Bénin.
2 Université Jean Lorougnon Guédé, Unité de Formation et de Recherche en Environnement, Daloa, Côte d'Ivoire.
3 Université Libre de Bruxelles, Ecole Interfacultaire de Bioingénieurs, Service d'Ecologie du Paysage et Systèmes de Production Végétale, Bruxelles, Belgique.
4 Université de Liège, Gembloux Agro-Bio Tech, Unité Biodiversité et Paysage, Gembloux, Belgique.
* Corresponding author: E-mail: mireille.toyi@gmail.com

OPEN ACCESS Freely available online

PLOS ONE

Nest Grouping Patterns of Bonobos *(Pan paniscus)* in Relation to Fruit Availability in a Forest-Savannah Mosaic

Adeline Serckx[1,2,3,4]*, Marie-Claude Huynen[1], Jean-François Bastin[3,5,6], Alain Hambuckers[1], Roseline C. Beudels-Jamar[2], Marie Vimond[1], Emilien Raynaud[1], Hjalmar S. Kühl[4,7]

1 Behavioural Biology Unit, University of Liege, Liege, Belgium, **2** Conservation Biology Unit, Royal Belgian Institute of Natural Sciences, Brussels, Belgium, **3** Ecole Régionale Post-Universitaire d'Aménagement et de Gestion Intégrés des Forêts et Territoires Tropicaux, University of Kinshasa, Kinshasa, Democratic Republic of the Congo, **4** Department of Primatology, Max Planck Institute for Evolutionary Anthropology, Leipzig, Germany, **5** Landscape Ecology and Vegetal Production Systems Unit, Université Libre de Bruxelles, Brussels, Belgium, **6** Biodiversity and Landscape Architecture Unit, Gembloux AgroBio-Tech, University of Liege, Gembloux, Belgium, **7** German Centre for Integrative Biodiversity Research, Leipzig, Germany

Abstract

A topic of major interest in socio-ecology is the comparison of chimpanzees and bonobos' grouping patterns. Numerous studies have highlighted the impact of social and environmental factors on the different evolution in group cohesion seen in these sister species. We are still lacking, however, key information about bonobo social traits across their habitat range, in order to make accurate inter-species comparisons. In this study we investigated bonobo social cohesiveness at nesting sites depending on fruit availability in the forest-savannah mosaic of western Democratic Republic of Congo (DRC), a bonobo habitat which has received little attention from researchers and is characterized by high food resource variation within years. We collected data on two bonobo communities. Nest counts at nesting sites were used as a proxy for night grouping patterns and were analysed with regard to fruit availability. We also modelled bonobo population density at the site in order to investigate yearly variation. We found that one community density varied across the three years of surveys, suggesting that this bonobo community has significant variability in use of its home range. This finding highlights the importance of forest connectivity, a likely prerequisite for the ability of bonobos to adapt their ranging patterns to fruit availability changes. We found no influence of overall fruit availability on bonobo cohesiveness. Only fruit availability at the nesting sites showed a positive influence, indicating that bonobos favour food 'hot spots' as sleeping sites. Our findings have confirmed the results obtained from previous studies carried out in the dense tropical forests of DRC. Nevertheless, in order to clarify the impact of environmental variability on bonobo social cohesiveness, we will need to make direct observations of the apes in the forest-savannah mosaic as well as make comparisons across the entirety of the bonobos' range using systematic methodology.

Citation: Serckx A, Huynen M-C, Bastin J-F, Hambuckers A, Beudels-Jamar RC, et al. (2014) Nest Grouping Patterns of Bonobos *(Pan paniscus)* in Relation to Fruit Availability in a Forest-Savannah Mosaic. PLoS ONE 9(4): e93742. doi:10.1371/journal.pone.0093742

Editor: Cédric Sueur, Institut Pluridisciplinaire Hubert Curien, France

Received January 5, 2014; **Accepted** March 7, 2014; **Published** April 2, 2014

Funding: This project was funded by the National Fund for Scientific Research (FNRS, Belgium), the Fonds Leopold III from the Royal Belgian Institute of Natural Sciences (Belgium) and the Ecole Régionale post-universitaire d'Aménagement et de gestion Intégrés des Forêts et Territoires tropicaux (ERAIFT, Democratic Republic of Congo). The funders had no role in study design, data collection and analysis, decision to publish, or preparation of the manuscript.

Competing Interests: The authors have declared that no competing interests exist.

* E-mail: adelineserckx@gmail.com

Introduction

Nest-building is an important behavioural feature shared by all species of great apes and is considered to be a basal adaptation underlying the aptitude of great apes for manipulating objects in their environment. The deep ancestry of this trait has possible implications for our understanding of the cognitive evolution of early hominoids [1], as it permits higher-quality sleep by providing thermoregulation [2,3], reduced vulnerability to predators [2,4,5], more comfortable sleeping postures [4,6,7], and protection against pathogens [2,4,8]. The impact of environmental factors on the location of great ape nests has been the subject of a number of studies [6,9–18], and nest counts are frequently used to estimate ape population density [19–29]. However the functionality of great ape nesting sites in relation to the dynamics of their social organization has been much less well-documented [1]. Bonobo nesting behaviour has not been as thoroughly investigated compared to that of chimpanzees [6,16,30,31]. Nonetheless, several studies have already shown that nesting patterns could play an important role in their social behaviour. Fruth and Hohmann suggested that the aggregation of bonobos at nest sites at night could facilitate information transfer on the quality of food patches visited during the day [1], and that nests could serve as 'taboo zones' which can help bonobos avoid conflicts with group members [32]. Variation in the size and location of nest groups could reflect differences in social organisation and could provide us with insight into the species-specific elements of bonobo social structure [1].

Comparisons between the social organization of bonobos and chimpanzees have been made using data from a number of habituated populations and show that bonobos live in more cohesive communities and with a larger relative party size (i.e., the percentage of the total community size) [33–36]. The composition of chimpanzee parties changes more frequently than that of bonobos. Individual chimpanzees, usually adult females with infants, more often travel at a distance from the main parties,